Total Intensity Light Scattering from Solutions of Macromolecules

CHAPTER · NOVEMBER 2008

DOI: 10.1007/978-1-4020-4465-6_2

1 AUTHOR:

Guy Berry
Carnegie Mellon University
107 PUBLICATIONS **1,713** CITATIONS

Prepared for submission to "SOFT MATTER: SCATTERING, MANIPULATION & IMAGING" BOOK SERIES, R. Pecora, R. Borsali Editors

Total Intensity Light Scattering from Solutions of Macromolecules

Guy C. Berry
Department of Chemistry
Carnegie Mellon University
Pittsburgh, PA 15213

Abstract

The analysis of total intensity light scattering from solutions of macromolecules is discussed, covering the concentration range from infinite dilution to concentrated solutions, with a few examples for the scattering from colloidal dispersions of particles and micelles. The dependence on scattering angle is included over this entire range. Most of the discussion is limited to the Rayleigh-Gans-Debye scattering regime, but Mie scattering from large spheres is also discussed. Examples include the effects of heterogeneity of molecular weight and chemical composition, optically anisotropic chain elements, deviations from flexible chain conformational statistics and intermolecular association.

Keywords

Light scattering, second virial coefficient, radius of gyration, dilute solution, moderately concentrated solution, concentrated solution, scaling behavior.

November 2004

Contents

1. Introduction

2. General Relations

3. Scattering at infinite dilution and zero scattering angle

3.1 The basic relation

3.2 Identical scattering elements

3.3 Optically diverse scattering elements

3.4 Optically anisotropic scattering elements

3.5 Scattering beyond the RGD regime.

4. Scattering at infinite dilution and small q

4.1 The basic relation

4.2 Identical scattering elements

4.3 Optically diverse scattering elements

4.4 Optically anisotropic scattering elements

4.5 Scattering beyond the RGD regime

5. Scattering at infinite dilution and arbitrary q

5.1 The basic relation

5.2 Identical scattering elements

5.3 Optically diverse scattering elements

5.4 Optically anisotropic scattering elements

5.5 Scattering beyond the RGD regime

6. Scattering from a dilute solution at zero scattering angle

6.1 The basic relation

6.2 Monodisperse solute, identical optically isotropic scattering elements

6.3 Heterodisperse solute, identical optically isotropic scattering elements

6.4 Optically diverse, isotropic scattering elements

6.5 Optically anisotropic scattering elements

7. Scattering from non dilute solutions at zero scattering angle

7.1 The basic relation

7.2 The third virial coefficient

7.3 Concentrated solutions

7.4 Moderately concentrated solutions

8. Scattering dependence on q for arbitrary concentration

8.1 The basic relation

8.2 Dilute to low concentrations

8.3 Concentrated solutions

8.4 Moderately concentrated solutions

8.5 Behavior for a charged solute

9. Special topics

9.1 Intermolecular association in polymer solutions

9.2 Intermolecular association in micelle solutions

9.3 Online monitoring of polymerization systems

References

Symbols

Tables

Figures

1. Introduction

Electromagnetic scattering (light, x-ray and neutron) has long been used to characterize a wide variety of material properties, including especially thermodynamic, dynamic and structural features. This chapter is limited to a relatively narrow subset of these studies, focusing on properties that may be obtained via measurements of the total intensity, or so-called elastic or static, scattering of light, as a function of the scattering angle ϑ and other relevant parameters, such as temperature and the composition of mixtures, with occasional digressions to include the scattering of x-rays and neutrons. Here, the term total scattering refers to the intensity of light measured under conditions designed to average over the fluctuations in the intensity that are used with advantage in quasi elastic, or dynamic, light scattering. Further, this chapter will focus principally on static scattering of light from polymer solutions, encompassing solute concentrations from dilute to moderately concentrated, with a few remarks on the scattering from concentrated solutions, and some digressions to include the static scattering of light from dispersions. Here, a moderately concentrated polymer solution is one for which the concentration c (wt/vol) of the solute is much less than the density ρ of the undiluted polymer, but in the range of the reciprocal of the volume swept out by the chain in rotation about its center of mass, see below for a more precise definition. Static light scattering from solutions in this concentration range will principally focus on optically isotropic polymers (or particles), but will also include some discussion of isotropic solutions of optically anisotropic polymers. The former will emphasize polarized scattering, whereas the latter will emphasize depolarized scattering (Here, polarized and depolarized scattering refer to scattering in the horizontal plane, with vertically polarized incident light and vertically or horizontally polarized scattered light, respectively). The general principles of polarized and depolarized static light scattering may be found in a number of monographs or reviews [1-37]—the nomenclature here will follow than in reference 1 for the most part. The interesting topic of the scattering from nematic solutions will not be included, but see elsewhere for a review [9]. Similarly, dynamic light scattering, discussed elsewhere in this book, as well as in a number of monographs and review chapters [4, 8-11, 22, 38-41], will receive only a brief mention in this chapter.

In many cases, it may safely be assumed that the electric field giving rise to the dipole radiation of the scattered light is that of the incident radiation propagating in the medium. That is, in a solution, the field acting on all parts of a solute is the same as that acting on the solvent. This simplification,

usually valid for polymer solutions, is termed Rayleigh-Gans-Debye (RGD) scattering [1, 23, 30, 33], with the term Rayleigh scattering preserved for the scattering from solute very small in comparison to the wavelength of light. In the RGD regime, the scattering from a single solute may be taken as an appropriate sum of independent Rayleigh scattering from the elements comprising the solute. Aside from the scattering from strongly absorbing media, deviations from this for the scattering from solutions (or suspensions) will almost always involve the scattering from large particles, suspended in a medium with a rather different refractive index from that of the particles In such cases, the incident radiation is altered as it propagates through a solute particle, and the simplicity of the additivity of the scattering from different elements in the particle generated by an unaltered incident beam cannot be adopted. In fact, detailed attention to scattering beyond the RGD regime will be limited to the scattering from spherical particles, called Mie scattering.

Most of the discussion in this chapter, will concern the scattering in a single plane containing the incident ray, and with the plane-polarized components of that ray either in the scattering plane or orthogonal to it; an exception to this, with the electric vector of the incident ray at an angle φ to the scattering plane will be introduced in the discussion of the Mie theory of scattering for large spheres. With φ either 0 or $\pi/2$, it is sufficient to use notation that specifies the scattering angle ϑ between the incident and scattered rays, and the polarization state of the incident and scattered light. Unless otherwise noted, it will be assumed that the incident light is plane polarized, and for most of the scattering discussed in this chapter, the notation $\mathbf{R}_{Si}(q,c)$ will suffice to designate the Rayleigh ratio from a solution with solute concentration c, where the subscripts S and i designate the polarization state of the electric vectors of the scattered and incident light, respectively, relative to the scattering plane. Here, $\mathbf{R}_{Si}(q,c)$ is given by $r^2 I_{Si}(\vartheta)/V_{obs} I_{INC}$, with r the distance between the scattering centers and the detector, V_{obs} the observed scattering volume and $I_{Si}(\vartheta)$ and I_{INC} the intensities of the scattered and incident light, respectively. More precisely, we will be interested in the excess Rayleigh ratio, equal to the Rayleigh ratio for the solution less that for the solvent, but notation to this effect is suppressed for convenience. Thus, for vertically polarized incident light (i.e., $\varphi = \pi/2$), and horizontally or vertically polarized scattered light, the components $\mathbf{R}_{Hv}(q,c)$ and $\mathbf{R}_{Vv}(q,c)$, respectively, will comprise contributions designated $\mathbf{R}_{iso}(q,c)$, $\mathbf{R}_{aniso}(q,c)$ and $\mathbf{R}_{cross}(q,c)$:

$$\mathbf{R}_{Hv}(q,c) = \mathbf{R}_{aniso}(q,c) \quad (1)$$

$$\mathbf{R}_{Vv}(q,c) = \mathbf{R}_{iso}(q,c) + (4/3)\mathbf{R}_{aniso}(q,c) + \mathbf{R}_{cross}(q,c) \quad (2)$$

where $\mathbf{R}_{aniso}(q,c)$ and $\mathbf{R}_{cross}(q,c)$ vanish for a solute comprising optically isotropic scattering elements, and $\mathbf{R}_{cross}(0,c) = 0$ in any case. The terms polarized and depolarized scattering will generally refer to $\mathbf{R}_{Vv}(q,c)$ and $\mathbf{R}_{Hv}(q,c)$, respectively, in this Chapter. In the following, the subscript "iso" will be suppressed for convenience when considering the behavior for isotropic scattering elements, to designate $\mathbf{R}_{iso}(q,c)$ and $\mathbf{R}_{Vv}(q,c)$ simply as $\mathbf{R}(q,c)$. If unpolarized incident light is used, as was often the case prior to the now nearly universal use of plane polarized light generated by lasers as the source for the incident light, the scattered light will comprise $\mathbf{R}_{Vv}(q,c) + \mathbf{R}_{Vh}(q,c)$ if a vertical polarization analyzer is used, or these plus $\mathbf{R}_{Hv}(q,c) + \mathbf{R}_{Hh}(q,c)$ if no analyzer is used, with $\mathbf{R}_{Hh}(q,c) = \cos^2(\vartheta)\mathbf{R}_{Vv}(q,c)$ in the RGD regime; for a solute with isotropic scattering elements $\mathbf{R}_{aniso}(q,c) = \mathbf{R}_{cross}(q,c) = 0$, and $\mathbf{R}_{Vh}(q,c) = \mathbf{R}_{Hv}(q,c) = 0$.

The modulus of the wave vector **q**, with the units of a reciprocal length, plays a central role in this chapter, setting the length-scale over which features of the structure giving rise to interference effects on the total intensity that provide information on the polymer in solution. Here, **q** is the vector difference between the vectoral wave numbers $\mathbf{k_0}$ and **k**, which lie in the directions of the incident and scattered light, respectively:

$$\mathbf{q} = \mathbf{k_0} - \mathbf{k} \tag{3}$$

For elastically scattered light medium, $|k_0| = |k| = (4\pi/\lambda)$, with λ the wavelength of light in the scattering medium ($\lambda = \lambda_0/\hat{n}$, with $\hat{n}$ the refractive index of the medium), and the modulus of **q** becomes

$$q = (4\pi/\lambda)\sin(\vartheta/2) \tag{4}$$

In the RGD regime, both $\mathbf{R}_{Vv}(q,c)$ and $\mathbf{R}_{Hv}(q,c)$ depend on ϑ through q, but even in that regime, as noted above, $\mathbf{R}_{Hh}(q,c) = \cos^2(\vartheta)\mathbf{R}_{Vv}(q,c)$ depends explicitly on ϑ. Nevertheless, the nomenclature used here instead of, say the alternate notation $\mathbf{R}_{Vv}(\vartheta,c)$ which would take account of such situations, is convenient for special situations, and serves to emphasize the importance of the parameter q. In a few cases, the alternate notation will be employed in the interests of clarity.

2. General Relations

Certain general relations used with the polarized static scattering from isotropic solutions in the RGD regime are gathered in this section to introduce notation used in the following sections. In this section, attention will be focused on the scattering from a monodisperse solute comprising

identical isotropic scattering elements. More complex situations involving heterogeneity of various kinds and anisotropic scattering elements will be discussed subsequently. Thus, here, $\mathbf{R}_{Vv}(q,c)$, designated simply $\mathbf{R}(q,c)$, may be expressed in the form [1, 5, 18, 20, 27, 29-31]

$$\mathbf{R}(q,c)/K_{op} = cMP(q,c) - [cMP(q,c)]^2\widetilde{B}(c)Q(q,c) \quad (5)$$

with M the molecular weight, K_{op} an optical constant, P(q,c) the intramolecular structure factor, and the second term arising from interference effects among the rays scattered from different molecules. Both P(0,c) and Q(0,c) are equal to unity. (Note: the nomenclature for Q(q,c) here differs from that sometimes used.) Variations of this expression to account for heterodispersity and anisotropy are considered in the following. An alternative nomenclature introduces the so-called structure factor S(q,c):

$$\mathbf{R}(q,c) = K_{op}cM\,S(q,c) \quad (6a)$$

$$S(q,c) = P(q,c)F(q,c) \quad (6b)$$

(Note: again, the reader should be aware that S(q,c) is sometimes used to denote a different function than that defined here.) Two expressions are commonly employed to represent F(q,c). With the preceding,

$$F(q,c) = 1 - cB(c)P(q,c)Q(q,c) \quad (7)$$

where $B(c) = M\widetilde{B}(c)$ and Q(q,c) depend on intermolecular interference. Alternatively, the inverse of F(q,c) may be expressed in terms of an interference function H(q,c):

$$F(q,c)^{-1} = 1 + c\Gamma(c)P(q,c)H(q,c) \quad (8)$$

which, together with the requirement H(0,c) = 1, may be considered to define H(q,c) and $\Gamma(c)$ in terms of the more direct functions B(c) and Q(q,c), i.e.,

$$\Gamma(c) = B(c)/[1 - cB(c)] \quad (9)$$

$$H(q,c) = Q(q,c)\,\frac{[1 - cB(c)]}{[1 - cB(c)P(q,c)Q(q,c)]} \quad (10)$$

Although theoretical considerations will usually be developed in a form based on Equation 7, for experimental purposes, it is largely a matter of convenience as to which form is used for F(q,c), e.g., one of the functions H(q,c) or Q(q,c) might be less dependent on ϑ than the other, and therefore more convenient to use. With the use of Equation 9,

$$\frac{K_{op}cM}{\mathbf{R}(q,c)} = \frac{1}{S(q,c)} = \frac{1}{P(q,c)} + c\Gamma(c)H(q,c) \qquad (11)$$

Some approximate theories discussed below lead directly to Equation 9 or 11 with H(q,c) equal to unity for all q.

With Equation 9, thermodynamic information is found in the function $\Gamma(c)$, and thermodynamic and conformational information is represented in the functions P(q,c) and H(q,c). As is well known, in the limit of infinite dilution, both H(q,0) and Q(q,0) tend to unity for all q [1, 20, 27, 29, 42, 43] (the "single-contact" approximation), and as discussed below, R_G may be determined from P(q,0) in the limit $qR_G << 1$. In the limit $qR_G >> 1$, F(q,c) tends to unity, as then the scattering can only be sensitive to short-range correlations among the scattering elements, and will be dominated by intramolecular interference effects reflected in P(q,0), i.e., $c\Gamma(c)P(q,c)H(q,c) << 1$ (or $cB(c)P(q,c)Q(q,c) << 1$) for large q, and in consequence, F(q,c) tends to unity. This asymptotic behavior will require larger q with increasing $\Gamma(c)$, and may generally be beyond that available in light scattering experiments for moderately concentrated solutions, for which $c\Gamma(c)$ is large.

For a monodispersed solute, F(0,c) is related to the equilibrium osmotic modulus K_{OS} [12, 20, 27, 30, 31, 37, 44-47]:

$$F(0,c) = (M/cRT)\, K_{OS} \qquad (12)$$

$$K_{OS} = c\, \partial\, \Pi/\partial c \qquad (13)$$

where Π is the osmotic pressure. It should be noted, however, that the expression between F(0,c) and K_{OS} is not valid for a heterodisperse solute; the effects of heterodispersity are developed below. With this expression, for a monodispersed solute,

$$c\Gamma(c) = \frac{M}{RT}\frac{\partial \Pi}{\partial c} - 1 \qquad (14)$$

This relation will find use in the following.

Another, and very different, source for the dependence of **R**(q,c) on c can arise if the solute components form aggregated structures, with the extent of the intermolecular (or interparticle) association dependent on c, but with an aggregate structure that is stable at a particular c. In some cases, the association may be at equilibrium at each c, but often that is not the case, and one has to consider metastable structures, the form of which may depend on the pathway used to form the solution. The hemoglobin tetramer, a well known example of an aggregate that forms at equilibrium, has been studied by lights scattering methods [48], and certain worm-like micelles provide another example, as discussed further below. Solutions of semiflexible polymers may exhibit metastable association, even to the extent that the molecular weight observed does not change with concentration over an appreciable range, but can be markedly affected by the solvent used; examples are cited below.

In the following sections, the application of the preceding expressions will be applied over a range of concentrations, from the infinitely dilute limit obtained by extrapolation to concentrated solutions. Methods to effect the extrapolations to infinite dilution and zero scattering angle are addressed in a subsequent section. The discussion is presented in several principal sections:

3. Scattering at infinite dilution and zero angle;
4. Scattering at infinite dilution and small q;
5. Scattering at infinite dilution and arbitrary q;
6. Scattering from a dilute solution at zero scattering angle;
7. Scattering from non dilute solutions at zero scattering angle;
8. Scattering dependence on q for arbitrary concentration; and
9. Special topics.

The discussion of behavior at infinite dilution in the first three sections permits a significant simplification, with F(q,0) = 1. Thus, for the general case at infinite dilution, in which there may be a heterodispersity among the solute molecules in their molecular weight, composition and structure, but with all components comprising isotropic scattering elements may be expressed in the

form (suppressing the subscript "iso" for convenience until needed for discussions involving anisotropic scattering elements)

$$[\mathbf{R}(q,c)/c]^0 = K'\hat{n}_s^2(\partial\hat{n}/\partial c)_w^2 M_{LS}P_{LS}(q,0) \tag{15}$$

where the subscript LS denotes an averaging over heterodispersity appropriate for light scattering (or, indeed, x-ray or neutron scattering), the superscript 0 denotes the limiting value at infinite dilution, $\hat{n}$ is the refractive index, subscript s denotes the medium, the refractive index increment $(\partial\hat{n}/\partial c)_w$ is taken at constant weight fractions of the solvent components in the case of a mixed solvent, and $K' = 4\pi^2/N_A\lambda_0^4$, with λ_0 the wavelength of in the incident light in vacuum. It is assumed that $(\partial\hat{n}/\partial c)_w \neq 0$, except where noted otherwise. For scattering in the RGD regime from a system comprising a solvent and C components differing in some way (e.g., molecular weight, refractive index, etc.), with $\tilde{\psi}_{j,\nu}$ and $m_{j,\nu}$ the refractive index increment and the molecular weight, respectively, of the j-th element on the ν-th component, and n_ν is the number of elements in the ν-th component, with a component, comprising structures identical in composition, molecular weight and (statistical) structure, present at weight fraction w_ν:

$$M_{LS} = \tilde{\psi}^{-2}\sum_{\nu}^{C} w_\nu M_\nu^{-1}\{\sum_{j}^{n_\nu}\tilde{\psi}_{j,\nu}m_{j,\nu}\}^2 \tag{16}$$

$$P_{LS}(q,0) = \frac{\sum_{\nu}^{C} w_\nu M_\nu^{-1}\sum_{j}^{n_\nu}\sum_{k}^{n_\nu}\tilde{\psi}_{j,\nu}\tilde{\psi}_{k,\nu}\, m_{j,\nu}m_{k,\nu}\langle[\sin(q|r_{jk}|_\nu)]/q|r_{jk}|_\nu\rangle}{\sum_{\nu}^{C} w_\nu M_\nu^{-1}[\sum_{j}^{n_\nu}\tilde{\psi}_{j,\nu}m_{j,\nu}]^2} \tag{17}$$

$$\tilde{\psi} = (\partial\hat{n}/\partial c)_w = \sum_{\nu}^{C} w_\nu\tilde{\psi}_\nu \tag{18}$$

$$\tilde{y}_n = (\partial\hat{n}/\partial c_\nu)_w \tag{19}$$

where $M_\nu = \Sigma_j^{n_\nu} m_{j,\nu}$, $|r_{ij}|_\nu$ is the scalar separation of scattering elements i and j on the ν-th chain and, as usual, the brackets $\langle ... \rangle$ indicate an ensemble average [1, 27, 29, 49-51]. These expressions will be applied to an number of examples in the following, along with extensions required to account

for the presence of optically anisotropic scattering elements, or scattering for which the RGD approximation is not valid.

3. Scattering at infinite dilution and zero scattering angle

3.1 The basic relation

With the preceding, at zero scattering angle, $P_{LS}(q,0) = 1$, and the expressions given above a solute comprising isotropic scattering elements in the RGD reduce to the relation

$$M_{LS} = [\mathbf{R}(0,c)/c]^0/K'\hat{n}_s^2(\partial\hat{n}/\partial c)_w^2 \qquad (20)$$

A solute with anisotropic scattering elements or for conditions not in the RGD regime are discussed below. In the RGD limit for a solute comprising isotropic scattering elements, this expression may be evaluated as

$$M_{LS} = \tilde{\psi}^{-2}\sum_{\nu}^{C} w_\nu M_\nu^{-1}\{\sum_{j}^{n_\nu}\tilde{\psi}_{j,\nu}m_{j,\nu}\}^2 \qquad (21)$$

Expressions for M_{LS} are discussed in this section, starting with the simplest case of a solute comprising optically identical scattering elements in the RGD regime, and culminating in an example for which the RGD approximation may not be utilized.

3.2 Identical scattering elements

For a single solute comprising scattering elements all with the same refractive index so that $\tilde{\psi}_\nu = \tilde{\psi}$ independent of ν, but heterodisperse in molecular weight, as for a homologous series of a polymer, and remembering that $M_\nu = \sum_j^{n_\nu} m_{j,\nu}$, inspection the expression for M_{LS} in the RGD limit results in the well-known result

$$M_{LS} = \sum_{\nu}^{C} w_\nu M_\nu = M_w \qquad (22)$$

or $M_{LS} = M$ for a monodisperse solute.

If the system contains mixed solvent components, then preferential distribution of the solvent components in the vicinity of the polymer can complicate the analysis, but use of the refractive index increment $(\partial\hat{n}/\partial c_\nu)_\Pi$ determined at constant temperature, pressure and at osmotic equilibrium

of the solution and the solute-free solvent mixture (e.g., by dialysis) gives the simple result [26, 27]

$$M_{LS} = \frac{(\partial \hat{n}/\partial c)_{\Pi}^{2}}{(\partial \hat{n}/\partial c)_{w}^{2}} M_w \tag{23}$$

permitting evaluation of M_w from $[\mathbf{R}(0,c)/c]^0$. The ratio $(\partial \hat{n}/\partial c)_{\Pi}^{2}/(\partial \hat{n}/\partial c)_{w}^{2}$ provides a measure of the preferential solvation of the solute by a component of the solvent, with deviations from unity most prevalent when the preferentially solvating component is present at low concentration in the mixed solvent [26, 27, 52, 53]. Mixed solvents are often used in studies on polyelectrolytes, with low molecular weight salts added to increase the ionic strength of the solvent, and to screen electrostatic interactions among the charged solute molecules. It is sometimes necessary to resort to mixed organic solvents of uncharged polymers to achieve solubility.

3.3 Optically diverse scattering elements

To consider a solute disperse in composition, an instructive form of the expression for M_{LS} expression is obtained [20, 27, 54, 55] with the definitions $m_\nu = M_\nu/n_\nu$ and

$$\Delta m_{j,\nu} = m_{j,\nu} - m_\nu \tag{24}$$

$$\Delta \tilde{\psi}_{j,\nu} = \tilde{\psi}_{j,\nu} - \tilde{\psi}_\nu \tag{25}$$

such that $\Sigma_j \Delta m_{j,\nu} = \Sigma_j \Delta \tilde{\psi}_{j,\nu} = 0$,

$$M_{LS} = \tilde{\psi}^{-2} \sum_{\nu}^{C} w_\nu M_\nu^{-1} \{\tilde{\psi}_\nu M_\nu + \sum_{j}^{n_\nu} \Delta \tilde{\psi}_{j,\nu} \Delta m_{j,\nu})\}^2 \tag{26}$$

If either $\Delta \tilde{\psi}_{j,\nu}$ or $\Delta m_{j,\nu}$ are zero for all ν, as for a homologous series of chains heterodisperse in chain length, or blends of such chains, this expression simplifies to give

$$M_{LS} = \tilde{\psi}^{-2} \sum_{\nu}^{C} \tilde{\psi}_\nu^2 w_\nu M_\nu \tag{27}$$

For a system comprising two monomer units, such that $\tilde{\psi}_\nu$ takes on one of two values, $\tilde{\psi}_A$ or $\tilde{\psi}_B$, for the two scattering elements with molecular weights m_A and m_B, respectively, so that $\tilde{\psi} = w_A \tilde{\psi}_A + (1 - w_A)\tilde{\psi}_B$, M_{LS} may be written in the form

$$M_{LS} = (1 + 2\mu_1 Y + \mu_2 Y^2) M_w \tag{28}$$

where

$$Y = \frac{\tilde{\psi}_A - \tilde{\psi}_B}{\tilde{\psi}} \tag{29}$$

with (for n equal 1 or 2)

$$\mu_n = \sum_{\nu}^{C} w_\nu M_\nu \Delta w_\nu^n / M_w \tag{30}$$

$$\Delta w_\nu = w_{A\nu} - w_A = w_B - w_{B\nu} \tag{31}$$

where $w_{A\nu}$ and $w_{B\nu} = 1 - w_{A\nu}$ are the weight fractions of A and B in component ν, respectively, and w_A and $w_B = 1 - w_A$ are the weight fractions of types A and B, respectively, in the total sample. Consequently, in this case, M_{LS} is a parabolic function of Y, and evaluation of μ_1, μ_2 and M_w requires determination requires the determination of $[\mathbf{R}(0,c)/c]^0$ and $(\partial\hat{n}/\partial c)_w$ in at least three solvents differing in refractive index, but each a solvent for both of the blend components.

Obviously, this reduces to $M_{LS} = M_w$ for a homopolymer, as then $\tilde{\psi}_A = \tilde{\psi}_B$. Furthermore, this result also holds systems for which $\Delta w_\nu = 0$, such as random and alternating copolymers or regular block copolymers, with uniform structures among the molecules. It should be noted that M_w for the entire block copolymer is obtained, even though one of the blocks may be isorefractive with the solvent, and therefore not contribute to the observed scattering. More generally, if the composition is independent of molecular weight, then μ_1 vanishes, and μ_2, falling in the range $0 \le \mu_2 \le w_A w_B$, depends on the composition. Further examples have been discussed in detail [54], along with another, equivalent form of the μ_n, obtained from the preceding with the definition $M_{X,w} = w_X^{-1}\Sigma_\nu w_\nu w_{X,\nu} M_{X,\nu}$, where $M_{X,\nu} = w_{X,\nu} M_\nu$, and X is A or B. With this definition,

$$2\mu_1 = \{(1 - w_A)(M_w - M_{B,w}) - w_A(M_w - M_{A,w})\}/M_w \tag{32}$$

$$\mu_2 = w_A w_B (M_{A,w} + M_{B,w} - M_w)/M_w \tag{33}$$

For example, if $\tilde{\psi}_B = 0$, then $Y = 1/w_A$, and

$$M_{LS} = M_{A,w}/w_A \tag{34}$$

with a corresponding expression applicable if $\tilde{\psi}_A = 0$. The vertex of the parabola describing M_{LS} as a function of Y occurs with $Y = -\mu_1/\mu_2$ and, of course, $M_{LS} = M_w$ for $Y = 0$ ($\tilde{\psi}_A = \tilde{\psi}_B$).

The preceding parabolic form may also be developed for a blend of two homopolymers of type A and B, or to copolymers comprising monomers of type A and B, present at weight fractions w_A and $w_B = 1 - w_A$ with weight-average molecular weights $M_{A,w}$ and $M_{B,w}$, respectively, to give

$$2\mu_1 = w_A w_B (M_{A,w} - M_{B,w})/M_w \tag{35}$$

$$\mu_2 = w_A w_B(M_{A,w} + M_{B,w} - M_w)/M_w \quad (36)$$

As with the evaluation of M_{LS} for copolymers, application of this expression to determine M_w of a copolymer requires the determination of $[\mathbf{R}(0,c)/c]^0$ and $(\partial\hat{n}/\partial c)_w$ in at least three solvents differing in refractive index, but each a solvent for the copolymer. Experimental tests of these relations have been discussed [54].

3.4 Optically anisotropic scattering elements

The depolarized scattering in the RGD regime from a solute with anisotropic scattering elements may conveniently be expressed in the form [1, 20, 56, 57]:

$$[\mathbf{R}_{aniso}(0,c)/c]^0 = (1/15)K'(2\pi N_A)^2 \sum_{\nu}^{C} w_\nu M_\nu^{-1} \langle \gamma_\nu^2 \rangle \quad (37)$$

where $\langle \gamma_\nu^2 \rangle$ is the ensemble-averaged mean-square optical anisotropy per molecule, with polarizability components given by

$$\langle \gamma_\nu^2 \rangle = \{(3/2)[(\alpha_{11} - \alpha_{22})^2 + (\alpha_{11} - \alpha_{33})^2 + (\alpha_2 - \alpha_{33})^2] + 3[\alpha_{12}^2 + \alpha_{13}^2 + \alpha_{23}^2]\}_\nu \quad (38)$$

For isotropic scatters, $\alpha_{ij} = (\alpha_{iso}/3)\delta_{ij}$, and $\langle \gamma_\nu^2 \rangle = 0$, so that in that case, $[\mathbf{R}_{aniso}(0,c)/c]^0 = 0$. As elaborated below, to a very good approximation, this is the usual case for high molecular weight flexible chain polymers. Detailed evaluation of $\langle \gamma^2 \rangle$ has been given for some polymers in the frame of the rotational isomeric state model [25]. A useful simplification arises for polymers with identical cylindrically symmetric polarizabilities for all chain elements, in which case (for $(\partial\hat{n}/\partial c)_w \neq 0$) Equation 38 may be put in the form

$$M_{LS,aniso} = \{[\mathbf{R}_{aniso}(0,c)/c]^0/K'\hat{n}_s^2(\partial\hat{n}/\partial c)_w^2\} = (3/5)M_w\delta_{LS}^2 \quad (39)$$

$$\delta_{LS}^2 = M_w^{-1} \sum_{\nu}^{C} w_\nu M_\nu \delta_\nu^2 \quad (40)$$

where δ_ν^2 is given by

$$\delta_v^2 = \frac{\delta_0^2}{n_v} \sum_j^{n_v} \sum_k^{n_v} (3/2)[\langle \cos^2 \beta_{ij} \rangle - 1] \quad (41)$$

where β_{ij} is the angle between the major axes associated with scattering elements i and j on a chain with n_v elements, each with molecular weight m_0. Here, $\langle ... \rangle$ indicates an ensemble average, and δ_0 is given by

$$\delta_0 = \frac{\alpha_\parallel - \alpha_\perp}{\alpha_\parallel + 2\alpha_\perp} \quad (42)$$

where $\alpha_\parallel$ and $\alpha_\perp$ are the principal polarizabilities of the scattering elements. Two limiting cases for chain molecules may be considered: a rodlike chain, with $\beta_{ij} = 0$ for all i and j, so that $\delta_v = \delta_0$, and a random coil with uncorrelated orientations among the scattering elements, such that only terms with i = j contribute to the double sum, giving $\delta_v = \delta_0/n_v = m_0\delta_0/M_v$. For these cases:

rod: $$M_{LS,aniso} = (3/5)\delta_0^2 M_w \quad (43)$$

coil: $$M_{LS,aniso} = (3/5)\delta_0^2 m_0 \quad (44)$$

so that the overall molecular weight is not reflected in $M_{LS,aniso}$ for the random coil chain even if δ_0 approaches its maximum value of unity. For a solute with a distribution of M, the values of $M_{LS,Hv}$ and $M_{LS,Vv}$ determined from $(R_{Hv}(0,c)/c)^0$ and $(R_{Vv}(0,c)/c)^0$, respectively, are given by

$$M_{LS,Hv} = (3/5)\delta_{LS}^2 M_w \quad (45)$$

$$M_{LS,Vv} = \{1 + (4/5)\delta_{LS}^2\} M_w \quad (46)$$

with δ_{LS}^2 expressed above in terms of δ_v^2 and the molecular weight distribution. One model that provides a crossover between rod and coil chain limits is that for the wormlike chain, with persistence length â, contour length L and mass per unit length $M_L = M/L$. For this chain,

$$\delta_v^2/\delta_0^2 = (2Z_v/3)\{1 - (Z_v/3)[1 - \exp(-3Z_v^{-1})]\} \quad (47)$$

where $Z_\nu = \hat{a}/L_\nu$. A numerically equivalent result may be obtained for the freely rotating chain model with fixed valence angles between bonds [20]. Inspection of Equation 47 shows that that δ_ν^2/δ_0^2 decreasing from unity for $L_\nu/\hat{a} << 1$ (rodlike) to approach $2\hat{a}/3L_\nu$ for $L_\nu/\hat{a} >> 1$ (coil like). An example of δ_{LS}^2/δ_0^2 as a function of $L_w/\hat{a}$ for a sample hetereodisperse in L may be seen in Figure 1 [1].

<<Figure 1>>

3.5 Scattering beyond the RGD regime.

Although the preceding based on the use of the RGD approximation will almost always be adequate for (nonabsorbing) threadlike molecules, such as flexible or semiflexible coils, rodlike or helical chains, etc, owing to sparse density of scatters in an "intramolecular" domain, that approximation may fail for particles if they are large enough, depending on the refractive index of the solvent in which they are dispersed. Although the scattering for a number of particle shapes has been treated [1, 13, 19, 21, 23, 33, 58, 59], usually requiring numerical evaluation of the results, in this chapter attention is focused on he Mie theory describing the scattering for spherical solute beyond the RGD approximation. Two parameters are critical in evaluating the crossover from scattering for which the RGD approximation may be used, and that for which the Mie theory is required: $\tilde{\alpha} = 2\pi R/\lambda$, with R the sphere radius, and $\tilde{n} = \hat{n}_{solute}/\hat{n}_{medium}$. As mentioned above, the complexity arises from the fact that unlike the case with the RGD approximation, the scattering from a particle may no longer be taken as a sum over independent Rayleigh scatters. Evaluation of M_{LS} for homogeneous spheres may be accomplished within the Mie theory by the introduction of two functions, a function $h_{sph}(\tilde{n}) = 3(\tilde{n} + 1)/2(\tilde{n}^2 + 2)$ used to define a modified $\tilde{\psi}$, equal to $h_{sph}(\tilde{n})\tilde{\psi}$, in the calculation of M_{LS} from the experimental observations, and another function $m_{sph}(\tilde{n},\tilde{\alpha})$ appearing in the ratio between M_{LS} (calculated with the modified $\tilde{\psi}$) and the true molecular weight. Thus, for a system of nonabsorbing spheres polydispersed in size and with the same $\tilde{n}$ and particle shape, the Mie theory gives

$$M_{LS} = \sum_{\nu}^{C} w_\nu M_\nu [m_{sph}(\tilde{n},\tilde{\alpha}_\nu)]^2 \geq M_w \qquad (48)$$

Analytic expressions are available for $m_{sph}(\tilde{n},\tilde{\alpha})$, and these find use in a variety of applications. A plot of $M_{LS}/M = [m_{sph}(\tilde{n},\tilde{\alpha})]^2$ as a function of $\tilde{n} - 1$ for monodispersed spheres with several values of α is shown in Figure 2 [1]. The dashed lines in that figure correspond to an approximation to $m_{sph}(\tilde{n},\tilde{\alpha}_v)$ based on an expansion for small $\tilde{\alpha}^2|\tilde{n} - 1|$:

$$m_{sph}(\tilde{n},\tilde{\alpha}) = 1 + j_{sph}(\tilde{n})\,\tilde{\alpha}^2|\tilde{n} - 1| + \ldots \quad (49)$$

$$j_{sph}(\tilde{n}) = (\tilde{n} + 1)(\tilde{n}^4 + 27\tilde{n}^2 + 38)/[15(\tilde{n}^2 + 2)(2\tilde{n}^2 + 3) \quad (50)$$

As may be seen in Figure 2, this expression provides a useful approximation to M_{LS}/M provided $\tilde{\alpha}^2|\tilde{n} - 1| < 0.1$ and $\tilde{\alpha} < 1$. An iterative process is needed in using Figure 2 to determine M from the light scattering data, to insure consistency between the value of M deduced from the ratio M_{LS}/M and the value of $R = (3M/4\pi\rho M)^{1/3}$ used to compute $\tilde{\alpha}$.

<<Figure 2>>

The deviations of M_{LS}/M from unity seen in Figure 2 can have important impact on, for example, the use of a light scattering detector to study the effluent in a chromatographic separation to determine the size distribution of a polydisperse sample of spheres. As implied by the inequality given above, M_{LS} does not correspond to any of the usually defined molecular weight averages, nor to any single average over a wide range in $\tilde{\alpha}$ and $\tilde{n}$. For the range of small $\tilde{\alpha}^2|\tilde{n} - 1|$ discussed above for the expansion of $m_{sph}(\tilde{n},\tilde{\alpha})$ (for particles with a homogeneous refractive index),

$$M_{LS} \approx M_w[1 + 2(2\pi R/\lambda M^{1/3})^2 M_z^{2/3} j_{sph}(\tilde{n})] \quad (51)$$

(where $2\pi R/\lambda M^{1/3}$ is independent of M). In principle, the dependence of M_{LS} on λ incorporated in the preceding expressions provides a means analyze M_{LS} as a function of λ to determine the size distribution, and methods of this type have been proposed [23, 30, 60]. They have, however, been largely superceded by methods involving measurements of the scattering as a function of q. Finally, it may be noted that much of the literature on the Mie theory for nonabsorbing spheres at infinite dilution is cast in terms of the extinction efficiency $Q_{sca}(\tilde{n},\tilde{\alpha})$, where $\pi R^2 Q_{sca}(\tilde{n},\tilde{\alpha})$ is the turbidity τ of the sample (e.g., the fraction of light transmitted by a sample with thickness b and

concentration ν is $\exp(-\tau b\nu)$). For example, in terms of $Q_{sca}(\tilde{n},\tilde{\alpha})$, for a monodisperse sample of spheres with $\tilde{n} > 1.4$ and $\tilde{\alpha} > 4$,

$$M_{LS} \approx M\{3Q_{sca}(\tilde{n},\tilde{\alpha})/4\tilde{\alpha}^2(\tilde{n}-1)h_{sph}(\tilde{n})\}^2 \tag{52}$$

In the so-called Fraunhofer scattering regime discussed below ($\tilde{\alpha} >> 1$ and $\tilde{n} > 1.1$), $Q_{sca}(\tilde{n},\tilde{\alpha})$ tends to 2, leading to simpler expressions sometimes exploited in analytical applications [21, 61-66].

Although much of the available literature refers to the Mie theory for spheres studies are available on a nonspherical particles, for which the expression given above for spheres may be modified to read

$$M_{LS} = \sum_{\nu}^{C} w_\nu M_\nu [m(\tilde{n},\lambda,M_\nu)]^2 \tag{53}$$

where the function $m(\tilde{n},\lambda,M_\nu)$ is specific for each particle shape [1, 13, 19, 21, 23, 33, 58, 59].

4. Scattering at infinite dilution and small q

4.1 The basic relation

Expansion of the ensemble average in $P_{LS}(q,0)$ given above for small q for the expression in the RGD regime gives

$$P_{LS}(q,0) = 1 - (1/3)q^2R_{G,LS}^2 + \ldots \tag{54}$$

$$R_{G,LS}^2 = \frac{\sum_{\nu}^{C} w_\nu M_\nu^{-1} \sum_{j}^{n_\nu}\sum_{k}^{n_\nu} \tilde{\psi}_{j,\nu}\tilde{\psi}_{k,\nu}\, m_{j,\nu}m_{k,\nu}\langle|r_{jk}|_\nu^2\rangle}{2\sum_{\nu}^{C} w_\nu M_\nu^{-1}[\sum_{j}^{n_\nu}\tilde{\psi}_{j,\nu}m_{j,\nu}]^2} \tag{55}$$

Following the order in the preceding, expressions for $R_{G,LS}^2$ are discussed in the following, starting with the simplest case of a solute comprising optically identical scattering elements in the RGD regime, and culminating in an example for which the RGD approximation may not be utilized.

4.2 Identical scattering elements

Specialization to the important case with m_i and $\tilde{\psi}_i$ the same for all scattering elements, as for a homologous series of a homopolymer, leads to considerable simplification:

$$R^2_{G,LS} = \frac{1}{M_w}\sum_{\nu}^{C} w_\nu M_\nu R^2_{G,\nu} \tag{56}$$

$$R^2_{G,\nu} = \frac{1}{2n_\nu^2}\sum_{j}^{n_\nu}\sum_{k}^{n_\nu} \langle |r_{jk}|^2_\nu \rangle \tag{57}$$

with $R^2_{G,\nu}$ the mean-square radius of gyration for the ν-th component; here components may differ in molecular weight and/or structure. Expressions for $R^2_{G,\nu}$ for a few specific models that are often encountered are tabulated in Table 1. One can often (but not always) express $R^2_{G,\nu}$ in a power-law to facilitate calculation of $R^2_{G,LS}$ for samples heterodisperse in molecular weight:

$$R^2_{G,\nu} = (R^2_G/M^\varepsilon)M^\varepsilon_\nu \tag{58}$$

where R^2_G/M^ε is a constant for the monodispersed solute, e.g., $R^2_G/M = \hat{a}/3M_L$ or $R^2_G/M^2 = 1/12M^2_L$ for the random-flight and rod models, respectively, with $M_L = M/L$ and $\hat{a}$ the persistence length. Theoretical considerations can assign the constant (R^2_G/M^ε) and a value to ε for a variety of models, e.g., 2/3 for a sphere, 1 for a random-flight coil chain, 7/6 for a flexible chain with full excluded volume, and 2 for a rodlike chain. With this power-law representation, $R^2_{G,LS}$ may then be evaluated to give the results presented in Table 2; as may be seen, a special notation is introduced for averages involving non-integral ε [67]. Although the use of dynamic light scattering to determine the light-scattering averaged hydrodynamic radius $R_{H,LS}$ is not discussed in this chapter, in the interests of completeness, expressions are given for $R_{H,LS}$ for the special case $R_{H,\nu} = (R_H/M^\varepsilon)M^\varepsilon_\nu$ using the expression (for a homologous series of a homopolymer)

$$R^2_{H,LS} = M_w/\sum_{\nu}^{C} w_\nu M_\nu R^{-1}_{H,\nu} \tag{59}$$

Because of the appearance of M_z in the expression for $R^2_{G,LS}$ for a random coil chain, $R^2_{G,LS}$ is often referred to as a "z-average" value, but inspection of the Table 2 shows the limitations of this designation.

<<Table 1>>

<<Table 2>>

The wormlike chain with persistence length â and contour length L is not represented in Table 2, as for that model the expressions for R_G^2 for monodisperse solute does not reduce to a power law, except for the coil or rod extremes with small or large â/L, respectively. Thus, inspection of the expression in Table 1 shows that R_G^2 for the persistent chain reduces to power-laws $R_G^2 = âL/3$ or $R_G^2 = L^2/12$ for $â/L << 1$ (coil limit) or $â/L >> 1$ (rod limit), respectively, with a crossover between these two limiting forms for $â/L \approx 1$. Consequently, $R_{G,LS}^2$ varies from proportionality to M_z or M_zM_{z+1} in these extremes. If it assumed that the well-known Schulz-Zimm (two-parameter exponential) distribution of M may be applied, then $R_{G,LS}^2$ may be evaluated for cases that do not result in forms based on the standard molecular weight averages (M_n, M_w, M_z, etc.). For example, for the persistent coil model use of that distribution function gives [67],

$$R_{G,LS}^2 = (L_z â/3)S_{LS}(â/L_z) \tag{60}$$

$$S_{LS}(Z_z) = 1 - 3Z_z + 6Z_z^2\frac{h+2}{h+1} - 6Z_z^3\frac{(h+2)^2}{h(h+1)^2}\{1 - [1 + (Z(_zh + 2))^{-1}]^{-h}\} \tag{61a}$$

$$\approx [1 + 4Z_z(h + 2)/(h + 3)]^{-1} = [1 + 4â/L_{z+1}]^{-1} \tag{61b}$$

where $Z_z = â/L_z$;. As expected, this result ranges from $R_{G,LS}^2 = L_zL_{z+1}$ for $â/L_z >> 1$ (rod limit) to $R_{G,LS}^2 = âL_z/3$ for r $â/L_z << 1$ (coil limit), with the crossover between these two limits seen for $â/L_z \approx 1$. Moreover, the final Padé approximation with $R_{G,LS}^2 \approx (L_zâ/3)[1 + 4â/L_{z+1}]^{-1}$ obtained using the Schulz-Zimm distribution in M provides the correct limits for large or small $â/L_z$, and might be expected to apply as well with other distributions in M.

The expressions for the random-flight chain in Tables 1 and 2 and its limitations for flexible chain polymers requires some comment. The random-flight model is based on the assumptions that excluded volume interactions are suppressed (as under Flory theta conditions, with $A_2 = 0$) and that the ensemble averaged mean square separation $\langle r_{ij}^2 \rangle$ of scattering elements i and j is proportional to $|i - j|$, requiring very large L, even for a flexible chain [5, 12, 20, 25, 27, 29, 37, 44, 45]; it may be noted that for practical purposes, the determination of R_G^2 by light scattering tends to be limited to larger L in any case, to achieve sufficiently large $u \propto R_G^2/\lambda^2$, but that limitation is relaxed to permit determinations of R_G^2 for smaller L with scattering using radiation with smaller wavelength (e.g., neutron or x-ray scattering). The effects of the assumption that $\langle r_{ij}^2 \rangle \propto |i - j|$ has been examined

within models eliminating this approximation, so that, for example, the true value of R_G^2 may no longer equal âL/3 for smaller L . These models include the rotational-isomeric-state (RIS) model with an atomistic representation of the polymer chain [25], and the more coarse-grained helical-wormlike chain (HW) model [5]. With both models, the deviation of R_G^2/L at low L from its constant value at large L may be adequately represented. The HW model introduces an additional parameter in comparison with those for the wormlike chain, and the RIS model requires a realistic potential for bond rotations, including the effects of the rotational state of nearby bonds. The original version of the RIS model, with bond rotation potentials assumed to be independent of the rotational state of neighboring bonds, exhibits dependence of R_G^2/L on L at low L [5, 25, 37, 68], but cannot capture realistic behavior owing to the inadequacy of the assumed independent bond rotation potentials.

The effects of excluded volume interactions become increasingly important with increasing L for systems for which $A_2 > 0$; in so-called "good solvents", the ratio A_2M^2/R_G^3 of the "thermodynamic volume" per mol A_2M to the geometric volume per mole R_G^3/M tends to a constant at large L [12, 27, 29, 45, 69-71]. The effects of excluded volume interactions are usually embodied in the expansion factor α, defined as

$$\alpha^2 = R_G^2/R_{G,0}^2 \tag{62}$$

where $R_{G,0}^2 = âL/3$ for large L; as seen below, $\alpha \approx 1$ for small L. With the so-called "two-parameter" treatments of α and A_2 for flexible chains,

$$\alpha^5 - \alpha^3 = a_1 z h(â/L,z) \tag{63}$$

$$A_2 = A_2^{(R)} a(â/L,z) \tag{64a}$$

where

$$A_2^{(R)} = (\pi N_A/4M_L^2)\, d_{Thermo} \tag{64b}$$

$$z = (3d_{Thermo}/16â)\,(3L/\pi â)^{1/2} \tag{64c}$$

$$a(â/L, z) \approx \{1 + b_1(â/L)\, z/\alpha^3\}^{-1} \tag{64d}$$

Both h(â/L,z) and a(â/L,z) are unity for z = 0, $M_L = M/L$ and $A_2^{(R)}$, the value of A_2 that would obtain if the chain were rodlike, is proportional to the binary cluster integral [12, 29, 44, 45, 70]. In the limits of small â/L (coil conformation), the dependence on â/L is suppressed, whereas for large â/L (rodlike chain), α and a(â/L, z) tend to unity for any z. The thermodynamic diameter d_{Thermo} of the

chain a measure of the length scale of the segmental interactions, reducing to zero at the Flory theta temperature Θ (for which $A_2 = 0$). To a good approximation [45], for small â/L, $a(\hat{a}/L,z) \approx \{1 + b_1 z/\alpha^3\}^{-1}$, $b_1 \approx 2.865$ and for linear flexible chains (â/L << 1) $a_1 = 134/105$ and h(â/L,z) tends to the constant $A_2M^2/4\pi^{3/2}N_AR_G^3$ for large z [45, 70, 72]. At the present time, it is beyond the scope of theory to provide reliable estimates of $A_2^{(R)}$, despite an interesting proposal to base estimates on the properties of small molecule mixtures [73]. However, d_{Thermo} increases from zero at the Flory Theta temperature to become about equal to the geometrical chain diameter d_{geo} for chains interacting through a hard-core repulsive potential, and can be much larger than d_{geo} for polyelectrolyte chains. With h(â/L,z) a constant for large z, $\alpha^2 \propto z^{2/5} \propto (L/\hat{a})^{1/5}$, and as a consequence, $R_G^2/\hat{a}^2 = (L/\hat{a})\alpha^2/3 \propto (L/\hat{a})^{6/5}$. For the scattering regime of usual interest in light scattering, it usually adequate to use the random-flight expression for P(q,0), with the value $R_G^2 =$ âL/3 appearing therein replaced by $\hat{a}L\alpha^2/3$.

Although it is beyond the scope here, it should be noted that the wormlike chain model can also be adapted to include excluded volume interactions, in which case both a_1 and $b_1$are replaced by functions of â/L, and z is replaced by a similar parameter that includes an additional function of â/L [45, 74-76].

In addition to the expressions listed in Table 1, R_G^2 has been derived for a wide range of branched chain structures for the random-flight model, including comb and star shaped molecules, randomly branched chains and hyperbranched structures [22, 77, 78]. For example, detailed expressions for R_G^2 for regular star- and comb-shaped branched chains within the random-flight approximation can be approximated very well by the simple expression [45, 79]

$$R_G^2 = gR_{G,LIN}^2 \quad (65)$$

$$g = \lambda_{br} + g_{star}(1 - \lambda_{br})^{7/3} \quad (66)$$

where $R_{G,LIN}^2$ refers to a linear chain of the same M as the branched molecule, f is the number of branches, $g_{star} = (3f - 2)/f^2$, and λ_{br} is the ratio of the mass in the branches to that in the backbone, i.e., $\lambda_{br} = 0$ for a star-shaped molecule, and $\lambda_{br} = 1$ for a linear chain. The parameters a_1 and b_1 introduced above in Equations 63 and 64, respectively, have been computed for comb and star-shaped branched polymers [45, 78, 80, 81]

4.3 Optically diverse scattering elements

As would be anticipated from the expression given above for $R^2_{G,LS}$, the evaluation of $R^2_{G,LS}$ for structures with m_i and $\tilde{\psi}_i$ differing among the scattering elements is complex, even for a copolymer for which all chains have the same molecular weight and composition, allowing only for variation in the sequence of the scattering elements among the chains (or in a particles), e.g., a block or alternating copolymer, stratified particles, etc ., such that Equation 55 reduces to

$$R^2_{G,LS} = \frac{\sum_{\nu}^{C} \sum_{j}^{n_\nu} \sum_{k}^{n_\nu} \tilde{\psi}_{j,\nu}\tilde{\psi}_{k,\nu}\, m_{j,\nu}m_{k,\nu}\langle|r_{jk}|^2_\nu\rangle}{2[\sum_{\nu}^{C} \sum_{j}^{n_\nu} \tilde{\psi}_{j,\nu}m_{j,\nu}]^2} \tag{67}$$

Restricting further to the special case of only two scattering elements, A and B, and making use of the relations $w_A = 1 - w_B = n_A m_A/(n_A m_A + n_B m_B)$ and $\tilde{\psi} = w_A\tilde{\psi}_A + w_B\tilde{\psi}_B$,

$$R^2_{G,LS} = \tilde{\psi}^{-2}\{w^2_A\tilde{\psi}^2_A R^2_{G,A} + w^2_B\tilde{\psi}^2_B R^2_{G,B} + 2w_A w_B\tilde{\psi}_A\tilde{\psi}_B R^2_{G,AB}\} \tag{68}$$

$$R^2_{G,AB} = [R^2_{G,A} + R^2_{G,B} + \Delta^2_{AB}]/2 \tag{69}$$

Here, Δ^2_{AB} is the mean-square separation of the centers of gravity of the structures comprising only A or B units, and

$$R^2_{G,\nu} = \frac{1}{2n^2_\nu}\sum_{j}^{n_\nu} \sum_{k}^{n_\nu} \langle|r_{jk}|^2_\nu\rangle \tag{70}$$

for ν equal to either A or B, with, for example, only the type A elements being considered in the sum for $R^2_{G,A}$, i.e., $R^2_{G,A}$ is the value of $R^2_{G,LS}$ for conditions with $\tilde{\psi}_B = 0$, etc. A further simplification in form is made using the definition $\tilde{w}_A = 1 - \tilde{w}_B = w_A\tilde{\psi}_A/\tilde{\psi}$, to give

$$R^2_{G,LS} = \tilde{w}_A R^2_{G,A} + (1 - \tilde{w}_A)R^2_{G,B} + \tilde{w}_A(1 - \tilde{w}_A)\Delta^2_{AB} \tag{71}$$

This expression may be used, for example, for copolymers or stratified spheres, etc. [30, 54, 55, 82]. In applying this expression, it is assumed that $R^2_{G,A}$, $R^2_{G,B}$ and Δ^2_{AB} do not depend on the solvent; this may be reasonable with particles, such as stratified spheres, but can compromise the interpretation of data on flexible chain polymers, which are susceptible to excluded volume effects, or even collapse of one component in certain block copolymers. For copolymers with either random or strictly alternating placements of the A and B units, $\Delta^2_{AB} = 0$. By contrast, for a block copolymer Δ^2_{AB} may be comparable to $R^2_{G,A}$ and $R^2_{G,B}$. For example, with a block copolymer with a random-flight chain conformation, and with N each of A and B blocks, $\Delta^2_{AB} = 2(R^2_{G,A} + R^2_{G,B})/N$. Consequently, Δ^2_{AB} tends to zero for large N, as for an alternating copolymer, but Δ^2_{AB} cannot be neglected for a diblock copolymer (N = 1). Values of Δ^2_{AB} are available for a few additional model structures [54, 55]. It is important to note that since x may be positive, negative or zero, $R^2_{G,LS}$ may also take on positive, negative or zero values, in distinction from the geometric mean square radius of gyration $R^2_{G,geo}$, which must be positive. Thus, for $R^2_{G,geo}$, the dependence on $\tilde{\psi}_A$ and $\tilde{\psi}_B$ is suppressed, and for copolymers with a random-flight conformation,

$$R^2_{G,geo} = w_A R^2_{G,A} + (1 - w_A) R^2_{G,B} + w_A(1 - w_A)\Delta^2_{AB} \tag{72}$$

by comparison with $R^2_{G,LS}$ given above.

For a stratified spherical structure with a shell (or coating) surrounding a spherical core, $\Delta_{AB} = 0$, and for monodispersed solute, with outer diameter R_B and inner core diameter $R_A < R_B$,

$$R^2_{G,LS} = (3/5)\left(\tilde{w}_A R^2_A + (1 - \tilde{w}_A)\frac{R^5_B - R^5_A}{R^3_B - R^3_A}\right) \tag{73}$$

where $\tilde{w}_A$ and $\tilde{w}_B = 1 - \tilde{w}_A$ are calculated, respectively, using the weight fractions w_A in the core and $w_B = 1 - w_A$ in the shell [30]. For a thin shell enclosing the solvent, such that $\tilde{w}_A = 0$, as might be appropriate for some solvent-filled spherical micelles , this expression reduces to

$$R^2_G = (3/5)R^2_B\left(\frac{1 - [1 - (\Delta_{shell}/R_B)^5]}{1 - [1 - (\Delta_{shell}/R_B)^3]}\right) \tag{74}$$

where $\Delta_{shell} = (R_B - R_A)$. The ratio of the volume of the shell to its surface area may be expressed as [1, 7, 83, 84]

$$v_2M/N_A = 4\pi R_B^2\Delta_{shell}\{1 - (\Delta_{shell}/R_B) - ((\Delta_{shell}/R_B)^2\} \quad (75)$$

with specific volume v_2 of the shell. Thus, for a thin shell, with $\Delta_{shell}/R_B << 1$, combination of these expressions to present Δ_{shell} in terms of the experimental parameters R_G^2, M and v_2 gives

$$\Delta_{shell} \approx (v_2M/4\pi N_A R_G^2)\{1 + (1.3)\beta^2 + 0.06\beta^3 + \ldots\}^{-1} \quad (76)$$

where $\beta = v_2M/4\pi N_A(R_G^2)^{3/2}$, providing a means to determine Δ_{shell} by light scattering measurements, even though $\Delta_{shell} << \lambda$.

Expressions for R_G^2 are available for other of hollow particle shapes [30, 85, 86].

4.4 Optically anisotropic scattering elements

The restriction to optically isotropic scattering elements may be relaxed to give

$$[\mathbf{R}_{Hv}(q,c)/c]^0 = K'\hat{n}_s^2(\partial\hat{n}/\partial c)_w^2M_{LS,Hv}P_{LS,Hv}(q,0) \quad (77)$$

$$[\mathbf{R}_{Vv}(q,c)/c]^0 = K'\hat{n}_s^2(\partial\hat{n}/\partial c)_w^2M_{LS,Vv}P_{LS,Vv}(q,0) \quad (78)$$

for a homologous homopolymer comprising scattering elements with cylindrical symmetry, where $M_{LS,Vv}$ and $M_{LS,Hv}$ are discussed in the preceding section on scattering at infinite dilution and zero scattering angle, and

$$P_{LS,Hv}(q,0) = 1 - (3/7)R_{G,LS,Hv}^2q^2 + \ldots \quad (79)$$

$$P_{LS,Vv}(q,0) = 1 - (1/3)R_{G,LS,Vv}^2q^2 + \ldots \quad (80)$$

with

$$R_{G,LS,Hv}^2 = \frac{\sum_{\nu}^{C} w_\nu M_\nu \delta_\nu^2 f_{3,\nu}^2 R_{G,\nu}^2}{\sum_{\nu}^{C} w_\nu M_\nu \delta_\nu^2} \quad (81)$$

$$R_{G,LS,Vv}^2 = \frac{\sum_{\nu}^{C} w_\nu M_\nu (1 + 4\delta_\nu^2/5) J(\delta_\nu) R_{G,\nu}^2}{\sum_{\nu}^{C} w_\nu M_\nu (1 + 4\delta_\nu^2/5)} \quad (82)$$

where $R^2_{G,\nu}$ is given in Table 1. It may be noted that the expressions for $[\mathbf{R}_{Vv}(q,c)/c]^0$ and $[\mathbf{R}_{Hv}(q,c)/c]^0$ require that $[\mathbf{R}_{cross}(q,c)/c]^0$ is not zero unless q = 0, with $[\mathbf{R}_{cross}(q,c)/c]^0 \propto q^2$ for small q. For the persistent coil model,

$$J(\delta_\nu) = \frac{1 - (4/5)f_{1,\nu}\delta_\nu + (4/7)(f_{2,\nu}\delta_\nu)^2}{1 + (4/5)\delta_\nu^2} \tag{83}$$

with the parameters $f_{i,}$ shown in Figure 3 as functions of L/â [20]. As may be seen, these parameters all unity for small L/â < 1(rod limit), and decrease essentially proportionally to â/L for L/â > 3 as the conformation approaches the coil limit. Consequently, in the latter regime, $J(\delta_\nu) \approx 1$, and the expression for $R^2_{G,LS,Vv}$ reduces to that with isotropic scattering elements. In the opposite limit with $\delta_\nu \approx \delta_0$ as for L/â << 1 (rod limit), all of the $f_{i,\nu}$ approach unity. An example of $R^2_{G,LS,Vv}$ divided by the expression $L_z L_{Z+1}/12$ appropriate in the rodlike limit for a sample heterodisperse in L is shown in Figure 1. In a practical sense, for the use of these expressions coupled with experimental δ^2_{LS}, the values of δ^2_{LS} will be so small if the chain is not nearly rodlike that one can set all of the f_i equal to unity with negligible effect.

<<Figure 3>>

A complication can occur if the optically anisotropic polymer is also chiral, as that may introduce rotations of the polarization states of both incident and scattered beams, complicating the analysis. Mention is made at the close of the next section of the scattering from particles comprising anisotropic scattering elements.

4.5 Scattering beyond the RGD regime

The preceding expressions must be modified if the RGD approximation fails. For compositionally homogeneous scatters, the results may be cast in the form [1]

$$R^2_{G,LS} = \frac{\sum_\nu^C w_\nu M_\nu y(\tilde{n},\lambda,M_\nu)[m(\tilde{n},\lambda,M_\nu)]^2 R^2_{G,RGD,\nu}}{\sum_\nu^C w_\nu M_\nu [m(\tilde{n},\lambda,M_\nu)]^2} \tag{84}$$

where $R^2_{G,RGD,\nu}$ is the mean-square radius of gyration that would be computed for the RGD formulation, $m(\tilde{n},\lambda,M_\nu)$ is defined above in the discussion of M_{LS} and $y(\tilde{n},\lambda,M_\nu)$ is an additional function of the same variables, with $y(\tilde{n},\lambda,M_\nu)$ tending to unity as the RGD conditions are approached. For homogeneous spheres, the Mie scattering theory may be adopted, to give

$$R^2_{G,LS} = (3/5)\frac{\sum_{\nu}^{C} w_\nu M_\nu [m_{sph}(\tilde{n},\tilde{\alpha}_\nu)]^2 y_{sph}(\tilde{n},\tilde{\alpha}_\nu) R^2_\nu}{\sum_{\nu}^{C} w_\nu M_\nu [m_{sph}(\tilde{n},\tilde{\alpha}_\nu)]^2} \tag{85}$$

where the functions $y_{sph}(\tilde{n},\tilde{\alpha}_\nu)$ and $m_{sph}(\tilde{n},\tilde{\alpha}_\nu)$ may be evaluated using the Mie theory [1, 23, 30, 33, 59]. The result for a monodisperse solute, given in Figure 4, reveals a very complex behavior as a function of $\tilde{\alpha} = 2\pi R/\lambda$ and $\tilde{n}$, with oscillations in R^2_G/R^2 as a function of $\tilde{\alpha}$ dominant for larger $\tilde{n}$. Although these oscillations would tend to smooth for a solute heterodisperse in R, complicated behavior may still be expected. Similar treatments have been applied with other spherically symmetric structures, including stratified spheres [87-90].

<<Figure 4>>

5. Scattering at infinite dilution and arbitrary q

5.1 The basic relation

The intramolecular (intraparticle) scattering form factor P(q,0) given by Equation 17 in the RGD regime, is reproduced here for convenience,

$$P_{LS}(q,0) = \frac{\sum_{\nu}^{C} w_\nu M_\nu^{-1} \sum_{j}^{n_\nu}\sum_{k}^{n_\nu} \tilde{\psi}_{j,\nu}\tilde{\psi}_{k,\nu}\, m_{j,\nu}m_{k,\nu}\langle[\sin(q|r_{jk}|_\nu)]/q|r_{jk}|_\nu\rangle}{\sum_{\nu}^{C} w_\nu M_\nu^{-1}[\sum_{j}^{n_\nu}\tilde{\psi}_{j,\nu}m_{j,\nu}]^2} \tag{17}$$

This expression has been calculated for a wide variety of structures. Most of these models tend to be coarse-grained representations of the solute structure, in keeping with the length scale given by

q^{-1} for light scattering; more detailed atomistic models would be appropriate, for example, for the q–range sampled by wide angle neutron and x-ray scattering.

Following the order in the preceding, expressions for $P_{LS}(q,0)$ are discussed in the following, starting with the simplest case of a solute comprising optically identical scattering elements in the RGD regime, and culminating in an example for which the RGD approximation may not be utilized.

5.2 Identical scattering elements

Turning first to the important case with m_i and $\tilde{\psi}_i$ the same for all scattering elements, as for a homologous series of a homopolymer (or particles), the expression given above for examples for $P_{LS}(q,0)$ may be simplified to read:

$$P_{LS}(q,0) = \frac{1}{M_w} \sum_{\nu}^{C} w_\nu M_\nu P_\nu(q,0) \tag{86}$$

$$P_\nu(q,0) = \frac{1}{n_\nu^2} \sum_{j}^{n_\nu} \sum_{k}^{n_\nu} \langle [\sin(q|r_{jk}|)/q|r_{jk}|\rangle \tag{87}$$

Tables of expressions for P(q,0) for a wide range of polymer and particle structures are available, some of which are elaborated in the following [22, 30].

Calculations of P(q,0) in the RGD approximation often employ an integral form of the expression for $P_\nu(q,0)$, using a continuous chain model with a chain of contour length L comprising optically isotropic scattering elements [5, 91], such that (suppressing the subscript ν for convenience when considering a monodisperse solute):

$$P(q,0) = (2/L^2)\int_0^L (L - x)\, \tilde{g}(\mathbf{q},x)\, dx \tag{88}$$

where $\tilde{g}(\mathbf{q},x)$ is the Fourier transform of the distribution function $G(\mathbf{r},x)$ for chain sequences of contour length x with end-to-end vector separation **r**:

$$\tilde{g}(\mathbf{q},x) = (4\pi/q)\int_0^\infty r \sin(rq)\, G(\mathbf{r}; x)\, dr \tag{89}$$

The form used for G(**r**,x) then distinguishes different models, e.g., random-flight chains with a Gaussian form for G(**r**,x) [1, 22, 30, 31, 79, 85], with a non-Gaussian G(**r**,x) for persistent or rodlike chains. Other forms for P(q,0) are applied in calculations for particles [30]. The results of model calculations with isotropic scattering elements within the RGD approximation for a few cases that lead to concise analytical expressions for some commonly encountered structures for a monodisperse solute are tabulated in Table 3, and a selection of those are shown in Figure 5. The P(q,0) for the examples shown coalesce for small $R_G^2q^2$, as should be anticipated given the invariant form for P(q,0) for small q, i.e., $\partial P(q,0)/\partial q^2 = R_G^2/3$. It may be noted that as shown in the insert, P(q,0) vs $R_G^2q^2$ are essentially numerically equivalent for $R_G^2q^2$ less than about 2.

<<Table 3>>

<<Figure 5>>

The well-known result of Debye for P(q,0) given in Table 3 for the linear, monodisperse random-flight chain model with large L is obtained on the assumption of a Gaussian G(**r**,x) for all x. It finds nearly universal use with flexible chain polymers. Consideration of this expression shows that for large R_G^2, the experimental range of u conveniently accessed at small angle accessible might be restricted to u large enough to lead to inaccuracy in the determination of the true q = 0 intercept of $[c/\mathbf{R}(q,c)]^0$ vs q and the initial tangent $\partial[c/\mathbf{R}(q,c)]^0/\partial q^2$ for small q needed to determine R_G^2 (see above). It has been noted that a fortuitous partial suppression of the higher order terms in u in the function $P(q,0)^{-1/2}$ can help alleviate this difficulty [72]. Thus, expansions in terms of u give

$$P(q,0)^{-1} = 1 + u/3 + u^2/36 + \ldots \quad (90)$$

$$P(q,0)^{-1/2} = 1 + u/6 - u^3/1080 + \ldots \quad (91)$$

In using this strategy, the investigator would examine plots of $[c/\mathbf{R}(q,c)]^{1/2}$ versus q^2 for each concentration studied, and extrapolate the intercepts and initial tangents to infinite dilution (the means for such extrapolations are considered in the following); this strategy is not useful for linear chains with a most-probable distribution of L, see below.

The random-flight model has been applied to compute P(q,0) for a wide range of branched homopolymers, including star, ring and comb-shaped molecules, randomly branched chains and

dentritic structures [1, 2, 22, 79, 85]. As would be expected P(q,0) for these structures is not given by the expression above for linear chains. Nevertheless, that form is provides a useful approximation to the calculate P(q,0) if R_G^2 in that expression is taken to be the value $R_G^2 = g\, R_{G,LIN}^2$ of the branched chain in place of $R_{G,LIN}^2$ for the linear chain of the same molecular weight; the branching parameter g is discussed in the preceding. An example of this comparison shown in Figure 6 demonstrates the utility of this approximation.

<<Figure 6>>

Consideration of the behavior of the Debye expression for P(q,0) for large u gives:

$$\lim_{u >> 1} P(q,0)^{-1} = C + u/2 + O(u^{-1}) \tag{92}$$

where C = 1/2 for the linear chain (see below for a discussion of branched flexible chains). With this result, for the (monodisperse) linear random-flight chain [20, 27, 55]

$$\lim_{u >> 1} [K_{o\pi} c/\mathbf{R}(q,c)]^0 = (1/2)[M^{-1} + (R_G^2/M)q^2 + \ldots] \tag{93}$$

or a tangent $\partial[K_{o\pi} c/\mathbf{R}(q,c)]^0/\partial q^2 = \hat{a}L/6M = \hat{a}/6M_L$, dependent only on the short-range features of the chain conformation. The limiting value of 2 for the Debye result for uP(q,0) at large u is easily seen by inspection of the expression. However, numerical evaluation demonstrates that this limit is not attained until u is rather large, e.g., uP(q,0) is 1.800 and 1.980 for u equal to10 and 100, respectively. Moreover, the assumption in the random-flight model that G(**r**,x) is Gaussian for all sequence lengths x cannot be a good representation for small x, corresponding to the scattering regime sampled at large q [5, 91]. As elaborated in the following paragraphs, one might anticipate that G(**r**,x) would approach the behavior for a rodlike chain for small x. The expression for P(q,0) for a rodlike chain given in Table 3 tends to a very different limit for large L [92, 93]:

$$\lim_{u >> 1} P(q,0)^{-1} = C + Lq/\pi + O(q^{-1}) = C + (12u)^{1/2}/\pi + O(q^{-1}) \tag{94}$$

with $C = 2/\pi^2$ and $u = R_G^2q^2 = L^2q^2/12$. As a consequence, in this limit the $\partial[K_{o\pi}c/\mathbf{R}(q,c)]^0/\partial q = 1/\pi M_L$, with this value independent of any distribution in M for a homologous series. With this expression, uP(q,0) is linear in $u^{1/2}$ for large u, i.e., $uP(q,0) \sim \pi(u/12)^{1/2}$, rather than the limit $uP(q,0) \sim 2$ for the random-flight chain.

Persistent chain models attempt to account for the inherent non-Gaussian behavior for realistic chains. A number of calculations based on the wormlike chain model have been presented [5, 47, 74, 75, 91, 94-99], none of which provide a physically acceptable result for large q, as they do not represent the crossover to the rodlike behavior that would be anticipated in that limit, with the models based on Gaussian statistics lacking that limit altogether. However, following early analyses based on that model, the effects of the chain structure on P(q,0) are often discussed in terms of regimes noted in the functions $(âL/3)q^2P(q,0)$ and $(L/\pi)qP(q,0)$ vs qâ: region I behavior for $R_G^2q^2 << 1$, with $(âL/3)q^2P(q,0)$ increasing monotonically with increasing $R_G^2q^2$; region II behavior for $1/R_G^2 < q^2 < â^2$, with $(âL/3)q^2P(q,0)$ tending to plateau with $(âL/3)q^2P(q,0) = 2$, the development of which depends on the value of l/â; and region III, with $(âL/3)q^2P(q,0)$ increasing with increasing q, a region not accurately captured by the early models for rodlike chains. Although this behavior is usually not observed in light scattering data owing to the range of q accessible in the physically available range of angles, the behavior is important in the scattering with radiation at smaller wavelength (e.g., neutron and x-ray scattering), and is elaborated in the following.

Calculations designed to overcome the deficiencies noted above in P(q,0) obtained with early treatments based on the wormlike chain have been given for what has been called the Kratky-Porod chain [5, 91, 96, 100, 101]. On the basis that P(q,0) for persistent chains should be similar to that for the random-flight model for $R_G^2q^2 << 1$, transforming to the behavior for a rodlike chain for $âq >> 1$, a model was developed based on complicated numerical representations for $G(\mathbf{r},x)$ [5, 91]. The results provide a crossover from a function $P_{RF}(q,0)$ for $R_G^2q^2 << 1$ to P(q,0) for the rodlike chain for $âq >> 1$, where numerical results for $P_{RF}(q,0)$ (for $0.1 \le L/â \le 20{,}000$) are well-represented by the expression for the random-flight chain (see Table 3), using $R_G^2 = (âL/3)S(â/L)$ for the wormlike chain (in place of the value (âL/3 for the random-flight chain), see Table 1. The results for P(q,0) are presented as a fairly complicated expression involving a number of numerical parameters chosen to fit the numerical results of the calculation of P(q,0). Examples of $(L/2â)P(q,0)$ vs 2âq calculated with that expression have been presented in graphical bilogarithmic

form for twelve values of L/â, ranging from 0.6 to 1,280 [102]; the plot exhibits a family of curves that decrease gradually (as given by $(L/2â)P_{RF}(q,0)$, until a crossover range of 2âq is reached, with a fairly rapid transition to the rodlike behavior for larger âq; the span in âq over which the crossover occurs shortens with decreasing L/â, i.e., as the chain becomes more rodlike. Although the crossover expression, presented in a form requiring the use of a number of numerical parameters, is involved, one might anticipate that a Padé approximation for P(q,0) calculated for persistent chain models will provide a useful approximation in many cases if L/â > 1. An alternative form, based on a different computational method, and resulting in a result requiring numerical integrations provides similar numerical results [101], and both are similar to the results obtained by numerical simulations on the wormlike chain [100]. Inspection of these results shows that the expression

$$P(q,0) \approx \left(P_{RF}(q,0)^m + \left(\frac{1 - \exp(-(âq)^2)}{1 + Lq^2/\pi} \right)^m \right)^{1/m} \qquad (95)$$

with m = 3 provides a good representation of the more complex crossover expression for L/â > 5; the second term in the brackets is devised to go to zero as q tends to zero, and to give the correct asymptotic behavior for a rodlike chain for larger q. The deviation of the Padé approximation with m = 3 from the numerical P(q,0) for smaller L/â reflects the sharpening character of the crossover noted above, and accordingly, may be minimized by permitting m to increase with decreasing L/â, e.g., m equal to 6 for L/â of 2.5 to 0.6. An alternate approximate treatment [96], designed to match a certain power-series expansion of $P_{RF}(q,0)$ at small q, and the rod behavior at large q results in an integral form requiring numerical evaluation; the results for L/â > 5 are fitted reasonably well with the Padé expression for m = 6, showing a sharper crossover than that with the first Kratky-Porod model discussed above.

Plots $(âL/3)q^2P(q,0)$ and $(L/\pi)qP(q,0)$ vs qâ are given in Figure 7 for the first of the two Kratky-Porod models described above, using data extracted from the bilogarithmic plot of $(L/2â)P(q,0)$ vs 2âq mentioned there. Following a monotone increase of $(âL/3)q^2P(q,0)$ with increasing âq (region I), the plots reveal a tendency to form a horizontal branch arising from the approach of $(âL/3)q^2P_{RF}(q,0)$ to its limiting value of $2âL/3R_G^2 = 2/\{S(â/L)\}$ with increasing q (region II), and a linearly increasing branch given by $(\pi/3)âq$ at larger q (region III). The intersection of the extrapolated lines for regions II and III occurs at a crossover q* given by

$$\hat{a}q^* \approx (6/\pi)S(\hat{a}/L)^{-1} \approx (6/\pi)(1 + 4\hat{a}/L) \qquad (96)$$

where the approximate form given above for S(â/L) is used in the final approximation. Given the physical limitation on the scattering angle (i.e., $\vartheta \leq \pi$), â/λ must be larger than about $(3/2\pi^2)(1 + 4\hat{a}/L) \approx 0.24$ if the transition to regime III is to be observed. That would place the transition outside the range for scattering using visible light except for a long, nearly rodlike chain, but the transition marked by q* has been used with an expression such as this in the analysis of $q^2P(q,0)$ from neutron or x-ray scattering to evaluate â for semiflexible polymers, see below.

<<Figure 7>>

The examples of $(Lq/\pi)P(q,0)$ vs qâ in Figure 7 show a maximum, corresponding to the maximum in $u^{1/2}P_{RF}(q,0)$ for $u \approx 2.149$, or $q = q^{**} = \{2.149/R_G^2\}^{1/2}$, with a rapid decrease to the asymptotic form $(Lq/\pi)P(q,0) \approx 1$ for $q >> q^*$. As may be seen in Figure 7, the height of the maximum in $(Lq/\pi)P(q,0)$ above the asymptotic limiting value decreases with decreasing L/â, with no maximum at all for the rodlike chain (the limit as â/L goes to zero). In addition, the appearance of the maximum is sensitive not only to the value of L/â, but also to the distribution in L present in the sample; q** remains proportional to $(R_{G,LS}^2)^{-1/2}$, with a proportionality constant that depends on both L/â and the molecular weight distribution, and with $R_{G,LS}^2$ changing from proportionality with L_z to proportionality with $(L_zL_{z+1})^{1/2}$ with decreasing L/â (see below). For example, for a most-probable distribution of M ($M_w/M_n = 2$), $q^{**} \approx \{3/(R_G^2/M)M_z\}^{1/2}$ for the random-flight chain model. The effects of the distribution in M have been evaluated for a range of parameters using the second (and apparently less accurate) of the crossover models mentioned above, showing suppression of the maximum with increasing heterodispersity in L [103].

More recently, the use of expressions for the persistent coil have been applied to light scattering studies on wormlike micelles; the large values of L and â for these makes investigation of this large âq behavior possible, but it should be noted that all of the above is for an "infinitely thin" chain, and neglects chain thickness effects that could affect the scattering at high q [104]. Although this may usually be negligible in light scattering, it may be important for the scattering with smaller wavelengths, e.g., neutron scattering. A simple approximation is usually used to extract the radius

R_c of the (assumed) circular cross-section of the chain in such cases from the scattering in region III, with a factorization given by [30, 104]

$$P_{III}(q,0) \approx (\pi/Lq)P_{section}(q,0) \tag{97a}$$

$$P_{section}(q,0) \approx \left(\frac{2J_1(R_cq)}{R_cq}\right)^2 \approx \exp[-(R_cq)^2/4] \tag{97b}$$

where $J_1(x)$ is the first-order Bessel function of the first kind; inspection shows that the exponential (Guinier) approximation is within 10 % of the Bessel function relation for $R_cq < 2$, with the deviation increasing rapidly for larger qR_c. Expressions for $P_{section}(q,0)$ for other cross-section geometries are available, including hollow structures [30, 86, 104] The assumed factorization has been examined in a more rigorous treatment, and found to be useful provided $R < L/20$ [95], which is often satisfactory for use with the scattering from wormlike or cylindrical micelles, for which R is of the order on 1 nm. The example in Figure 8a shows data on a wormlike micelle demonstrating the several features described in the preceding; the data were obtained by small-angle neutron scattering as light scattering data would not access only the smallest range of q for the data shown [105]. The example in Figure 8b shows data comprising both light and small-angle neutron scattering on a wormlike micelle characterized by $L/â \approx 3$ which, coupled with the dispersity in L, is too small to support the maximum in $(Lq/\pi)P(q,0)$ [106].

<<Figure 8 a & b>>

The helical-wormlike (HW) chain model represents a further and substantial refinement on the preceding, including the example with the most detailed $G(\mathbf{r},x)$ given above as a special case. For example, as mentioned above, the HW model is able to represent behavior in which R_G^2/L depends markedly on L at low L, including situations with an extremum in R_G^2/L. Similarly, the HW model can reproduce more complex behavior in P(q,0) appear in the wormlike persistent chain model, including behavior in which $(âq)^2P(q,0)$ can exhibit an extremum at intermediate âq, before entering the rodlike form for large âq [5, 91]. The expression for HW involves the use of the relation for P(q,0) calculated using R_G^2 for the HW chain, in a form with P(q,0) calculated for a rodlike chain with the same L (either the Padé form given above, or a more accurate expression involving a power series), with the P(q,0) so derived modified by multiplication by a fairly

complex function involving several power series, using tabulated coefficients. Unfortunately, this calculation of P(q,0) is rather tedious, and seems likely to find use only in laboratories where the repeated need for such an analysis will motivate the preparation of a computer based implementation of the calculation.

The preceding has addressed the limitations in G(**r**,x) for chain sequences with small contour length x for chains without excluded volume interactions (i.e., in very dilute solutions at the Flory Theta temperature). The other major limitation in the calculation of P(q,0) is the neglect of excluded volume interactions. Although several attempts to deal with this have been published, often through the use of a form assuming that $\langle r_{ij}^2 \rangle \propto |i - j|^{\varepsilon}$, with $\varepsilon > 1$ to represent the effects of excluded volume interactions [98]. Consideration of the effects of excluded volume interactions on G(**r**,x) for $x << (\hat{a}L)^{1/2}$ leads to a Fourier transform I(**q**,x) that produces asymptotic behavior for $qR_G^2 >> 1$ with $P(q,0) \sim (\hat{a}q)^{-5/3}$ [46, 107]. Verification of this asymptotic behavior for polymer chains has proved to be elusive by light scattering owing to limitations on the upper bound on q. A simple strategy that incorporates much of the effect of excluded volume interactions on P(q,0) is to use P(q,0) for the random-flight chain, with the R_G^2 for the chain with excluded volume in place of the value âL/3 for the random-flight chain. In the adaptation of this to persistent chains, the second term in the Padé expression (involving L) would not be modified. It appears that this provides a reasonable fit to experiment, as indeed it must for $R_G^2 q^2 << 1$.

Use of the Debye expression to evaluate $P_{LS}(q,0)$ for a linear random-flight chain heterodisperse in M gives

$$P_{LS}(q,0) = (2/rM_w q^2)\{1 - (1/rM_n q^2)[1 - M_n \sum_{\nu}^{C} w_\nu M_\nu^{-1} \exp(-rM_\nu q^2)]\} \qquad (98)$$

with $r = R_G^2/M = \hat{a}/3M_L$ a polymer-specific, independent of chain length in the random-flight model. For large $rM_\nu q^2$ for any M_ν in the distribution, this results in the asymptotic form [55]

$$\lim_{rM_\nu q^2 >> 1} P(q,0)^{-1} = (M_w/M_n)\{C + rM_n q^2/2 + O(u^{-1})\} \qquad (99)$$

where C = 1/2 for the linear chain; as remarked above, non-Gaussian chain statistics for short chain segments may suppress the limiting behavior predicted by the random-flight model for large q . With this result, for the linear random-flight chain,

$$\lim_{rM_{LS}q^2 >> 1} [K_{o\pi}c/\mathbf{R}(q,c)]^0 = (1/2)[M_n^{-1} + rM_nq^2 + \ldots] \qquad (100)$$

Thus, if the asymptotic behavior can be observed, it will provide information on the molecular weight distribution. For a heterodispersity in M characterized by the Schulz-Zimm distribution function, the final summation in $P_{LS}(q,0)$ may be completed to give

$$P_{LS}(q,0) = (2/rM_wq^2)\{1 - (1/rM_nq^2)[1 - (1 + rM_nq^2/h)^{-h}]\} \qquad (101)$$

For the most-probable distribution of M (for which h = 1, and $M_w/M_n = 2$ and $M_z/M_w = 3/2$), this reduces to

$$P_{LS}(q,0)^{-1} = 1 + rM_zq^2/3 \qquad (102)$$

Note that in this case, since $P_{LS}(q,0)$ is linear in q^2, the use of the square-root analysis discussed above to aid determination of the initial tangent of for flexible chains would be inappropriate. With R_G^2 is replaced by $g(R_G^2)_{LIN}$ in the definition of r this same result may be applied to give $P_{LS}(q,0)$ for randomly branched chains, as obtain in certain polymerization [22].

Use of the Schulz-Zimm distribution in M leads to an explicit representation of $P_{LS}(q,0)$ for rodlike chains [108]

$$P_{LS}(q,0) = \frac{2}{(1+h)\xi}\left\{\arctan(\xi) + \sum_{j=1}^{h-1}\left(\frac{1}{h-j} - \frac{1}{h}\right)(1+\xi^2)^{(j-h)/2}\sin[(h-j)\arctan(\xi)]\right\} \qquad (103)$$

where $\xi = qM_w/M_L(1 + h)$. Of course, as expected, this expression gives the approximation $P_{LS}(q,0) \sim \pi M_L/M_wq$ for large qM_w/M_L, making $K_{o\pi}c/\mathbf{R}(q,c)]^0$ independent of the molecular weight

distribution in that limit, with a dependence on q that provides an estimate for M_L. For a most-probable distribution of M,

$$P_{LS}(q,0) = (2M_L/qM_w)\arctan(qM_w/2M_L) \quad (104)$$

5.3 Optically diverse scattering elements

In this case, the full expression for $P_{LS}(q,0)$ given above must be applied, with obvious complications for structures with m_i and $\tilde{\psi}_i$ differing among the scattering elements, even for the case of a copolymer even for a copolymer for which all chains have the same molecular weight and composition, allowing only for variation in the sequence of the scattering elements among the chains (or in a particles), e.g., a block or alternating copolymer, stratified particles, etc ., such that

$$P_{LS}(q,0) = \frac{\sum_{\nu}^{C} w_\nu \sum_{j}^{n_\nu}\sum_{k}^{n_\nu} \tilde{\psi}_{j,\nu}\tilde{\psi}_{k,\nu}\, m_{j,\nu}m_{k,\nu}\langle[\sin(q|r_{jk}|_\nu)]/q|r_{jk}|_\nu\rangle}{\sum_{\nu}^{C} w_\nu[\sum_{j}^{n_\nu}\tilde{\psi}_{j,\nu}m_{j,\nu}]^2} \quad (105)$$

3As in the discussion of $R^2_{G,LS}$, restricting further to the special case of only two scattering elements, A and B, and making use of the relations $w_A = 1 - w_B = n_Am_A/(n_Am_A + n_Bm_B)$ and $\tilde{\psi} = w_A\tilde{\psi}_A + w_B\tilde{\psi}_B$, to give [54, 55]

$$P_{LS}(q,0) = \tilde{\psi}^{-2}\{w_A^2\tilde{\psi}_A^2P_A(q,0) + w_B^2\tilde{\psi}_B^2P_B(q,0) + 2w_Aw_B\tilde{\psi}_A\tilde{\psi}_BQ_{AB}(q,0)\} \quad (106)$$

where, similar to the expression used with $R^2_{G,LS}$

$$P_\nu(q,0) = \left(\frac{1}{n_\nu^2}\sum_{j}^{n_\nu}\sum_{k}^{n_\nu}\langle[\sin(q|r_{jk}|_\nu)]/q|r_{jk}|_\nu\rangle\right) \quad (107)$$

for ν equal to either A or B, with, for example, only the type A elements being considered in the sum for $P_A(q,0)$, i.e., $P_A(q,0)$ is the value of $P_{LS}(q,0)$ for conditions with $\tilde{\psi}_B = 0$, etc., and

$$Q_{AB}(q,0) = \frac{1}{n_A n_B} \sum_{j}^{n_A} \sum_{k}^{n_B} \langle [\sin(q|r_{jk}|)]/q|r_{jk}| \rangle \qquad (108)$$

As in the discussion of $R^2_{G,LS}$, a further simplification in form is made using the definition $\tilde{w}_A = 1 - \tilde{w}_B = w_A\tilde{\psi}_A/\tilde{\psi}$, to give an expression parallel to that for $R^2_{G,LS}$,

$$P_{LS}(q,0) = \tilde{w}_A^2 P_A(q,0) + (1 - \tilde{w}_A)^2 P_B(q,0) + 2\tilde{w}_A(1 - \tilde{w}_A)Q_{AB}(q,0) \qquad (109)$$

As above, $\tilde{w}_A = w_A\tilde{\psi}_A/\tilde{\psi}$, and parallel to the preceding discussion of $R^2_{G,LS}$ for this same case, $P_A(q,0)$ and $P_B(q,0)$ are refer to those structures, respectively, i.e., $P_A(q,0)$ is the value of $P_{LS}(q,0)$ for conditions with $\tilde{\psi}_B = 0$, etc. Defining a function $P_{AB}(q,0)$ parallel to the corresponding function in the expression for $R^2_{G,LS}$ in Equation 71,

$$Q_{AB}(q,0) = [P_A(q,0) + P_B(q,0) + P_{AB}(q,0)]/2 \qquad (110)$$

to give

$$P_{LS}(q,0) = \tilde{w}_A P_A(q,0) + (1 - \tilde{w}_A)P_B(q,0) + \tilde{w}_A(1 - \tilde{w}_A)P_{AB}(q,0) \qquad (111)$$

In applying these expressions, it is assumed that $P_A(q,0)$, $P_B(q,0)$ and $Q_{AB}(q,0)$ do not depend on the solvent, which may not be a good approximation with flexible chain polymers, owing to the possible effects of excluded volume, or even collapse of one component in certain block copolymers. The function $P_{AB}(q,0)$ (or $Q_{AB}(q,0)$) must be computed for each case, but expansion of $P_{AB}(q,0)$ in q^2 gives a leading term $\Delta^2_{AB}q^2/3$, with Δ^2_{AB} defined above in the discussion of $R^2_{G,LS}$, showing that $P_{AB}(0,0) = 0$, as must be the case to give $P_{LS}(0,0) = 1$ for arbitrary $\tilde{w}_A$. Since $\tilde{w}_A$ may be positive, negative or zero, inspection of $P_{LS}(q,0)$ shows that $\partial[P_{LS}(q,0)]^{-1}/\partial q^2$ may likewise be positive, negative or zero, as mentioned in the discussion of $R^2_{G,LS}$. Examples of $P_{AB}(q,0)$ are available for a linear random-flight diblock copolymer demonstrating this behavior [54]. For a sphere with radius R_A and scattering elements of type A, coated by a shell with outer radius $R_B > R_A$, comprising scattering elements of type B [30],

$$P_{LS}(q,0) = \left(\tilde{w}_A[P_A(q,0)]^{1/2} + (1-\tilde{w}_A)\frac{R_B^3[P_B(q,0)]^{1/2} - R_A^3[P_A(q,0)]^{1/2}}{R_B^3 - R_A^3}\right)^2 \quad (112)$$

where $P_A(q,0)$ and $P_B(q,0)$ are the functions for spheres with radii R_A and R_B, respectively. This expression reduces to $P_{LS}(q,0)$ for a shell of thickness $\Delta = R_B - R_A$ filled with solvent for $\tilde{w}_A = 0$, or to the expression for a sphere of radius R_A if $\tilde{w}_A = 1$. If $\tilde{\psi} = 0$, then $[\mathbf{R}(0,c)/K_{op}c]^0 = 0$, but $[\mathbf{R}(q,c)/K_{op}c]^0$ for $\vartheta > 0$ may be computed with Equation 111 with $\tilde{w}_A$ and $1 - \tilde{w}_A$ replaced by $w_A\tilde{\psi}_A$ and $w_B\tilde{\psi}_B$, respectively. The result will exhibit a series of maxima in $\mathbf{R}(q,c)$ for $\vartheta > 0$, with a superficial similarity to $[\mathbf{R}(q,c)/K_{op}c]^0$ observed with charged spheres, arising from electrostatic interactions among the spheres, see below.

5.4 Optically anisotropic scattering elements

As given above, with anisotropic scattering elements, expressions are required for both $[\mathbf{R}_{Hv}(q,c)/c]^0$ and $[\mathbf{R}_{Vv}(q,c)/c]^0$, given by the expressions

$$[\mathbf{R}_{Hv}(q,c)/c]^0 = K'\hat{n}_s^2(\partial\hat{n}/\partial c)_w^2 M_{LS,Hv}P_{LS,Hv}(q,0) \quad (113)$$

$$[\mathbf{R}_{Vv}(q,c)/c]^0 = K'\hat{n}_s^2(\partial\hat{n}/\partial c)_w^2 M_{LS,Vv}P_{LS,Vv}(q,0) \quad (114)$$

where $M_{LS,Hv}$ and $M_{LS,Vv}$ are discussed in the preceding. Further, $[\mathbf{R}_{Vh}(q,c)/c]^0 = [\mathbf{R}_{Hv}(q,c)/c]^0$ and, in the RGD regime assumed here, $[\mathbf{R}_{Hh}(q,c)/c]^0 = \cos^2(\vartheta)[\mathbf{R}_{Vv}(q,c)/c]^0$. For rodlike chains with anisotropic scattering elements and monodisperse in M, with x = Lq, [20, 27, 56, 57, 94]

$$(1 + 4\delta^2/5)P_{Vv}(q,0) = p_1(x) + \delta^2\{(4/5)p_3(x) - (2 - \delta^{-1})m_1(x) + (9/8)m_2(x) + m_3(x)\} \quad (115)$$

$$P_{Hv}(q,0) = p_3(x) + (5/8)\sin^2(\vartheta/2)m_2(x) \quad (116)$$

Here, δ is the nondimensional optical anisotropy, discussed in the preceding for rodlike and wormlike chain models, $p_1(x)$ is given in Table 3 for a rodlike chain with optically isotropic scattering elements, and

$$p_2(x) = (6/x^3)[x - \sin(x)] \quad (117)$$

$$p_3(x) = (10/x^5)[x^3 + 3x\cos(x) - 3\sin(x)] \quad (118)$$

$$m_1 = p_1 - p_2 \quad (119)$$

$$m_2 = 3p_1 - p_2 - p_3 \quad (120)$$

$$m_3 = p_3 - p_2 \quad (121)$$

The expression for $P_{Hv}(q,0)$ provides an example of case for which the scattering comprises contributions explicit in ϑ, in addition to the dependence on q. Although these expressions are derived explicitly for a rodlike chain, in the form given, incorporating δ as an explicit parameter, owing to the rapid decrease of δ/δ_0 with increasing $L/\hat{a}$ for the wormlike chain model, they also provide a reasonable approximation to the behavior for that model as a function of $L/\hat{a}$, consistent with behavior for both the rodlike limit ($L/\hat{a} << 1$) and flexible coil ($L/\hat{a} >> 1$) limits [20, 109]. For the latter limit, the $(\delta/\delta_0)^2 \propto \hat{a}/L$, and the terms in δ may be neglected in the expression for $[\mathbf{R}_{Vv}(q,c)/c]^0$, and $[\mathbf{R}_{Hv}(q,c)/c]^0$ is expected to be much smaller than $[\mathbf{R}_{Vv}(q,c)/c]^0$. Similarly, for helical chains, δ_0 is often small owing to the projections of the components of the elemental polarizability on the helical axis, and the effects of the optical anisotropy may be negligible on $[\mathbf{R}_{Vv}(q,c)/c]^0$, with weak, but measurable, $[\mathbf{R}_{Hv}(q,c)/c]^0$, making it a useful function to estimate the persistence length from the dependence of $[\mathbf{R}_{Hv}(q,c)/c]^0$ on molecular weight.

5.5 Scattering beyond the RGD regime

The RGD approximation fails as the size of the solute becomes large enough, and with a sufficiently strong optical contrast with the medium, to result in a phase shift of the incident beam as it propagates through the solute too large to be neglected. As mentioned in the Introduction, for nonabsorbing solute this effect will be negligible for macromolecules with a basic threadlike structure, even for structures with a very large $R^2_{G,LS}$, as the domain occupied by the macromolecule is mostly filled with solvent. By contrast, the conditions for a phase shift that may not be neglected can be met with particles under realistic conditions. Numerical methods are available to compute $P_{Vv}(q,0)$ for a number of particle shapes [13, 23, 110, 111]. Here, attention will be focused on the Mie theory for spheres comprising nonabsorbing, optically isotropic scattering elements [23, 30, 33, 59]. In considering some aspects of the Mie theory, it is necessary to expand the nomenclature to include the azimuthal angle φ describing the angle of the scattering plane relative to the polarization direction of vertically polarized incident light; in the examples considered to this point, $\varphi = \pi/2$. This may be accomplished using the notation in $P_{Vv}(\vartheta,\varphi,0)$, $P_{Hh}(\vartheta,\varphi,0)$ and $P_{Hv}(\vartheta,\varphi,0)$ if

$\varphi \neq \pi/2$ or the simpler notation used to this point, suppressing φ if $\varphi = \pi/2$, i.e., $P_{Vv}(q,0) = P_{Vv}(\vartheta,\pi/2,0)$ or $P_{Hh}(q,0) = P_{Hh}(\vartheta,\pi/2,0) = P_{Vv}(q,0,0)$. In the following, the simpler notation will suffice for $P_{Vv}(q,0)$ and $P_{Vv}(q,0)$, but the more complete notation will be used for $P_{Hv}(\vartheta,\varphi,0)$. The Mie theory provides expressions for $P_{Vv}(q,0)$, $P_{Hh}(q,0)$ and $P_{Hv}(\vartheta,\varphi,0)$ as the square of sums of functions of ϑ, φ and the relevant refractive indices. Although the deviation of these from the comparable functions obtained within the RGD approximation depend in a complicated way on $\tilde{\alpha}$ and $\tilde{n}$, the deviations are usually small if $\tilde{\alpha}|\tilde{n} - 1| < 0.25$. Examples shown in Figure 9 present $P_{Vv}(q,0)$ as a function of $q^2R_{G,LS}^2$ for a particular value of $\tilde{\alpha} = 2\pi R/\lambda$, over a range of $\tilde{n}$ [1]; the value chosen for $\tilde{\alpha}$ would correspond to an aqueous suspension of spheres with $R \approx 300$ nm, and $\lambda_0 = 633$ nm. For small $q^2R_{G,LS}^2$, the data are all well represented by the simple Gainer approximation [36]

$$P_{Vv}(q,0) = \exp(-q^2R_{G,LS}^2/3) \tag{122}$$

where $R_{G,LS}^2$ is itself a complicated function of $\tilde{\alpha}$ and $\tilde{n}$, as discussed above; values of $R_{G,LS}^2$ for these parameters may be seen in Figure 4. For larger $q^2R_{G,LS}^2$, the first minimum in $P_{Vv}(q,0)$ occurs near that for $P_{Vv}(q,0)$ computed in the RGD approximation (see Table 3), but with the minimum becoming broadened, less pronounced shifted toward smaller $q^2R_{G,LS}^2$ with increasing $\tilde{n}$. These same features are observed in the second minimum except for the largest $\tilde{n}$. These features make it evident that without *a priori* knowledge of $\tilde{n}$, it would be difficult to discriminate between the effects of heterodispersity of particle size and deviations from the behavior anticipated in the RGD regime.

<<Figure 9>>

For both $\tilde{n} >> 1$ and a phase shift magnitude $\tilde{\alpha}|\tilde{n} - 1| > 10$, the angular dependence reduces to a regime termed the Fraunhofer diffraction limit [23, 30, 33, 112]. In that regime, the angular dependence is independent of $\tilde{n}$, and is the same for absorbing and nonabsorbing particles. For example, for a monodisperse spheres, the angular dependence is that for Fraunhofer diffraction from a circular aperture:

$$\lim_{R/\lambda >> 1} P_{Vv}(q,0) \quad = \quad \{2J_1(\tilde{\alpha}\sin(\vartheta))/\tilde{\alpha}\sin(\vartheta)\}^2 \tag{123}$$

where $\tilde{\alpha} = 2\pi R/\lambda$, and $J_1(...)$ is the Bessel function of the first kind and first order. For polydisperse solute in this regime,

$$\lim_{R/\lambda >> 1} [\mathbf{R}_{Vv}(q,c)/c]^0 \quad \propto \quad \sum_v n_v \tilde{\alpha}_v^6 \{2J_1(\tilde{\alpha}_v \sin(\vartheta))/\tilde{\alpha}_v \sin(\vartheta)\}^2 \tag{124}$$

where n_v is the number fraction of spheres with radius R_v. When applicable, the simplicity of this expression is useful in methods to estimate the size distribution from data on $[\mathbf{R}_{Vv}(q,c)/c]^0$. Similar results obtain for other particle shapes. For example, for cylinders of length L_{cyl} and radius R, in the same limit, with $L_{cyl} >> R >> \lambda$,

$$\lim_{R/\lambda >> 1} P_{Vv}(q,0) \quad = \quad \sin^2(\tilde{\alpha}\vartheta))/(\tilde{\alpha}\vartheta)^3 \tag{125}$$

Since the patterns for the extrema are similar for the functions for spheres and cylinders, it is not possible to differentiate between solutes with these two shapes from the scattering in this limit. Neither can the expression for $L_{cyl} >> R >> \lambda$ be used to determine the distribution of scattering lengths.

Although it cannot be accurate for small ϑ, and is inaccurate in the RGD regime, it has been noted that the expression given above for $P_{Vv}(q,0)$ for spheres with $R/\lambda >> 1$ in the Fraunhofer limit may serve as a reasonable approximation to $P_{Vv}(q,0)$ in the Mie scattering regime even if R/λ is not much larger than unity [30, 113], providing a useful simplification in some cases for size estimation from light scattering data.

A regime termed anomalous diffraction arises for $\tilde{\alpha} >> 1$, but $\tilde{n} \approx 1$, so that the phase shift $\tilde{\alpha}|\tilde{n} - 1|$ is small, as could occur for large particles immersed in a nearly refractive index matching solvent [30, 33, 113]. The angular dependence then differs appreciably from that for Fraunhofer diffraction, and so-called anomalous diffraction approximations to the Mie theory for $P_{Vv}(q,0)$ have

been calculated for spheres in the regime $|\tilde{n} - 1| < 0.1$, $2\tilde{\alpha}|\tilde{n} - 1| < 0.1$, and $\tilde{\alpha} > 1$ [33, 114]. Use of the expression in the Fraunhofer limit would lead to serious error in size determination in this regime.

With the RGD approximation, $P_{Hh}(q,0) = \cos^2(\vartheta)P_{Vv}(q,0)$, but this simple relation does not obtain if the phase shift is not small. Similarly, although $P_{Hv}(q,0) = P_{Hv}(\vartheta,\pi/2,0)$ is zero for spheres comprising optically isotropic scattering elements, $P_{Hv}(\vartheta,\pi/4,0)$ does not vanish for all ϑ, exhibiting a maximum that may be used to estimate the radius of the sphere [115]. Calculations in both the RGD and the anomalous diffraction regime of the Mie theory reveal a similar maximum for such spheres in [116], in agreement with observations on spheres thought to be optically isotropic [114].

The functions $P_{Vv}(\vartheta,\varphi,0)$ and $P_{Hv}(\vartheta,\varphi,0)$ have been computed for monodisperse spheres and other particle shapes comprising optically anisotropic scattering elements [18, 115, 117]. A principal result for such spheres is that $P_{Hv}(\vartheta,\pi/4,0)$ exhibits extrema as a function of qR. Calculations in both the RGD [117] and anomalous diffraction [114]regimes provide estimates of qR at the first maximum and the following minimum that may be used to estimate R.

6. Scattering from a dilute solution at zero scattering angle

6.1 The basic relation

With increasing concentration, the effects of interference among the scattered rays from different solute molecules (or particles) will result in a decrease in the scattering, with effects represented in the preceding by the functions F(q,c) and P(q,c). Consequently, with increasing concentration, it is necessary to consider effects contributing to the scattering beyond those linear in c that have been the subject of the preceding. These may appear in P(q,c), through a dependence of G(**r**,x) on concentration, for example as may be the case for a flexible chain with excluded volume interactions such that R_G^2 depends on c, but will principally appear in the contributions to F(q,c) embodied in the functions B(c) and Q(q,c). For a solute comprising identical optically isotropic, but not necessarily identical, scattering elements, in the RGD regime basic relation is given by Equation 5 with P(q,c) = 1 and [1, 20, 27, 29, 44, 49-51],

$$\widetilde{B}_{LS}(c)Q_{LS}(q,c) = \frac{\sum_{\nu}^{C}\sum_{\mu}^{C} w_\nu w_\mu \tilde{\psi}_\nu \tilde{\psi}_\mu M_\nu M_\mu P_\nu(q,c) P_\mu(q,c) \widetilde{B}_{\nu\mu}(c) Q_{\nu\mu}(q,c)}{[M_{LS} P_{LS}(q,c)]^2} \qquad (126)$$

Both $\widetilde{B}_{\nu\mu}(c)$ and $Q_{\nu\mu}(q,c)$ involve integrations over pairs of molecules (or particles). For dilute solutions, one can expect to utilize virial expansions of $P_\nu(q,c)$, $\widetilde{B}_{\nu\mu}(c)$ and $Q_{\nu\mu}(q,c)$, except possibly for special situations, such as solutions of polyelectrolytes with a very low ionic strength environment, see below. For rigid particles, the shape will not depend on c, and P(q,c) = P(q,0). However, as discussed below, this approximation may not be valid for flexible chain macromolecules subjected to excluded volume interactions. This expression will be developed in the following, beginning with the simplest case.

In this section, attention is focused on the scattering from dilute solutions in the RGD regime at zero scattering angle, so that Equation 126 may be simplified to read

$$\widetilde{B}_{LS}(c) = M_{LS}^{-2} \sum_{\nu}^{C}\sum_{\mu}^{C} w_\nu w_\mu \tilde{\psi}_\nu \tilde{\psi}_\mu M_\nu M_\mu \widetilde{B}_{\nu\mu}(c) \qquad (127)$$

or, for a solute with optically identical scattering elements,

$$\widetilde{B}_{LS}(c) = M_{w}^{-2} \sum_{\nu}^{C}\sum_{\mu}^{C} w_\nu w_\mu M_\nu M_\mu \widetilde{B}_{\nu\mu}(c) \qquad (128)$$

Since the discussion will begin with considerations for a solute monodisperse in M, the subscript "LS" will be suppressed until the discussion moves to a heterodisperse solute.

Most of the section will consider a solute comprising identical isotropic scattering elements, so that the subscript denoting the polarization state will be suppressed, as only $\mathbf{R}_{Vv}(q,c)$ will be of interest in this section unless otherwise specified. As will be seen, much of the discussion will center around the second virial coefficient A_2 derived from an expansion of $\widetilde{B}_{LS}(c)$ to give $2A_{2,LS}$ as the leading term. In defining what is meant by a dilute solution (or dispersion), it is useful to introduce

a dimensionless concentration $\hat{c}$ wherein the concentration c (mass/volume) is scaled by the average concentration $M/N_A R_G^3$ in the molecular (or particle) domain:

$$\hat{c} = cN_A R_G^3/M \tag{129}$$

A dilute solution is then one with $\hat{c} < 1$, so that on average, the solute species are separated by a distance larger than the average dimension. This is not to imply that this separation does not fluctuate, including fluctuations to a much smaller separation. For example, for flexible chain polymers, the monomer density $M/N_A R_G^3$ is so small in comparison with the solvent density that the centers of gravity of chains may approach separations much smaller than, say, $(R_G^2)^{1/2}$, so that the "domains" of polymer chains may overlap considerably, leading, for example, to the possibility of large values of A_2 in so-called good solvents [37]. By contrast, for hard spheres, the fluctuations may bring the centers of spheres no closer than 2R.

6.2 Monodisperse solute, identical optically isotropic scattering elements

As forecast above, the assumption of a dilute solution motivates the examination of Taylor series expansions (virial expansions) in c for the functions in F(q,c) [1, 9, 12, 20, 27, 29, 37, 44-46]. The nomenclature used for the expansion of $\Gamma(c)$ arises from the correspondence noted above between F(0,c) for a monodisperse solute comprising identical isotropic scattering elements and the osmotic pressure Π, such that, as given above, repeated here for convenience and emphasis:

$$c\Gamma(c) = \frac{M}{RT}\frac{\partial \Pi}{\partial c} - 1 \tag{14}$$

It may be remarked that the limitation of this expression to monodisperse solute is often forgotten in applications involving heterodisperse polymers. By long practice the virial expansion of Π is written as [37]

$$\frac{\Pi M}{RTc} = 1 + A_2 Mc + A_3 Mc^2 + \ldots = 1 + \psi_2 \hat{c} + \psi_3 \hat{c}^2 + \ldots \tag{130}$$

where A_2 and A_3 are the second and third virial coefficients, respectively, and the $\psi_j = A_j M(M/N_A R_G^3)^{j-1}$ are dimensionless virial coefficients. Consequently, to the same order,

$$c\Gamma(c) = 2A_2 Mc + 3A_3 Mc^2 + \ldots = 2\psi_2 \hat{c} + 3\psi_3 \hat{c}^2 + \ldots \tag{131}$$

and this suffices for the analysis of $c/\mathbf{R}(0,c)$ on dilute solutions, obtained by extrapolation of $c/\mathbf{R}(q,c)$ to $\vartheta = 0$ at each concentration, such that

$$c/\mathbf{R}(0,c) \quad = \quad [c/\mathbf{R}(0,c)]^0\{1 + 2A_2Mc + 3A_3Mc^2 + \ldots\} \tag{132}$$

It may be noted that under Flory theta conditions, $A_2 = 0$, and even though $A_3 > 0$ [9, 12, 37, 44, 45], $[\mathbf{R}(q,c)/c] \approx [\mathbf{R}(q,c)/c]^0$, provided $3A_3Mc^2 << 1$, as will usually be the case for a dilute solution.

In theoretical treatments, it is often convenient to express A_2M in terms of an excluded volume U per molecule, defined as [29, 37]

$$A_2M \quad = \quad \frac{N_AU}{M\,2} \tag{133}$$

For rigid particles interacting through a hard-core potential, U may be expressed in terms of the volume V_p of the particle and a factor f that depends on the particle shape, with $U = 8fV_p$, such that $f = 1$ for spheres, so that $U = (4\pi/3)(2R)^3$ and $A_2 \propto M^{-1}$, or $f = L/4d$ for rods of length L and diameter d, so that $U = \pi L^2 d/2$ and $A_2 \propto M_L^2 d$ as expressed in Equation 64b; f has been calculated for a variety of particle shapes [20, 29]. With flexible chain polymers, it is useful to express A_2M in a similar form [9, 27, 29, 45, 71, 72, 118]

$$\frac{A_2M^2}{N_AR_G^3} \quad = \quad \psi_2 \; = \; \Psi(U/R_G^3) \tag{134}$$

where $\Psi(0) = 0$, as at the Flory Theta temperature, and $\Psi(\infty) = \Psi_\infty$, a constant, in a so-called "good solvent" for a macromolecule . In this nomenclature, $\Psi_\infty = U/2R_G^3$ for rigid particles, e.g., $\Psi_\infty = 4V_p/R_G^3 = (16\pi/3)(5/3)^{3/2} \approx 36$ for spheres interacting through a hard-core potential. By comparison, $\Psi_\infty \approx$ 6-7 for linear flexible chain polymers, reflecting the soft intermolecular potential for such chains, permitting the substantial overlap of chain "domains" mentioned above. Cartoons that represent a dilute solution as a system of globular-like coiled chains that do not overlap fail to convey this aspect of a solution of flexible chain polymers. For spheres interacting through a hard-core potential, $A_3M = \Upsilon_3(A_2M)^2$ with $\Upsilon_3 = 5/8$ [119]. Inspection shows that in this case, the function $[c/\mathbf{R}(0,c)]^{1/2}$ will exhibit less curvature with increasing c than will $c/\mathbf{R}(0,c)$:

$$c/\mathbf{R}(0,c) = [c/\mathbf{R}(0,c)]^0\{1 + 2A_2Mc + 3\Upsilon_3(A_2Mc)^2 + \ldots\} \quad (135)$$

$$[c/\mathbf{R}(0,c)]^{1/2} = \{[c/\mathbf{R}(0,c)]^0\}^{1/2}\{1 + A_2Mc + [(3\Upsilon_3 - 1)/2](A_2Mc)^2 + \ldots\} \quad (136)$$

with $(3\Upsilon_3 - 1)/2 = 7/16 \approx 0.44$ for the hard sphere case. A similar strategy is also useful with dilute solutions of macromolecules in good solvents, to enhance the reliability of the extrapolation to determine $[c/\mathbf{R}(0,c)]^0$ by creating a larger span in c for which linearity obtains to a good approximation [27, 72].

The preceding strategy may not be appropriate with solutions of polyelectrolytes, depending on the overall ionic strength of the solution. The ionic strength is often increased by the addition of small molecule electrolyte, forming a multicomponent solvent, in which case, as discussed above, the solutions should be dialyzed against the multicomponent solvent to prepare the solution used for light scattering and measurement of the refractive index. At very low ionic strength, it is possible that the range of the spatial range of the electrostatic interactions among the polyelectrolyte solute will approach or exceed q^{-1}, in which case the assumed independence of solute concentration fluctuations in neighboring regions of order q^{-3} may be invalid, vitiating the statistical fluctuation theory for scattering [26]. The Debye screening length κ^{-1} provides a measure of the range of the electrostatic interactions, where

$$\kappa^{-1} = (8\pi N_A L_B I_o)^{-1/2} \quad (137)$$

where $L_B = e^2/\varepsilon kT$ is the Bjerrum length, with ε the dielectric strength ($L_B/\text{nm} \approx 57/\varepsilon$ at 25°C, or $L_B \approx 0.7$ nm for water), and I_o is the ionic strength ($I_o = \Sigma\nu_i^2 m_i/2$, with ν_i and m_i the molarity and charge of species i). To insure that assumed statistical independence is valid, one should have $\kappa^{-1} < q^{-1}$ For example, $q^{-1} > 40$ nm for 633nm wavelength light in an aqueous medium, compared $\kappa^{-1} < 10$ nm for with $I_o > 10^{-3}$ M, showing that the necessary conditions would normally be met with visible light; the situation may not be as favorable with small-angle x-ray scattering. Assuming the validity of the independent statistical fluctuations in neighboring scattering volumes, the expressions given above may be used, but one still may be faced with much larger virial coefficients than would be obtained with neutral systems, to the extent that reliable extrapolation to

infinite dilution may be compromised. In addition to these considerations, as discussed below, the intramolecular excluded volume interactions, and hence the size of flexible chains, may change with the solute concentration, with a corresponding effect on the effective second virial coefficient at each concentration. These effects may all be suppressed by the addition of a simple electrolyte, and unless one is particularly interested in the behavior at low ionic strength is very low, that is to be recommended. The aforementioned potential variation of the solute dimension with concentration is suppressed for rodlike molecules, thereby removing that possible contribution to the observed behavior. Data on $c/\mathbf{R}_{Vv}(0,c)$ for a rodlike polyelectrolyte (*cis*-PBO) and a structural variant of that chain introducing rotational isomers that deviate from the rodlike structure (*ab*-PBO) are given for different values of the ionic strength shown in Figure 10a demonstrate the behavior described above, with extreme curvature in $c/\mathbf{R}_{Vv}(0,c)$ for the system at low ionic strength, and tending to give more normal behavior for $c/\mathbf{R}_{Vv}(0,c)$ and values of $A_{2,LS}$ expected for a neutral rodlike chain with an ionic strength sufficiently high to screen intermolecular electrostatic interactions. That is, the observed A_2 is approximated by Equation 64 with $a(\hat{a}/L,z) = 1$ for $A_2^{(R)}$ given above:

$$A_2 \;=\; A_2^{(R)} \;=\; (\pi N_A/4M_L^2)\, d_{Thermo} \tag{138}$$

where $d_{Thermo} \approx \kappa^{-1}$ [76, 120]. The data on $c/\mathbf{R}_{Hv}(0,c)$ included in this figure are discussed in the section below on chains with optically anisotropic scattering units.

<<Figure 10 a & b>>

6.3 Heterodisperse solute, identical optically isotropic scattering elements

The effect of molecular weight heterogeneity on $B_{LS}(c)$ determined at zero scattering angle for a solute heterodisperse in M, but comprising optically identical isotropic scattering elements, is given by expansion of $\widetilde{B}_{\nu\mu}(c)$ in c, and retaining only the first term,

$$\widetilde{B}^0_{LS} \;=\; M_w^{-2} \sum_{\nu}^{C} \sum_{\mu}^{C} w_\nu w_\mu M_\nu M_\mu \widetilde{B}^0_{\nu\mu} \tag{139}$$

With the use of this with the preceding evaluation of $c\Gamma_{LS}(c)$ for a dilute solution, $\widetilde{B}^{0}_{LS} \approx 2A_{2,LS}$and $\widetilde{B}^{0}_{\nu\mu} \approx 2A_{2,\nu\mu}$ to this order in c, so that

$$A_{2,LS} = M_w^{-2} \sum_{\nu}^{C} \sum_{\mu}^{C} w_\nu w_\mu M_\nu M_\mu A_{2,\nu\mu} \tag{140}$$

By comparison, for measurements of the osmotic pressure for the same material [37],

$$\frac{\Pi M_n}{RTc} = 1 + A_{2,\Pi} M_n c + \ldots \tag{141}$$

$$A_{2,\Pi} = \sum_{\nu}^{C} \sum_{\mu}^{C} w_\nu w_\mu A_{2,\nu\mu} \tag{142}$$

Theoretical evaluations of the "cross-terms" $A_{2,\nu\mu}$ for $\nu \neq \mu$ for flexible chain polymers have proved elusive, in contrast to the rigorous solution available for spheres interacting through a hard-core potential. For example, several experimental studies spread over a number of years, conducted by a number investigators, on solutions in good solvents of mixtures of two flexible chain polymers differing only in M have shown that the dependence of the "cross-term" $A_{2,12}$ on the composition and molecular weight ratio of the components is poorly predicted by available theoretical estimates [121-134]. The exact solution is available for spherical solutes interacting though a hard-core potential, giving $A_{2,\nu\mu}$ in terms of the excluded volume $U_{\nu\mu}$ for spheres of radii R_ν and R_μ, with 2R in U for the monodisperse case replaced by the arithmetic mean $(R_\nu + R_\mu)/2$ for the interacting pair, and M^2 replaced by $M_\nu M_\mu$ [119], so that,

$$M_\nu M_\mu A_{2,\nu\mu} = [(M_\nu^2 A_{2,\nu\nu})^{1/3} + (M_\mu^2 A_{2,\mu\mu})^{1/3}]^3/2 \tag{143}$$

where the $A_{2,\nu\nu}$ are the second virial coefficients for monodispersed spheres, i.e., $A_{2,\nu\nu} \propto R_\nu^3/M_\nu^2 \propto M_\nu^{-\gamma}$, with $\gamma = 1$ for spheres interacting through a hard core potential.

Given the lack of a definitive theory for mixed solute for flexible chain polymers, resort is made to approximations for systems with a distribution of M. Thus, in one approximation, the observation that A_2 can often be approximated by a power-law for a monodisperse polymeric solute, say $A_2 =$

$k_{A_2}M^{-\gamma}$, provides motivation to use this form to estimate $A_{2,LS}$ and $A_{2,\Pi}$ for heterodisperse polymeric solute, using the a generalization of the expression for spherical solute given above [29, 135]:

$$M_\nu M_\mu A_{2,\nu\mu} = k_{A_2}\left[M_\nu^{(2-\gamma)/3} + M_\mu^{(2-\gamma)/3}\right]^3/2 \quad (144)$$

For example, in the so-called good solvent limit for flexible chain polymers, for which $A_2M^2/N_AR_G^3$ approaches a constant and $R_G^2 \propto M^\varepsilon$, then $\gamma = 2 - 3\varepsilon/2$, or $\gamma \approx 1/5$ with $\varepsilon \approx 6/5$. Alternatively, a simpler empirical form to use is given by the geometric mean $A_{2,\nu\mu} = (A_{2,\nu\nu}A_{2,\mu\mu})^{1/2}$. [67, 127, 133, 135] In either case, one can compute $A_{2,LS}$ and $A_{2,\Pi}$ as would be deduced from light scattering and osmometry, respectively, in the forms

$$A_{2,LS} = k_{A_2}M_W^{-\gamma}\,\Omega_{LS} \quad (145)$$

$$A_{2,\Pi} = k_{A_2}M_n^{-\gamma}\,\Omega_{\Pi} \quad (146)$$

Thus, the functions Ω_{LS} and Ω_Π provide measures, respectively, of the deviation of the functions $A_{2,LS}$ vs M_w and $A_{2,\Pi}$ vs M_n from the behavior for A_2 vs M that would be observed for a monodisperse sample of the same solute. Using the first approximation above for $A_{2,\nu\mu}$, one obtains [29, 135]

$$\Omega_{LS} = \left\{M_{(2-\gamma)}^{2-\gamma} + 3M_{(2[2-\gamma]3)}^{2[2-\gamma]/3}M_{([2-\gamma]3)}^{[2-\gamma]/3}\right\}/4M_W^{2-\gamma} \quad (147)$$

$$\Omega_\Pi = \left\{M_{(1-\gamma)}^{1-\gamma}M_n^{-1} + 3M_{([1-2\gamma]3)}^{[1-2\gamma]/3}M_{(-[1+\gamma]3)}^{-[1+\gamma]/3}\right\}/4M_n^{-\gamma} \quad (148)$$

where the molecular weight averages $M_{(\ldots)}$ are defined in footnote (b) of Table 2. With the use of the geometric mean approximation for $A_{2,\nu\mu}$ [67]

$$\Omega_{LS} = (M_{(1-\gamma/2)}/M_w)^{2-\gamma} \quad (149)$$

$$\Omega_\Pi = (M_{(-\gamma/2)}/M_n)^{-\gamma} \quad (150)$$

In this case, use of the Schulz-Zimm distribution of molecular weight, for which

$$M_{(a)} = (1/y)\{\Gamma(1 + h + a)/\Gamma(1 + h)\}^{1/a} \quad (151)$$

with $1/y = M_n/h = M_w/(1+h)$, etc., gives $A_{2,\Pi}/A_{2,LS} = [(1 + h)/(1 + h - \gamma/2)]^2$ for the use of the geometric mean approximation, demonstrating the general result that $A_{2,\Pi} \geq A_{2,LS}$, with the equality holding for a sample monodisperse in molecular weight. The rather more complicated result for the use of Equations 147 and 148 gives somewhat larger $A_{2,\Pi}/A_{2,LS}$ for a given polydispersity, with the discrepancy increasing with increasing heterodispersity. Perhaps of more interest, both Ω_{LS} and Ω_{Π} decrease with decreasing h (increasing heterodispersity) for the geometric mean approximation, and increase with increasing h for the other model. The deviation of Ω_{LS} from unity is smaller than that for Ω_{Π} for both models, with deviations of Ω_{LS} from unity of about ten percent at most for $\gamma = 0.2$, showing that $A_{2,LS}$ vs M_w is predicted to be close to the behavior for A_2 vs M for a monodisperse solute with either model, see Figure 11.

<<Figure 11>>

6.4 Optically diverse, isotropic scattering elements

The scattering from dilute solutions of copolymers or mixtures of polymers differing in their chemical composition may introduce additional complications. For example, for such systems, in addition to the complications for M_{LS} discussed above, one has

$$\tilde{B}_{LS}(c) = M_{LS}^{-2} \sum_{\nu}^{C} \sum_{\mu}^{C} w_\nu w_\mu \tilde{\psi}_\nu \tilde{\psi}_\mu M_\nu M_\mu \tilde{B}_{\nu\mu}(c) \quad (152)$$

so that by expansion of $\tilde{B}_{\nu\mu}(c)$ in c, and retaining only the first term,

$$\tilde{B}^0_{LS} = M_{LS}^{-2} \sum_{\nu}^{C} \sum_{\mu}^{C} w_\nu w_\mu \tilde{\psi}_\nu \tilde{\psi}_\mu M_\nu M_\mu \tilde{B}^0_{\nu\mu} \quad (153)$$

With the use of this with the preceding evaluation of $c\Gamma_{LS}(c)$ for a dilute solution, $B^0_{LS} = 2A_{2,LS}$, and $\tilde{B}^0_{\nu\mu} = 2A_{2,\nu\mu}$, so that

$$A_{2,LS} = M_{LS}^{-2} \sum_{\nu}^{C} \sum_{\mu}^{C} w_\nu w_\mu \tilde{\psi}_\nu \tilde{\psi}_\mu M_\nu M_\mu A_{2,\nu\mu} \quad (154)$$

The case for mixtures of polymers with each component itself comprising identical scattering elements, but with differing composition among the components, may be treated by the use of the full expression for $B_{LS}(c)$ given above (at zero scattering angle) to account for variations in the refractive index and thermodynamic interactions among the polymeric components for pauci-dispersed solute, usually ternary systems, often with the objective of determining the cross-term" $A_{2,12}$ from experimental data [136-148]. In practice, the tendency for dissimilar polymers to separate into two phases places limitations on such work. Similarly, with the behavior of copolymers may be compromised by the formation of micelles with increasing c, requiring consideration of an effective molecular weight that increases with increasing c to form species that interact as particles, e.g., spheres or rods [86]. This complication is suppressed for a polymeric solute comprising random or alternating placements of the comonomers, but the interpretation of $A_{2,LS}$ in terms of the composition can be elusive [124, 125, 149-151].

6.5 Optically anisotropic scattering elements

For a monodisperse solute with identical, optically anisotropic scattering elements, the vertical and horizontal components of light scattered with vertically polarized incident light, $R_{Vv}(0,c)$ and $R_{Hv}(0,c)$, respectively, are given by [9, 20, 57, 75, 152-154]:

$$\frac{Kc}{\mathbf{R}_{Vv}(0,c)} = \left(\frac{1}{M(1+4\delta^2/5)}\right)\{1 + 2\left(\frac{1-\delta^2/10}{1+4\delta^2/5}\right) A_2 M\, c + \ldots\} \qquad (155)$$

$$\frac{Kc}{\mathbf{R}_{Hv}(0,c)} = \frac{5}{3M\delta^2}\{1 - A_2 M\, c/4 + \ldots\} \qquad (156)$$

with the latter limited to rodlike chains.

The dependence of the molecular anisotropy on the chain conformation and the intrinsic anisotropy δ_o of the scattering elements making up the chain are discussed above. As may be seen, the dependence of $Kc/\mathbf{R}_{Hv}(0,c)$ on c is expected to be much smaller than that of $Kc/\mathbf{R}_{Vv}(0,c)$ for a given value of A_2. Behavior of this kind is seen in Figure 10a for a rodlike polymer (*cis*-PBO),

albeit one heterodisperse in molecular weight ($M_w/M_n \approx 1.5$). Owing to the suppressed dependence on c, $Kc/\mathbf{R}_{Hv}(0,c) \approx [Kc/\mathbf{R}_{Hv}(0,c)]^0$ in dilute solutions.

7. Scattering from non dilute solution at zero scattering angle

7.1 The basic relation

In this section, attention is focused on the scattering in the RGD regime at zero scattering angle. As with the preceding section, most of the section will consider a solute comprising identical isotropic scattering elements, so that the subscript denoting the polarization state will be suppressed, as only $\mathbf{R}_{Vv}(q,c)$ will be of interest in this section unless otherwise specified. With these provisions, the basic equation is given by Equation 5 with $P(q,c) = 1$ and $B_{LS}(c)$ simplified to read

$$\widetilde{B}_{LS}(c) = M_{LS}^{-2} \sum_{\nu}^{C} \sum_{\mu}^{C} w_\nu w_\mu \widetilde{\psi}_\nu \widetilde{\psi}_\mu M_\nu M_\mu \widetilde{B}_{\nu\mu}(c) \tag{157}$$

which, together with Again, as in the preceding, since the discussion will begin with considerations for a solute monodisperse in M, the subscript "LS" will be suppressed until the discussion moves to a heterodisperse solute. As discussed above, the crossover from dilute to moderately concentrated solutions may be identified with the dimensionless concentration given by Equation 129, i.e., $\hat{c} = cN_AR_G^3/M$. A dilute solution is then one with $\hat{c} < 1$, so that on average, the solute species are separated by a distance larger than the average dimension. An additional characteristic concentration must be anticipated, marking the transition from a moderately concentrated to a concentrated solution, for which, for example, one might expect a mean-field treatment, such as some generalized form of the Flory-Huggins model, to be a reasonable approximation.

7.2 Low concentrations: The third virial coefficient

For solutions with $\hat{c} < 1$, but too large to neglect the term in c^2 in the virial expansion of $c/\mathbf{R}(0,c)$, the next highest order effect in c may be analyzed through the third virial coefficient A_3, see Equation 132. Indeed, some authors have examined $c/\mathbf{R}(0,c)$ for (nearly) monodispersed polymers in good solvents (for which $A_2M^2/N_AR_G^3 = \psi_2 \approx \Psi_\infty$) to evaluate A_3, to find behavior similar to that predicted theoretically for spherical solute interacting through a hard-core potential such that $A_3M = \Upsilon_3(A_2M)^2$, with Υ_3 independent of M in the good solvent limit (the symbol g has often been used in the literature in place of Υ_3, but that is avoided here owing to the use of g in connection with the

dimensions of branched chains). As mentioned above, for the spherical model, $\Upsilon_3 = 5/8$. Experimental data on linear flexible chain polymers in good solvents have given a similar result, but with $\Upsilon_3 \approx 0.2\text{-}0.3$ [126, 155, 156], in reasonable accord with Monte-Carlo simulations [157]and the predictions of a smoothed-density model for $A_2$and A_3 [158], and smaller than a number of theoretical results [29]; this observation was invoked above in writing Equation 136. It appears that Υ_3 is enhanced toward 5/8 for star-branched flexible chains, as may be reasonable in view of the higher repeat unit density in such configurations [159, 160].

Experimental evaluation of A_3 for dilute solutions under Flory Theta solvent conditions, for which $A_2 = 0$, show that that $A_3 > 0$ [161, 162], in accord with observations discussed below for moderately concentrated solutions. This result is similar to that for a gas at low pressure at the Boyle temperature for which the second virial coefficient vanishes but the third remains positive [119]. The nonzero value of A_3 in this case is attributed to a nonzero irreducible ternary cluster integral β_3, even though the binary cluster integral $\beta_2 = 0$ at the Flory theta temperature with $A_2 = 0$ [9]. In a good solvent, ternary interactions represented by pair-wise additivity of terms involving β_2 dominate contributions from , and one can apply the celebrated two-parameter theory with the neglect of β_3 to treat A_2 and A_3 [27, 29, 45]. Analytical theoretical treatments and simulations confirm this behavior for flexible chain polymers[157, 163, 164].

For a solute heterodisperse in M, the first two terms in the expansion of $B_{LS}(c)$ give

$$\widetilde{B}_{LS}(c) \approx M_{LS}^{-2} \sum_{\nu}^{C} \sum_{\mu}^{C} \tilde{\psi}_\nu \tilde{\psi}_\mu \left(w_\nu w_\mu M_\nu M_\mu \widetilde{B}^0_{\nu\mu} + \sum_{\kappa}^{C} w_\kappa \left[\widetilde{B}^0_{\nu\mu\kappa} - M_\kappa \widetilde{B}^0_{\nu\kappa} \widetilde{B}^0_{\mu\kappa} \right] c \right) \quad (158)$$

where the partial specific volume of each component has been approximated by its infinite dilution limit in obtaining the second term [44]. With the use of this in the virial expansion for $c/\mathbf{R}(0,c)$ for a solute comprising optically identical solute,

$$\begin{aligned} A_{3,LS} \approx\ & M_w^{-2} \sum_{\nu}^{C} \sum_{\mu}^{C} \sum_{\kappa}^{C} w_\nu w_\mu w_\kappa M_\nu M_\mu A_{3,\nu\mu\kappa} \\ & - (4/3) M_w^{-3} \sum_{\nu}^{C} \sum_{\mu}^{C} \sum_{\kappa}^{C} \sum_{\sigma}^{C} w_\nu w_\mu w_\kappa w_\sigma M_\nu M_\mu M_\kappa M_\sigma \left[A_{2,\nu\kappa} A_{2,\mu\kappa} - A_{2,\nu\kappa} A_{2,\mu\sigma} \right] \end{aligned} \quad (159)$$

where $A_{2,\nu\mu} = \widetilde{B}^{0}_{\nu\mu}/2$ (as above) and $A_{3,\nu\mu\kappa} = \widetilde{B}^{0}_{\nu\mu\kappa}/3$. This expression has been used to deduce the several cross-terms from measurements of $A_{3,LS}$ on a solute containing two homopolymers (C = 2) differing in molecular weight, but to show that none of the theoretically predicted Υ_3 fit experiment [126].

7.3 Concentrated solutions

Despite the special cases discussed in the preceding paragraph, for most systems, the virial expansion is inadequate unless the solution is dilute ($\hat{c} << 1$), and developments to treat non dilute solutions are often based on the use of Equation 14, which is valid for a monodisperse solute. For example, for monodispersed, optically homogeneous spheres interacting through a hard-core potential, calculations including three-body interactions give

$$c\Gamma(c) = \varphi\frac{8 - 2\varphi}{(1 - \varphi)^4} \qquad (160)$$

where the volume fraction $\varphi = (4\pi/3)N_A R^3 c/M$ for spheres of radius R, and $A_2Mc = 8\varphi$ [20, 165]. A treatment including interparticle interactions to all orders results in the addition of $4\varphi^2 - \varphi^3$ in the numerator [86], see the next section for a comparison of these two forms.

Similarly, the expression for Π derived from the Flory-Huggins theory of polymer solutions may be used to estimate $\Gamma(c)$ in the appropriate concentration range for an optically homogeneous solute; as will be seen below, this is most relevant for a concentrated solution (or melt of a mixture of polymers). Thus, for a monodisperse solute [37]:

$$\Pi V_1/RT = -\{\ln(1 - \varphi) + (1 - 1/r)\varphi + \chi\varphi^2\} \qquad (161)$$

where φ is the volume fraction of the polymer, r is the ratio of the molar volumes of the polymer to that of the solvent, V_1 is the molar volume of the solvent, and $\chi RT\varphi^2$ is the non-combinatorial part of the chemical potential as represented in the Flory-Huggins model; χ is expected to be a constant for a given polymer/solvent pair in that model, but invariably is observed to depend on φ. With this expression,

$$\Gamma(c) = \frac{v_2^2 M}{V_1}\left(\frac{1}{1-\varphi} - 2\chi - \varphi\frac{\partial\chi}{\partial\varphi}\right) \quad (162)$$

where v_2 is the specific volume of the polymer. In the early literature, this expression was applied to the entire range of concentration, usually on the assumption that any dependence χ on concentration could be accommodated by a virial expansion [12, 44, 45]:

$$\chi(\varphi) = \chi_1 + \chi_2\varphi + \chi_3\varphi^2 + \ldots \quad (163)$$

Thus, expansion of Equation 162 for $\Gamma(c)$ for small φ gives A_2 independent of M, and equal to $A_2^{(L)} = (v_2^2/V_1)[(1/2) - \chi_1]$. In subsequent developments for dilute solutions to account for the molecular weight dependence of A_2 leading to relations of the form expressed in Equation 64, $A_2^{(L)}$ is identified with $A_2^{(R)}$, with d_{Thermo} in $A_2^{(R)} \propto [(1/2) - \chi_1]$. This assignment give the well-known result that the Flory theta temperature Θ, for which both A_2, and d_{Thermo} are zero, occurs with $\chi_1 = 1/2$. Alternatively, in a commonly used nomenclature [37],

$$\frac{1}{2} - \chi_1 = \psi_1(1 - \Theta/T) \quad (164)$$

so that $(1/2) - \chi_1$ is zero for $T = \Theta$.

As an alternative to Equation 163 with arbitrary χ_i chosen to fit a set of data, since it appears that data for χ tends to 1/2 as φ goes to unity for solutions in good solvents [118], the constrain $\Sigma\chi_i = 1/2$ might reasonably be considered in conjunction with Equation 163. This seems to be consistent with data shown in Figure 12 showing bilogarithmic plots of $(\Pi M/RTc) - 1$ as a function of $\varphi/2$ for solutions of polyisobutylene in cyclohexane, from measurements of the osmotic pressure, or converted from measurements of the vapor pressure [166, 167]. The dashed curve is computed with a fit and 163 with $\chi(\varphi) = 0.42 + 0.08\varphi$, and this same expression was used with Equations162 compute the solid curve shown for $[K_{op}cM/\mathbf{R}(0,c)] - 1$ vs. φ. The straight line power-law portion of the behavior, given by the use of Equation 163 in this linear form, is consistent with the scaling expected for moderately discussed in the next section. The conditions for the transition from a moderately concentrated to a concentrated solution are somewhat murky, but are generally thought to lie in the range of 0.2-0.4 weight fraction polymer [9, 118, 168] (with the exception of the example for rodlike chains discussed in the preceding, for which that transition is marked by a change from a disordered, isotropic solution to an ordered mesophase). The deviation the power-

law regime, occurring for $\varphi \approx 0.2$ may be a reasonable estimate of the transition in this case, in reasonable accord with estimates found in the literature.

<<Figure 12>>

The approximation applied in the preceding paragraph for a good solvent need not be expected to apply under Flory Theta solvent conditions, for the reasons discussed in the preceding discussion. Data on the parameter χ in the Flory-Huggins expression given above are shown in Figure 13 on several polymer-solvent systems under Flory theta conditions, with all of the data at the higher concentrations arising from either osmotic pressure or vapor pressure measurements, reflecting the difficulty of obtaining "dust-free" preparations in this regime for light scattering investigations. The data are fitted rather well by the empirical expression

$$\chi = \chi_1 + \chi_2 \frac{\varphi}{\sqrt{1-\varphi}}; \quad \text{"Flory theta solvent conditions"} \tag{165}$$

with $\chi_1 = 1/2$, leaving χ_2, related to A_3M, as a disposable parameter; as with the series expansion of χ in φ given above, this form has no known basis in theory. With this expression for χ,

$$\Gamma(c) = \frac{v_2^2 M}{V_1}\left(\frac{1}{1-\varphi} - 2\chi_1 - \chi_2\varphi\left(2 + \frac{1-(1+n)\varphi}{(1-\varphi)^{1+n}}\right)\right) \tag{166}$$

with $n = 1/2$. Curiously, it appears that χ_2 is essentially invariant with system for these examples, with $\chi_2 \approx 0.30$. Deviation from power-law behavior is seen to develop for φ greater than about 0.5, suggesting that in this case that concentration marks the transition from moderately concentrated behavior to the response for a concentrated solution under Flory theta conditions, at least for these systems.

<<Figure 13>>

7.4 Moderately concentrated solutions

In general, for moderately concentrated solutions ($\hat{c} \approx$ 1-10), neither the virial expansions for dilute solutions nor the mean-field treatments for concentrated solutions will be adequate. There are,

however, exceptions: solutions of rodlike chains in good solvents and flexible chain polymers under Flory Theta conditions. Thus, a notable exception to the failure of the virial expansion in this regime may be the behavior for rodlike polymers, for which the constrained configuration of the chains limits interchain interactions, leading to simplified behavior for disordered solutions; such solutions will form a mesophase, often nematic or cholesteric (twisted nematic) as the concentration is increased beyond the limits of interest here. For example, as may be seen in Figure 14 , data on $Kc/\mathbf{R}_{Vv}(0,c)$ for moderately concentrated solutions of poly(benzyl glutamate) are well fitted by Equation 132, retaining only terms to order c, showing that terms involving A_3 and higher virial coefficients may be neglected in this case for the concentration range shown (although this material is slightly optically anisotropic, the effect of the $\mathbf{R}_{Hv}(0,c)$ is negligible in this context) [9, 169]. A similar simplified behavior is observed for flexible chain polymers under Flory theta conditions, for which A_2, but not A_3, is equal to zero. As may be seen in Figure 15, the simple expression obtained with neglect of terms in A_4 and higher virial coefficients suffices to describe the data shown on moderately concentrated solutions [9, 169]:

$$c\Gamma(c) \approx 3A_3Mc^2 \tag{167}$$

In Figure 15, the data on $c\Gamma(c)$ are shown as a function of $[\eta]c$ as a surrogate for $\hat{c}$ since for these solutions the intrinsic viscosity $[\eta]$ is proportional to R_G^3/M, and $\hat{c} \approx 6.8\,[\eta]c$. The data give $c\Gamma(c) \propto ([\eta]c)^2$, which is the behavior expected if $c\Gamma(c) = 3A_3Mc^2$, suggesting that the effects of the higher order terms in the virial expansion are negligible in this case. As discussed in the section on the third virial coefficient, the nonzero value of A_3 is attributed to a nonzero irreducible ternary cluster integral β_3, even though the binary cluster integral $\beta_2 = 0$ at the Flory theta temperature with $A_2 = 0$ [9].

<<Figure 14>>

<<Figure 15>>

The crossover from the dilute solution behavior of flexible chain polymers to an appropriated form in a concentrated solution remained unresolved for nearly thirty years until a simple scaling argument provided insight for the behavior in a good solvent [46]. The simplified argument for the

scaling starts with the assumption that the form given above in which ΠM/RTc is represented as a series in A_2Mc may be modified for a moderately concentrated solution to give a power-law dependence:

$$\Pi M/RTc \quad \propto \quad (A_2Mc)^{1+p} \tag{168}$$

with p to be determined by the stipulations that for a high molecular weight chain in a good solvent $A_2M^2/N_AR_G^3$ is a constant, with $R_G^2 \propto M^{\varepsilon}$ and $\varepsilon \approx 6/5$, and that Π should not depend on M for such a system in moderately concentrated solutions. It may be noted, that with the first assumption, $A_2Mc \propto c/\hat{c}$, and some authors start from that representation [9, 45, 118]. The stipulations require that $(1+p)[(3\varepsilon/2) - 1] = 1$, or $p = (4 - 3\varepsilon)/(3\varepsilon - 2) \approx 1/4$ in the limiting case of a good solvent and very large M. Consequently, the overall dependence gives $\Pi \propto c^{9/4}$, and

$$c\Gamma(c) \quad \propto \quad (A_2Mc)^{1+p} \tag{169}$$

Although it has not been generally noted, as remarked above, an approximate power-law behavior is implicit in the use of the mean-field expressions discussed in the preceding section over a similar range of concentrations, as should be anticipated as these forms have been fitted to experimental data on a wide range of polymer solutions. With these results, both ΠM/RTc and $KcM/\mathbf{R}(0,c)$ are expected to scale as power laws of A_2Mc (or $c/\hat{c}$) for moderately concentrated solutions of high molecular weight polymers in good solvents. In reality, for many systems in the molecular weight range of interest, ε lies between the value of unity observed at the Flory theta temperature, and the value 6/5 for the limiting good solvent. Moreover, this scaling must be absolutely inappropriate at the Flory theta temperature, since then $A_2 = 0$, but $A_3 > 0$. The preceding motivates representations of ΠM/RTc and cΓ(c) in a system with $A_2 > 0$ through the use of a Padé expressions in A_2Mc to cover both the behavior in dilute solution, expressed in Equation 135, and that in a moderately concentrated solution, expressed in Equations168 and 169:

$$\Pi M/RTc \quad \approx \quad 1 \; + \; A_2Mc\{1 + (\Upsilon_3/p)A_2Mc\}^p; \qquad \text{"good solvent"} \tag{170}$$

With this expression,

$$KcM/\mathbf{R}(0,c) \approx 1 + 2A_2Mc\{1 + (\Upsilon_3/p)(2A_2Mc)\}^pJ(A_2Mc); \quad \text{"good solvent"} \quad (171)$$

where $J(A_2Mc) \approx 1$ (ref hager2) and $\Upsilon_3 = A_3M/(A_2M)^2$ tends to a constant $\Upsilon_{3,\infty}$ in a good solvent. Data on $\Pi M/RTc$ and $KcM/\mathbf{R}(0,c)$ vs A_2Mc and $\Pi M/RTc$ vs $A_2Mc/2$ are shown superposed in Figure 16 for several polymers, in several solvents ranging in "goodness", with p calculated using known values of ε (all smaller than the limiting 6/5 appropriate for a very high molecular weight sample in a "good solvent"). The expression for $c\Gamma(c)$ may be represented in terms of $c/\hat{c}$, with some loss of information (i.e., suppression of the value of $A_2M^2/N_AR_G^3$) as

$$c\Gamma(c) \propto (c/\hat{c})\{1 + (k/p)c/\hat{c}\}^p \quad (172)$$

For use over the range from Flory theta conditions to a good solvent, with k empirically determined, and p = = $(4 - 3\varepsilon)/(3\varepsilon - 2)$ as above, so that p tends to 1/4 in a very good solvent ($\varepsilon \approx 6/5$), or to unity under Flory theta conditions ($\varepsilon \approx 1$). Alternatively, the expression involving A_2Mc may be modified by a term that is negligible in a good solvent, but important under when $A_2M^2/N_AR_G^3$ is much smaller than its limiting value for a good solvent:

$$c\Gamma(c) \approx 2A_2Mc\{1 + (\Upsilon_3/p)(2A_2Mc)\}^p + 3A_3Mc^2\{1 - 1/\Upsilon_3\} \quad (173)$$

This expression was used above to estimate A_3M from the data in Figure 16 for the scattering from a moderately concentrated solutions under Flory theta conditions.

<<Figure 16>>

The preceding has been limited to the behavior of monodisperse solute, and the behavior with a solute heterodisperse in M is likely to exhibit less universal behavior than that described above. Thus, for dilute solutions, the behavior will involve $A_{2,LS}$ (or $A_{2,\Pi}$), but it can be expected that this dependence on the chain length distribution will be suppressed as the concentration is increased toward the upper limits of the moderately concentrated regime, and will be absent for concentrated solutions.

8. Scattering dependence on q for arbitrary concentration

8.1 The basic relation

Here, attention will be restricted to solute comprising identical, isotropic scattering elements. In this regime, the full expression for c/**R**(q,c) must be employed, requiring consideration of the angular dependence embedded in the function

$$\frac{K_{op}cM}{\mathbf{R}(q,c)} = \frac{1}{P(q,c)} + c\Gamma(c)H(q,c) \qquad (174)$$

where in general one cannot expect P(q,c) = P(q,0) nor H(q,c) ≈ 1 over a wide range in c.

8.2 Dilute to low concentrations

As in the preceding section, the discussion begins in the concentration regime for which contributions from terms involving the third virial coefficient are important. In this regime, virial expansions in $\hat{c}$ of may be applied to obtain c/**R**(q,c) in the form given by Equation 174, with P(q,c) replaced by P(q,0), Γ(c) given by the virial expansion presented in the preceding, and H(q,c) replaced by a function $\hat{H}(q,c)$ that includes the variation of P(q,c) with c [9, 29, 170]:

$$\frac{K_{op}cM}{\mathbf{R}(q,c)} = \frac{1}{P(q,0)} + c\Gamma(c)\hat{H}(q,c) \qquad (175a)$$

$$\hat{H}(q,c) = \frac{2\psi_2 W_2(q)\hat{c} + \{3\psi_3 W_3(q) + 4[P(q,0)W_2(q)^2 - W_3(q)]\psi_2^2\}\hat{c}^2}{2\psi_2\hat{c} + 3\psi_3\hat{c}^2} + \ldots \qquad (175b)$$

where the functions $W_2(\vartheta)$ and $W_3(\vartheta)$ have been elaborated for special models and, as above, the $\psi_j = A_j M(M/N_A R_G^3)^{j-1}$ are dimensionless virial coefficients. The functions $W_2(\vartheta)$ and $W_3(\vartheta)$ involve the distribution of the center of gravity of pairs of solute molecules (or particles). For example, in the so-called "single-contact" approximation for dilute solutions of random-flight chain polymers, $W_2(\vartheta) = 1$ [43], to recover the simple result given above with $\hat{H}(q,c) = 1$ to order $\hat{c}$ in Equation 175. It may be noted that although the assumption of single-contacts among pairs of chains may be dubious for flexible chain molecules, it is appropriate for rodlike chains in a dilute solutions, on a purely geometric basis. Although $W_2(q)$ has been computed for a flexible chain with excluded volume interactions, experimental observations on dilute solutions suggest that data

on c/**R**(q,c) may be fitted by the use of the simple expression given above with H(q,c) = 1 and with P(q,c) approximated by the random-flight expression for P(ϑ,0), with âL/3 replaced by the value âLα^2/3 for a chain with excluded volume.

Under Flory theta conditions, for which $\psi_2 = 0$, the expression above simplifies to give P(q,c) = P(q,0) and $\hat{H}(q,c) = W_3(\vartheta)$ to order $\hat{c}^2$, a result discussed further in the following.

With Equation 175, if $\hat{H}(q,c) = 1$, as expected for a dilute solution, curves of c/**R**(q,c) versus q^2 at constant c are expected to be parallel, with intercepts $K_{op}c/\mathbf{R}(0,c) = M^{-1}[1 + c\Gamma(c)]$ and initial tangent $\partial[c/\mathbf{R}(q,c)]/\partial q^2 = R_G^2/3M$. Similarly, curves of c/**R**(q,c) versus c at constant q^2 are expected to be parallel, with intercepts $K_{op}c/\mathbf{R}(q,c) = [K_{op}c/\mathbf{R}(q,c)]^0 = M^{-1}P^{-1}(q,0)$ and initial tangent $\partial[c/\mathbf{R}(q,c)]/\partial c = 2A_2$. This dual parallelism gave rise to the double-extrapolation of the "Zimm-plot" in which $K_{op}c/\mathbf{R}(q,c)$ is plotted as a function of $q^2 + kc$, with k arbitrarily chosen to provide a satisfactory presentation of the data. It should be noted that this dual parallelism is lost if the analyses of $[K_{op}c/\mathbf{R}(q,c)]^{1/2}$ as a functions of c, advocated above, and q^2, suggested for high molecular weight linear flexible chain polymers, are adopted.

8.3 Concentrated solutions

For concentrated solutions, with $\hat{c} >> 1$, statistical mechanical treatments take advantage of the tendency for uniformity in the polymer repeat unit density. A treatment based on an application of the Ornstein-Zernicke formalism that uses approximations appropriate to this regime to permit summation of the many-body interaction terms appearing in the expression for **R**(q,c) leads to Equation 174 with H(q,c) = 1 [42, 124, 125, 171-173]. The method does not provide a prediction for Γ(c), and puts P(q,c) = P(q,0), which may be reasonable for a concentrated solution [9, 37, 46, 118]. The so-called random phase approximation applied to concentrated solutions leads to a similar result [46, 118, 173]. With this simplification, one can define a correlation length from the scattering observed at concentration c by the expression

$$b(q,c)^2 = \mathbf{R}(0,c)\{\partial \mathbf{R}^{-1}(q,c)/\partial q^2\} \quad (176)$$

$$b(q,c)^2 = \{1/[1 + c\Gamma(c)]\}\{\partial P^{-1}(q,c)/\partial q^2\} \quad (177)$$

As will be elaborated in the following, this simple form may be inadequate in moderately concentrated solutions owing to scattering with $H(q,c) \neq 1$, as discussed in the following. Data of this kind reported in the literature often are based on neutron or small-angle x-ray scattering, and tend to be restricted to large values of $R_G^2q^2$ than are characteristic of light scattering, e.g., often in the regime $1/R_G^2 < q^2 < 1/\hat{a}^2$ [118], so that the reported behavior would involve $b(q,c)^2$ determined in this range, or more likely an approximate to this, as the true value of $\mathbf{R}(0,c)$ might not be obtained. For example, in this regime $P(q,0)^{-1} \approx (1 + R_G^2q^2)/2 \approx R_G^2q^2/2$ for the random-flight chain model in the experimental range, for which the experimental data would yield $\partial[K_{o\pi}c/\mathbf{R}(q,c)]^0/\partial q^2 \approx \hat{a}L/6M = \hat{a}/6M_L$. A result of this sort is often inferred in the analysis of neutron or small-angle x-ray scattering in the form of the Ornstein-Zernike expression:

$$\frac{c}{\mathbf{R}(q,c)} = \frac{c}{\mathbf{R}_{app}(0,c)}\{1 + \xi_{O\text{-}Z}(c)^2q^2\} \qquad (178)$$

to express a scaling length $\xi_{O\text{-}Z}(c)$, where $\mathbf{R}_{app}(0,c)$ is the apparent value of $\mathbf{R}(0,c)$ obtained by extrapolation of data on $c/\mathbf{R}(q,c)$ vs q^2 over the limit range in q defined above.

The statistical treatment mentioned above based on the Ornstein-Zernicke approximation, leading $H(q,c) = 1$ for a concentrated solution of a homopolymer also provides a means to compute the scattering for concentrated solutions or melts of blends and copolymers [124, 149-151], as do treatments based on the random phase approximation [174]. These predictions have been used to analyze the scattering from such materials in terms of the "cross-terms" appearing in the model [122, 123, 138, 140-142].

8.4 Moderately concentrated solutions

As with the discussion for the scattering from moderately concentrated solutions at zero angle, the behavior for arbitrary q introduces new complexities as mean-field approximation no longer may be used. Thus, with increasing concentration to the regime for which $\hat{c}$ exceeds about unity, the virial expansions may not be useful, but $\hat{c}$ is not large enough to insure the utility of the mean-field methods. In this case, the scaling length b(q,c) defined above in terms of the angular dependence

of the scattering has the potential for increased complexity, as H(q,c) may not be equal to unity [1, 9]:

$$b(q,c)^2 = \xi_P(q,c)^2 + \xi_H(q,c)^2 \quad (179)$$

$$\xi_P(q,c)^2 = \{1/[1 + c\Gamma(c)]\}\{\partial P^{-1}(q,c)/\partial q^2\} \quad (180)$$

$$\xi_H(q,c)^2 = \{c\Gamma(c)/[1 + c\Gamma(c)]\}\{\partial H(q,c)/\partial q^2\} \quad (181)$$

If H(q,c) = 1, as in the preceding discussion on concentrated solutions, then $\xi_H(q,c) = 0$, and $b(q,c) = \xi_P(q,c)$ is the only correlation length in the problem. Of course, at infinite dilution, H(q,0) = 1, and $b(q,c)^2 = b(0,0)^2 = R_G^2/3$. Data on several systems for which $b(0,c)^2 > 0$ are given in Figures 17 and 18, including solutions of flexible chains in good solvents and under Flory theta conditions [175], and a solution of a helical rodlike chain in a good solvent [176]. The function $b(0,c)^2/b(0,0)^2 = 3b(0,c)^2/R_G^2$ calculated using the observed $\Gamma(c)$ and R_G^2 with the assumption that $\xi_H(0,c) << \xi_P(0,c)$, i.e., $b(0,c)^2/b(0,0)^2 \approx 3\xi_P(0,c)^2/R_G^2$ is also shown. A reasonable, though not complete agreement is observed between the calculated and experimental estimates confirm that this approximation is reasonable.

<<Figure 17>>

<<Figure 18>>

Experimental data on polymer solutions are discussed in the following, but it is convenient to consider first the behavior for (monodisperse) spheres interacting through a hard-core potential offers some insight to the general behavior in a concentrated solution. In this case, P(q,c) = P(q,0) and P(q,0)H(q,c) has been given in two approximations, with the first accounting for three-body interactions [36] and the second providing an approximation for the interactions between all spheres [177]:

$$P(q,0)H(q,c) = P(2q,0)^{1/2} = 3r_1(2y) \quad (182a)$$

$$r_1(x) = [\sin(x) - x\cos(x)]/x^3 \quad (182b)$$

for the first, where y = qR, and for the second treatment,

$$P(q,0)H(q,c) = |Z(2y,\varphi)|/Z(0,\varphi) \tag{183a}$$

$$Z(x,\varphi) = g_1(\varphi)r_1(x) + g_2(\varphi)r_2(x) + g_3(\varphi)r_3(x) \tag{183b}$$

$$g_1(\varphi) = (1 - 2\varphi)^2/(1 - \varphi)^4 \tag{183c}$$

$$g_2(\varphi) = (1 - \varphi/2)^2/(1 - \varphi)^4 \tag{183d}$$

$$g_3(\varphi) = (\varphi/2)g_1(\varphi) \tag{183e}$$

$$r_2(x) = [2x\sin(x) + (2 - x^2)\cos(x) - 2]/x^4 \tag{183f}$$

$$r_3(x) = \{24 - x^4\cos(x) + 4(3x^2 - 6)[\cos(x) + x\sin(x)\,]]\} \tag{183g}$$

With the second treatment, $c\Gamma(c)$ takes on the alternative expression mentioned above, with

$$c\Gamma(c) = 24\varphi Z(0,\varphi) = \varphi\,\frac{8 - 2\varphi + 4\varphi^2 - \varphi^3}{(1 - \varphi)^4} \tag{184}$$

for comparison with Equation 161; these forms are compared in Figure 19b. Owing to the singularities in P(q,0) for monodisperse spheres for certain values of q (or at least small values for heterodisperse spheres), it is convenient to consider the form

$$\frac{\mathbf{R}(q,c)}{K_{op}cM} = \frac{P(q,c)}{1 + c\Gamma(c)P(q,c)H(q,c)} \tag{185}$$

The functions P(q,c)H(q,c) for these two treatments are shown in Figure 19a. Although these results apply to spheres interacting through a hard-core potential, they have been utilized in the analysis of data on (nearly) spherical micelles, some authors have replaced y by $y = 2qR_{app}$, where R_{app} is adjusted to fit experiment [177]. As may be seen in Figures 5 and 9, $P(q,0) \approx \exp(-R_G^2 q^2/3)$ for a substantial range in $R_G^2q^2$ for $R_G^2q^2$ smaller than the value for the first minimum in P(q,0). Consequently, $H(q,c) \approx 1$ for $R_G^2q^2 <$ ca. 4 in this regime, allowing use of the simpler (and more familiar) form given by Equation 175a with $\hat{H}(q,c) = 1$. Substituting the expression given above for $\Gamma(c)$:

$$\frac{K_{op}cM}{\mathbf{R}(q,c)} = \frac{1}{P(q,0)} + \frac{8\varphi - 2\varphi^2 + 4\varphi^3 - \varphi^4}{(1 - \varphi)^4}; \qquad \text{spheres, } R_G^2q^2 < \text{ca. } 4 \tag{186}$$

with $A_2Mc = 8\varphi$.

<<Figure 19 a & b>>

Examples observed for polymer solutions both under Flory theta conditions and in a good solvent [178]are shown in Figures 20 and 21, respectively [9]. It is evident that H(q,c) is not unity, and that the contribution of $\xi_H(q,c)^2$ cannot be neglected for these data. Indeed, for most of the data shown, $\partial R^{-1}(q,c)/\partial q^2 < 0$ for small q, reflecting conditions with $\partial H(q,c)/\partial q^2 < 0$. Although a satisfactory theoretical treatment to estimate H(q,c) is lacking in this regime, it may be remembered that for spherical particles interacting through a hard-core potential, $H(q,c) = P(2q,0)^{1/2}/P(q,0)$. This function is plotted for a range of $u = R_G^2q^2$ in Figure 22 using P(q,0) for the random-flight chain model (in place of P(q,0) for the sphere), along with Q(q,c) calculated for two values of $c\Gamma(c)$ using this H(q,c); this same approximation is used for H(q,c) in Figure 21. The H(q,c) calculated in this rather arbitrary way has some of the features of the observed behavior, though it does not provide a quantitatively accurate fit. The trend in Figure 20 suggests that H(q,c) tends to unity with increasing concentration, as expected with the theoretical treatment discussed above for concentrated solutions.

<<Figure 20>>

<<Figure 21>>

<<Figure 22>>

8.4 Behavior for a charged solute

As noted above, $H(q,c) = P(2q,0)^{1/2}/P(q,0)$ in one treatment for uncharged spheres interacting through a hard-core potential, e.g., see Figure 19. A similar effect will obtain with charged particles in solutions, but at a smaller angle owing to the longer-range of the electrostatic interaction in comparison with that for the hard-core potential, e.g., as is well known, inter-particle electrostatic repulsion among spheres can be strong enough to lead to an ordered mesophase with increasing c if the average separation of the spheres is less than Debye electrostatic scaling length κ^{-1} [14, 179]. In addition, for macromolecules, the chain dimensions may expand with increasing κ^{-1} if $\kappa^{-1} > d_{geo}$, with d_{geo} the geometric diameter of the chain repeat unit; an example of this is

shown in Figure 10b, where it is seen that as expected, R_G^2 does not depend on κ^{-1} for the rodlike chain *cis*-PBO, but does increase markedly at low κ^{-1}, coincident with the large increase in A_2. It should be realized that an aqueous solution of an organic solute is often close to intermolecular association, and that the addition of salt, and consequent suppression of electrostatic interactions, may induce association. Thus, with amphoteric proteins, it is often found that association will occur if the pH is adjusted to the isoelectric point, a condition for which appreciable numbers of anionic and cationic sites coexist on the chain [26]. For a pH far from the isoelectric point, the amphoteric macromolecule behaves as either an anionic or cationic polyelectrolyte, and the net charge can help stabilize the solution against association. The effects of electrostatic interactions among charged spheres dispersed in a medium of low ionic strength can lead to a striking effect on $\mathbf{R}(q,c)/KMc$, resulting from large values of $c\Gamma(c)$ from electrostatic repulsion among the spheres. Thus, in this regime,

$$\mathbf{R}(q,c)/KMc = P(q,c)\{1 + c\Gamma(c)P(q,c)H(q,c)\}^{-1} \approx \{c\Gamma(c)H(q,c)\}^{-1} \quad (187)$$

where $H(q,c)^{-1}$ is expected to exhibit a maximum associated with the distance of average closest approach of the spheres, e.g., the expression for $H(q,c) = P(2q,0)^{1/2}/P(q,c)$ given above for uncharged spheres. Data on several dilute dispersion of charged polystyrene spheres (R = 45 nm) are given in Figure 23 [180]. Similar results are reported for solutions of polyelectrolytes and for other charged particles [180]. These curves bear a qualitative similarity to those obtaining for coated spheres under some conditions with the zero average refractive index increment, but their origin is very different, as is their shape in detail. A first-approximation to $H(q,c)$ might be obtained by using $\sin(\vartheta'/2) \approx (2L_\kappa/R)\sin(\vartheta/2)$ in the expression for hard spheres if $L_\kappa >> R$, where L_κ is an electrostatic length, expected to be related to κ^{-1} [180, 181]. This approximation gives far too sharp a maximum, and values of L_κ to match the position of the maximum that are far larger than κ^{-1} [180]. In addition to the weakness of the *ad hoc* model, at least a part of this discrepancy may reflect heterogeneity or fluctuation of the charge density, which may broaden the peak. Alternative treatments to model such data have been discussed [86].

<<Figure 23>>

9. Special Topics

9.1 Intermolecular association in polymer solutions

Light scattering methods provide a powerful means to investigate intermolecular (or interparticle) association. Intermolecular association is not uncommon in macromolecular solutions or dispersions of particles, especially in aqueous solvent. In general, two forms may be encountered in the extreme: association involving two or more components at equilibrium at any given concentration; and metastable association, in which the components present (i.e., including aggregated structures) depend on processing history, but do not change sensibly with concentration in the range of interest for light scattering. Of course, intermediate situations may also occur, and some of these have been considered in detail [182].

In some cases, metastable association may be revealed by a dependence of the molecular weight deduced from $Kc/\mathbf{R}(q,0)$ at infinite dilution on temperature or solvent, revealing the association. An example of this sort in which the nature of intermolecular association of a solute with a helical conformation was elucidated by the use of static and dynamic light scattering as a function of temperature, even though the scattering at any given temperature exhibited 'normal' behavior, and could not have been analyzed to reveal association if taken alone [183]. In a different and somewhat unusual, but not unique, example, it has been reported that $Kc/\mathbf{R}(q,c)$ is linear in q^2, albeit leading to a molecular weight that is much larger than the true value of M_w for the solute [184]. This was observed with a system that formed a gel at a higher solute concentration, suggesting that the observed scattering behavior reflects the anticipated P(q,c) for a randomly branched polymer [22]. More frequently, with intermolecular association involving flexible chain polymers, $Kc/\mathbf{R}(q,c)$ exhibits enhanced scattering at small q. This is often taken as evidence for the presence of an aggregated species mixed with solute that is either fully dissociated, or much less aggregated. Although reasonable, it should be realized that such an interpretation is not unique. These effects are illustrated in Figure 24.

<<Figure 24>>

The analysis of metastable behavior is sometimes facilitated by an approximate representation with a few 'pseudo components' (often two or three), each of which dominates the scattering over a limited range of q, with M, A_2 and P(q,c) replaced by their light scattering averages for each pseudo component. That is,

$$\mathbf{R}(q,c) = \sum_{\mu} \mathbf{R}_{\mu}(q,c) \approx K \sum_{\mu} \left(\frac{Mc}{P(q,c) + 2A_2Mc} \right)_{\mu,c} \qquad (193)$$

where the subscript "c" indicates that the parameters M and A_2, and the function P(q,c) may depend on c through the dependence of the state of aggregation on c. Note that this form does not properly account for the averaging among scattering elements, neglecting the so-called cross terms accounting for interference of the light scattered by different components, but it can provide a useful approximation if the components are few and widely separated in size, and especially if one component is much larger than the others, but present in minor content. The analysis of the suspected association with this relation is similar to the determination of the size distribution discussed above in the absence of association, but is made more complex as it involves data over a range of c, with concentration dependent parameters, and P(q,c) may not be the same, or even known, for all of the aggregates present, and may depend on c. In some of the literature on small–angle x–ray scattering, it has been common to assume that $P(q,c) \approx \exp[-(R^2_{G,LS}q^2/3]$ for each pseudo component, and frequently to assume that $2A_2c << 1$ in an analysis to estimate $(M_w)_\mu w_\mu$ and $[R^2_{G,LS}]_\mu$ for the assumed pseudo components, as a function of the overall concentration c [36]. Similar treatments are applied with light scattering, often restricted to small enough q that the expansion of P(q,c) for small $R^2_{G,LS}q^2$ may be applied. Although dynamic light scattering is outside the scope of this chapter, it may be noted that the advent of that technique has allowed some improvement in analyses of this type, since one can apply a similar expression for the (electric field) auto-correlation function $g^{(1)}(\tau; q,c)$ as a function of the correlation time τ obtained thereby in terms of pseudo components:

$$g^{(1)}(\tau; q,c) \quad \approx \quad \sum_\mu r_\mu(q,c)\exp[-\tau\, \gamma_\mu\,(q,c)] \tag{194}$$

where $r_\mu(q,c) = \mathbf{R}_\mu(q,c)\,/\mathbf{R}(q,c)$. Analysis of $g^{(1)}(\tau; q,c)$ then provides information on $(M_w)_\mu w_\mu$ and a hydrodynamic length $[a_{LS}]_\mu = kTq^2/6\pi\eta_{solvent}\gamma_\mu\,(q,c)$ for each component, and some degree of consistency is expected among the estimates for $(M_w)_\mu w_\mu$ obtained in the two experiments. Further, comparison of $[a_{LS}]_\mu$ and $[R^2_{G,LS}]_\mu$ can provide insight on the nature of the component. In some cases, it may be reasonable to estimate $(M_w)_\mu$ for the component with smallest $(M_w)_\mu$ with the assumption that $w_\mu \approx 1$ for that component, i.e., the scattering at small q reflects a small fraction of a large component. An example of a treatment of this kind may be found in study on aggregating rodlike polymers [185]. In some cases, the depolarized scattering can be particularly useful if the association induces order in the aggregated species [186, 187].

A well defined analysis is possible, at least in principle, for a case with equilibria among otherwise monodisperse monomers, dimers, etc., e.g., the equilibria obtaining among monomers, dimers and tetramers for hemoglobin in solution [188, 189]. Equilibrium association can lead to nonparallel plots of Kc/**R**(q,c) vs q^2 if the species are large enough. In the ideal situation, the ratio of R_G^2 for the aggregates to the unimer would be precisely known, as would be the effect of association on $A_{2,LS}$, permitting an assessment of the equilibrium constant for the association given a model [189]. An illustrative, if simplified, example of the effects of association is provided by the assumption that a monodisperse linear flexible coil chain of molecular weight M may undergo end-to-end dimerization to create a linear chain of molecular weight 2M, with equilibrium constant K_{eq}. This might, for example, result with chains each with a single end-group A, mixed with an equal number of chains also with a single end-group B that will form a stable complex the A groups at equilibrium. Further, "good solvent" conditions are assumed, with $\partial \ln R_G^2 = \partial \ln M = \varepsilon$, and $\partial \ln A_2 = \partial \ln M = \gamma$, with $\varepsilon = 2(2 - \gamma)/3$, following the usual approximation for flexible chain polymers, as discussed in the preceding. Since the dimers may be considered as components in the light scattering analysis, the values of the parameters $M_{LS}(c)$, $R_{G,LS}^2(c)$, and $P_{LS}(q,c)$ and $A_{2,LS}(c)$ obtaining at solute concentration c are of interest; these may be computed using Equations 22, 56, 86 and140, respectively, along with the approximations given by Equation 58 and the approximation $A_{2,\nu\mu} = (A_{2,\nu\nu}A_{2,\mu\mu})^{1/2}$ discussed above. The results give

$$M_{LS}(c) = M(2 - \zeta(c)) \tag{188}$$

$$R_{G,LS}^2(c) = R_{G,M}^2[\zeta(c) + 2^{1+\varepsilon}(1 - \zeta(c))]/(2 - \zeta(c)) \tag{189}$$

$$P_{LS}(q,c) = \{\zeta(c)[P(q,c)]_M + 2(1 - \zeta(c))[P(q,c)]_{2M}\}/(2 - \zeta(c)) \tag{190}$$

$$A_{2,LS}(c)M_{LS}(c) = A_{2,M}M\{\zeta(c) + 2^{1-\gamma/2}(1 - \zeta(c))\}^2/(2 - \zeta(c)) \tag{191}$$

$$\zeta(c) = (\tilde{K}_{eq}/2A_{2,M}Mc)\{(1 + 4A_{2,M}Mc/\tilde{K}_{eq})^{1/2} - 1\} \tag{192}$$

where $\zeta(c)$ is the fraction of polymer not associated at solute concentration c, and, for the postulated end-to-end association to form dimmers, with P(q,c) given by the expression in Table 3 for the random-flight chain, with L replaced by L^{ε} and $(2L)^{\varepsilon}$ for $[P(q,c)]_M$ and $[P(q,c)]_{2M}$, respectively. The calculations were completed for $\varepsilon = 7/6$ ($\gamma = 1/4$), over a range of $A_{2,M}Mc$ and $\tilde{K}_{eq}$

= $A_{2,M}M^2K_{eq}$. It may be noted that for large K_{eq}, the extrapolation to obtain the true molecular weight M at infinite dilution ($\zeta = 1$) may not be possible, and the experimenter may erroneously assume that the molecular weight of the polymer at infinite dilution is 2M. The effect of the association in producing nonparallel Kc/**R**(q,c) vs q^2 for data at different concentration is illustrated in Figure 25.

<<Figure 25>>

9.2 Intermolecular association in micelle solutions

The light scattering from micellar solutions, which has been of considerable interest in recent years, provides a realistic example of a system with a solute structure at equilibrium and therefore changing with the solute concentration. The behavior of Kc/**R**(0,c) as a function of c for aqueous solutions of wormlike micelles of hexaoxyethylene dodecyl ether, $E_{12}E_6$, is shown in Figure 26a [190]. The display in the bilogarithmic plot reveals a decrease in Kc/**R**(0,c) with increasing c attributed to an increase in $M_{LS}(c)$, largely offsetting the increase in Kc/**R**(0,c) that would usually be expected under good solvent conditions. Theoretical treatments on the association-dissociation equilibria for wormlike micelles suggest that for a range of c, M_w might increase as $M_w \propto c^{1/2}$ [191], motivating the dashed lines with slope –1/2 included in the plot; these are in a reasonable accord with the experiment. Futhermore, it may be noted that for c approaching the range of moderately concentrated solutions, Kc/**R**(0,c) is approaches proportionality with c^2, independent of the molecular weight, as with the behavior for rodlike chains shown in Figure 12. The authors of the cited work analyzed their data Kc/**R**(0,c) as a function of c using the equilibrium theory, that provided expressions for $M_w(c)$ and $\Gamma(c)$ in terms of several parameters, to obtain $M_w(c)$. Following the authors, those estimates are used in Figure 26b in a plot of $\Gamma(c)c = Kc/\mathbf{R}(0,c) - 1/M_w(c)$, which exhibits the anticipated behavior with $\Gamma(c)c \propto c^2$ at the higher concentrations.

<<Figure 26 a & b>>

9.3 Online monitoring of polymerization systems

The availability of instrumentation for parallel characterization of dilute solutions by a number of methods, including static and dynamic light scattering, viscosity, refractive index and UV-visible absorption, etc., has added substantially to the ability to elucidate the structure of polymeric solutes.

This is often used to characterize in eluent from size exclusion chromatography, a subject beyond the scope of this chapter [192], except to note that the topics discussed above for dilute solutions are relevant to the interpretation of static scattering from the eluent. Another application that is finding use is the real-time analysis of a polymerization product, by characterization of solutions obtained by dilution of aliquots obtained from the polymerization reactor or by direct characterization of the reactor solution if sufficiently dilute [193, 194]. With regard to the latter, as mentioned above, the proper transition from dependence on $A_{2,LS}$, to behavior that is essentially independent of the molecular weight distribution as the concentration is increased through the moderately concentrated to the concentrated regime appears to be unresolved.

Table 1

Mean-square radius of gyration for some commonly encountered models

Model	Length scales	R_G^2
Random-flight linear coil ("infinitely thin")	L = contour length â = persistence length	âL/3
Persistent (wormlike) linear chain[a] ("infinitely thin")	L = contour length â = persistence length	(âL/3)S(â/L)
Rod ("infinitely thin")	L = length	$L^2/12$
Disk ("infinitely thin")	R = radius	$R^2/2$
Cylinder	L = length R = radius	$L^2/12 + R^2/2$
Sphere	R = radius	$3R^2/5$
Spherical shell	R = radius (outer) Δ = shell thickness	$(3R^2/5)\left(\frac{1-[1-(\Delta/R)^5]}{1-[1-(\Delta/R)^3]}\right)$
Spherical shell ("infinitely thin")	R = radius (outer)	R
Spheroid	$2R_1$ = unique axis length $2R_2$ = transverse axis length	$R_1^2\left(\frac{2+(R_2/R_1)^2}{5}\right)$

a) $S(Z) = 1 - 3Z + 6Z^2 - 6Z^3[1 - \exp(-Z^{-1})] \approx (1 + 4Z)^{-1}$; $Z = â/L$

Table 2

Light scattering average mean-square radius of gyration and hydrodynamic radius for some power-law models

	$R^2_{G,LS}$	$R_{H,LS}$
Exact Relation[(a)]	$(1/M_w)\sum_{\nu}^{C} w_\nu M_\nu R^2_{G,\nu}$	$M_w/\sum_{\nu}^{C} w_\nu M_\nu R^{-1}_{H,\nu}$
Approximation for[(b)] $R_G \propto R_H \propto M^{\varepsilon/2}$	$(R^2_G/M^{\varepsilon})\, M^{\varepsilon+1}_{(\varepsilon+1)}/M_w$	$(R_H/M^{\varepsilon/2})\, M_w/M^{1-\varepsilon}_{(1-\varepsilon)}$
Random-flight coil[(c)] ; $\varepsilon = 1$	$(R^2_G/M)\, M_z$	$(R_H/M^{1/2})\, M_w/M^{1/2}_{(1/2)} \approx$ $(R_H/M^{1/2})\, M^{1/2}_w (M_w/M_n)^{0.10}$
Rodlike chain (thin)[(c)] ; $\varepsilon \approx 2$	$(R^2_G/M^2)\, M_z M_{z+1}$	$(R_H/M)\, M_w$
Sphere[(c)] ; $\varepsilon = 2/3$	$(R^2_G/M^{2/3})\, M^{5/3}_{(5/3)}/M_w \approx$ $(R^2_G/M^{2/3})\, M^{2/3}_z (M_w/M_z)^{0.10}$	$(R_H/M^{1/3})\, M_w/M^{2/3}_{(2/3)} \approx$ $(R_H/M^{1/3})\, M^{1/3}_w (M_w/M_n)^{0.10}$

(a) For optically isotropic solute, and with $\partial n/\partial c$ the same for all scattering elements.

(b) $M^{\mu}_{(\mu)} = \sum_{\nu}^{C} w_\nu M^{\mu}_\nu$; for example, $M_{(\mu)}$ is M_n, M_w, $(M_w M_z)^{1/2}$ and $(M_w M_z M_{z+1})^{1/3}$

for $\mu =$ 1, 1, 2 and 3, respectively [67].

(c) Approximations are for a solute with a Schulz-Zimm (two-parameter exponential) distribution of M, for which [67]

$M_{(\varepsilon)} \approx M_w \{\Gamma(1 + h + \varepsilon)/\Gamma(1+h)\}^{1/\varepsilon}/(1+h)$

with $(h+1)/h = M_w/M_n$, and $\Gamma(x)$ the gamma function of argument x.

Table 3

Particle scattering functions for some commonly encountered optically isotropic models[a]

Model	R_G^2 [b]		P(q,0)
Random-flight linear coil	âL/3	$u = âLq^2/3$	$p_c(u) = (2/u^2)[u - 1 + \exp(-u)]$
Persistent (wormlike) linear chain[c]	(âL/3)S(â/L)		See the text
Disk ("infinitely thin")[d]	$R^2/2$	y = Rq	$(2y^2)[1 - J_1(2y)/y]$
Sphere	$3R^2/5$	y = Rq	$(9/y^6)[\sin(y) - y\cos(y)]^2$
Shell ("infinitely thin")	R	y = Rq	$[\sin(y)/y]^2$
Rod ("infinitely thin")[f]	$L^2/12$	x = Lq	$p_1(x) = (2/x^2)[x\mathrm{Si}(x) - 1 + \cos(x)]$

(a) Unless given below, the original citations for the expressions presented above, and many more (including a circular cylinder of length L and radius R), may be found in reference 30.

(b) â is the persistence length, L is the contour length and R is the radius where appropriate.

(c) See Table 1 for S(â/L).

(d) $J_1(\ldots)$ is the Bessel function of the first order and kind.

(e) $\mathrm{Si}(x) = \int_0^x ds\{s^{-1}\sin(s)\}$ is the sine integral.

(f) See Equations 115-121 for a rod with optically anisotropic scattering elements.

Definitions of the principal symbols used throughout the text.

(Symbols with limited use in the vicinity of their definition may not be included.)

A_2, A_3	The second virial coefficient, the third virial coefficient, etc.; see Equation 132.
$A_2^{(R)}$	The second virial coefficient for a rodlike chain, appearing in an expression for A_2 for flexible chains, see Equation
B(c)	The thermodynamic interaction function $\{F(0,c) - 1\}/c$; see Equation 7.
$\widetilde{B}(c)$	A thermodynamic interaction function, equal to MB(c), see Equation 5.
F(q,c)	The intermolecular structure factor $\mathbf{R}_{iso}(q,c)/K_{op}cMP_{iso}(q,c)$; see Equation 6.
G(**r**; x)	The distribution function for chain sequences of contour length x and end-to-end vector separation **r**; $\tilde{g}(\mathbf{q},x)$ is the Fourier transform of G(**r**; x), see Equations 88 and 89.
H(q,c)	The function $\{F(q,c)^{-1} - 1\}/c\Gamma(c)P(q,c)$; see Equation 8.
K	An optical constant relating intensities to the Rayleigh ratio.
L	Chain contour length.
M	Molecular weight.
$M_{(\mu)}$	A generalized average molecular weight, (e.g., $M_{(\mu)}$ is M_n, M_w, $(M_wM_z)^{1/2}$ and $(M_wM_zM_{z+1})^{1/3}$ for μ = 1, 1, 2 and 3, respectively), see Table 2
M_L	The mass per unit length, M/L.
M_w	The weight average molecular weight, see Table 2
N_A	Avogadro's constant
P(q,c)	The intramolecular structure factor; see Equation 6.
$P_{Hv}(q,c)$	The intramolecular structure factor for the horizontally polarized component of the scattering with vertically polarized incident light.
$P_{Vv}(q,c)$	The intramolecular structure factor for the vertically polarized component of the scattering with vertically polarized incident light.
Q(c)	The function $\{F(q,c) - 1\}/cB(c)P(q,c)$; see Equation 7.
R_G^2	Mean–square radius of gyration.
R_H	Hydrodynamic radius, defined as $kT/6\pi\eta_s D_T$, with D_T the translational diffusion constant and η_s the solvent viscosity.
R(q,c)	The excess Rayleigh ratio at scattering angle ϑ, for a system with solute concentration c (wt/vol).
$\mathbf{R}_{aniso}(q,c)$	The anisotropic component of **R**(q,c).
$\mathbf{R}_{Hv}(q,c)$	The horizontally polarized component of **R**(q,c) for vertically polarized incident light.
$\mathbf{R}_{iso}(q,c)$	The isotropic component of **R**(q,c); sometimes denoted simply as **R**(q,c) if $\mathbf{R}_{aniso}(q,c) = 0$, and if confusion should not result in the context so used.

$\mathbf{R}_{Vv}(q,c)$	The vertically polarized component of $\mathbf{R}(q,c)$ for vertically polarized incident light.
$S(q,c)$	The total structure factor $\mathbf{R}_{iso}(q,c)/K_{op}cM$; see Equation 6.

$\hat{c}$	A reduced concentration, equal to $cN_AR_G^3/M$
$\hat{a}$	Persistence length for semiflexible chains.
$b(q,c)$	A correlation length obtained from the dependence of $\mathbf{R}_{Vv}(q,c)$ on q ; see Equation 176.
c, c_μ	The solute concentration (wt/vol); concentration of solute component μ.
d_{Thermo}	A thermodynamic chain segment diameter, equal to zero at the Flory Theta Temperature, see Equation 64
h	A parameter in the Schulz-Zimm molecular weight distribution function (e.g., $1 + h^{-1} = M_w/M_n$), see Table 2
k	Boltzmann's constant.
m_ν	The molecular weight of the ν-th scattering element.
$\tilde{n}$	The ratio $\hat{n}_{solute}/\hat{n}_{medium}$
$\hat{n}_{medium}$	Refractive index of the medium.
$\hat{n}_{solute}$	Refractive index of the solute.
$(\partial\hat{n}/\partial c)_w$	The refractive index increment.
$(\partial\hat{n}/\partial c)_\Pi$	The refractive index increment determined for osmotic equilibrium of the solute components with a mixed solvent.
q	The wave vector, with modulus $q = (4\pi/\lambda)\sin(\vartheta/2)$ for an isotropic medium.
w, w_μ	The solute weight fraction; weight fraction of solute component μ .

ϑ	The scattering angle.
Π	The osmotic pressure.
Θ	The Flory Theta Temperature, equal to the temperature for which $A_2 = 0$.
α	The expansion factor $(R_G^2/R_{G,0}^2)^{1/2}$ due to the excluded volume effect for a polymer chain.
$\tilde{\alpha}$	The parameter $2\pi R/\lambda$ for a sphere of radius R.
χ	The Flory-Huggins (reduced) intermolecular interaction parameter, see Equation 161
δ^2	Mean-square molecular optical anisotropy; see Equation 39.
δ_o	The optical anisotropy of a scattering element with molecular weight m_o.
φ	The solute volume fraction.
λ	The wavelength of light in the scattering medium; λ_o the same *in vaccuo.*
ρ	The density (wt/vol).

ψ_j	A reduced virial coefficient, equal to $A_j M(M/N_A R_G^3)^{j-1}$, see Equation 131.
$\tilde{\psi}_{solute}$, $\tilde{\psi}_{\mu}$	The contrast factor for optically isotropic media; the same for component μ.
$\Gamma(c)$	The thermodynamic interaction function $\{F(0,c)^{-1} - 1\}/c$; see Equation 8.

Definitions of the principal subscripts used throughout the text.

LS	A subscript to indicate the average of a function or parameter obtained in light scattering, e.g. M_{LS}, $R^2_{G,LS}$. etc.
μ	A solute component in a mixture; e.g. c_{μ}
iso	The isotropic component of a function, e.g. $\mathbf{R}_{iso}(q,c)$
aniso	The anisotropic component of a function, e.g. $\mathbf{R}_{aniso}(q,c)$
H_v	A property determined using the horizontally plane polarized component of the light scattered using vertically plane polarized incident light, e.g. $\mathbf{R}_{Hv}(q,c)$, $P_{Hv}(q,c)$, etc.
V_v	A property determined using the horizontally plane polarized component of the light scattered using vertically plane polarized incident light, e.g. $\mathbf{R}_{Vv}(q,c)$, $P_{Vv}(q,c)$, etc.
LIN	Denotes a property of a linear chain

References

[1] Berry GC. Light Scattering, Classical: Size and Size Distribution Classification. In: Encyclopedia of Analytical Chemistry; R.A. Meyers, ed. New York: John Wiley & Sons Ltd, 2000. 5413-48.

[2] Burchard W. Solution properties of branched macromolecules. Adv. Polym. Sci. 1999;143:113-194.

[3] Dingenouts N, Bolze J, Potschke D, Ballauff M. Analysis of polymer latexes by small-angle X-ray scattering. Adv. Polym. Sci. 1999;144:1-47.

[4] Berry GC, Cotts PM. Static and dynamic light scattering. In: Modern Techniques for Polymer Characterisation. R. A. Pethrick, J. V. Dawkins, eds. London: J. Wiley & Sons Ltd, 1999.

[5] Yamakawa H. Helical wormlike chains in polymer solutions. New York: Springer-Verlag, 1997.

[6] Sorensen CM. Scattering and absorption of light by particles and aggregates. In: Handbook of surface and colloid chemistry; K. S. Birdi, ed. Boca Raton, Fla: C. R. C. Press, 1997. 533-58.

[7] van Zanten JH. Characterization of vesicles and vesicular dispersions via scattering techniques. In: Vesicles; M. Rosoff, ed. New York: Marcel Dekker, Inc., 1996.

[8] Brown W, ed. Light scattering: Principles and development. New York: Oxford University Press, 1996.

[9] Berry GC. Static and dynamic light scattering on moderately concentrated solutions: Isotropic solutions of flexible and rodlike chains and nematic solutions of rodlike chains. Adv. Polym. Sci. 1994;114:233-90.

[10] Burchard W. Static and dynamic light scattering approaches to structure determination in biopolymers. In: Laser light scattering in biochemistry; S. E. Harding. D. B. Sattelle, V. A.Bloomfield, eds. Cambridge, UK: Royal Society Chemistry, 1992. 3-22.

[11] Schmitz KS. An introduction to dynamic light scattering by macromolecules. Boston: Academic Press, 1990.

[12] Fujita H. Polymer Solutions. Amsterdam: Elsevier, 1990.

[13] Barber PW, Hill SC. Light scattering by particles: Computational methods. Singapore: World Scientific, 1990.

[14] Russel RB, Saville DA, Schowalter WR. Colloidal dispersions. Cambridge: Cambridge University Press, 1989.

[15] Casassa EF. Particle scattering factors in Rayleigh scattering. In: Polymer Handbook; E H Immergut; J Branderup, eds. New York: John Wiley & Sons, 1989. pp VII/485-91.

[16] Sadler DM. Neutron scattering from solid polymers. In: Comprehensive Polymer Science; G. Allen, ed. New York: Pergamon Press, 1988. Chapt 32.

[17] Mitchell GR. X-ray scattering from non-crystalline and liquid crystalline polymers. In: Comprehensive Polymer Science; G. Allen, ed. New York: Pergamon Press, 1988. Chapt 31.

[18] Kerker M, ed. Selected papers on light scattering. Bellingham, WA: SPIE milestone series Vol. 951, SPIE Int. Soc. Opt. Eng., 1988.

[19] Gouesbet G, Grehan G, eds. Optical particle sizing: Theory and practice. New York: Plenum Press, 1988.

[20] Berry GC. Light scattering. In: Encyclopedia of Polymer Science and Engineering; H Mark et al, eds; Vol 8. New York: John Wiley & Sons, 1987. 721-94.

[21] Weiner BB. Particle and droplet sizing using Fraunhofer diffraction. In: Modern methods of particle size analysis; H. G. Barth, ed. New York: John Wiley & Sons, 1984. 135-72.

[22] Burchard W. Static and dynamic light scattering from branched polymers and biopolymers. Adv. Polym. Sci. 1983;48:1-124.

[23] Bohren CF, Huffman DR. Absorption and scattering of light by small particles. New York: John Wiley & Sons, 1983.

[24] Glatter O, Kratky O, eds. Small angle x-ray scattering; Academic Press: New York. 1982;p 510.

[25] Flory P. Statistical Mechanics of chain molecules. 1979;Wiley-Interscience, New York:

[26] Eisenberg H. Biological macromolecules and polyelectrolytes in solution. Monographs on Physical Biochemistry, W F Harrington; A R Peacocke, eds; Oxford Univ Press; London 1976;

[27] Casassa EF, Berry GC. Light scattering from solutions of macromolecules. In: Polym Mol Weights, Pt 1; P E Slade Jr, ed; Vol 4. New York: Marcel Dekker, Inc, 1975. 161-286.

[28] Huglin MB, ed. Light scattering from polymer solutions. London: Academic Press, 1972.

[29] Yamakawa H. Modern theory of polymer solutions. New York: Harper and Row, 1971.

[30] Kerker M. The scattering of light, and other electromagnetic radiation. New York: Academic Press, 1969.

[31] McIntyre D, Gornick F, eds. Light scattering from dilute polymer solutions. New York: International Science Review Series, L. Klein; Vol. 3, Gordon and Breach, 1964.

[32] Boll RH, Leacock JA, Clark GC, Churchill SW. Tables of light scattering functions; relative indices of less than unity, and infinity. Ann Arbor: University of Michigan Press, 1958.

[33] van de Hulst HC. Light scattering by small particles. New York: Wiley, 1957.

[34] Pangonis WJ, Heller W, Jacobson A. Tables of light scattering functions for spherical particles. Detroit: Wayne State University Press, 1957.

[35] Stacey KA. Light-scattering in physical chemistry. New York: Academic Press, 1956.

[36] Guinier A, Fournet G. Small-angle scattering of x-rays. New York: John Wiley & Sons, Inc., 1955.

[37] Flory PJ. Principles of polymer chemistry. Ithaca, N.Y.: Cornell University Press, 1953.

[38] Brown W, ed. Dynamic light scattering. Oxford, UK: Clarendon Press, 1993.

[39] Chu B. Laser light scattering 2nd ed. Boston: Academic Press, Inc., 1991.

[40] Dahneke BE. Measurement of suspended particles by quasi-elastic light scattering. 1983.

[41] Berne BJ, Pecora R. Dynamic light scattering. New York: John Wiley & Sons, Inc., 1976.

[42] Benmouna M, Reed WF. Theoretical developments in static light scattering from polymers. Monographs on the Physics and Chemistry of Materials 1996;53:1-29.

[43] Zimm BH. The scattering of light and the radial distribution function of high polymer solutions. J. Chem. Phys. 1948;16:1093-9.

[44] Kurata M. Thermodynamics of polymer solutions; translated by Hiroshi Fujita. New York: Harwood Academic Publishers, 1982.

[45] Casassa EF, Berry GC. Polymer solutions. In: Comprehensive Polymer Science; G. Allen, ed. New York: Pergamon Press, 1988. Chapt 3.

[46] de Gennes P-G. Scaling concepts in polymer physics. Ithaca, NY: Cornell University Press, 1979.

[47] Yamakawa H, Fujii M. Light scattering from wormlike chains Determination of the shift factor. Macromolecules 1974;7:649-54.

[48] Noren IBE, Bertoli DA, Ho C, Casassa EF. Tetramer-dimer equilibrium of carbon monoxyhemoglobin in 2M sodium chloride. Biochem. 1974;13:1683-6.

[49] Stockmayer WH. Reminiscences of "light scattering in multicomponent systems". J. Polym. Sci.: Part B: Polym. Phys. 1999;37:642-643.

[50] Kirkwood JG, Goldberg RJ. Light scattering arising from composition fluctuations in multi-component systems. J. Chem. Phys. 1950;18:54-7.

[51] Stockmayer WH. Light scattering in multi-component systems. J. Chem. Phys. 1950;18:58-61.

[52] Benoit HC, Strazielle C. Interpretation of preferential adsorption using random phase approximation theory. Coll. Czech. Chem. Comm. 1995;60:1641-52.

[53] Casassa EF. Interpretation of Rayleigh scattering by polymers in mixed solvents. Makromol. Chemie 1971;150:251-4.

[54] Benoit H, Froelich D. Application of light scattering to copolymers. In: Light scattering from polymer solutions; M. B. Huglin, ed. New York: Academic Press, 1972. 467-501.

[55] Benoit H. Light scattering by dilute solutions of high polymers. In: Electromagnetic scattering; M. Kerker, ed. Elmworth, NY: Pergamon Press, 1963. 285-301.

[56] Horn P. Light scattering in solutions of anisotropic macromolecules. Ann. Phys. 1955;10:386-434.

[57] Berry GC. Properties of an optically anisotropic heterocyclic ladder polymer (BBL) In solution. J. Polym. Sci.: Polym. Symp. 1978;65:143-72.

[58] Brown DJ, Weatherby EJ, Alexander K. Shape, concentration and anomalous diffraction effects in sizing solids in liquids. In: Optical particle sizing: Theory and practice; G. Gouesbet, G. Gréhan, eds. New York: Plenum Press, 1988. 351-62.

[59] Glatter O, Hofer M. Particle sizing of polydisperse samples by Mie-scattering. In: Optical particle sizing: Theory and practice; G. Gouesbet, G. Gréhan, eds. New York: Plenum Press, 1988. 121-33.

[60] Urwin JR. Molecular weight distribution by turbidimetric titration. In: Light scattering from polymer solutions; M. B. Huglin, ed. New York: Academic Press, 1972. 789-824.

[61] Hirleman ED, Dellenback PA. Adaptive Fraunhofer diffraction particle sizing instrument using a spatial light modulator. Appl. Opt. 1989;28:4870-8.

[62] Hirleman ED. Modeling of multiple scattering effects in Fraunhofer diffraction particle analysis. In: Optical particle sizing: Theory and practice; G. Gouesbet, G. Gréhan, eds. New York: Plenum Press, 1988. 159-75.

[63] Hirleman ED. Optimal scaling of the inverse Fraunhofer diffraction particle sizing problem: The linear system produced by quadrature. In: Optical particle sizing: Theory and practice; G. Gouesbet, G. Gréhan, eds. New York: Plenum Press, 1988. 135-46.

[64] Hirleman ED. Modeling of multiple scattering effects in Fraunhofer diffraction particle size analysis. Part. Part. Syst. Charact. 1988;5:57-65.

[65] Bertero M, Boccacci P, De Mol C, Pike ER. Particle-size distributions from Fraunhofer diffraction. In: Optical particle sizing: Theory and practice; G. Gouesbet, G. Gréhan, eds. New York: Plenum Press, 1988. 99-105.

[66] Hirleman ED. Optimal scaling of the inverse Fraunhofer diffraction particle sizing problem: The linear system produced by quadrature. Part. Charact. 1987;4:128-33.

[67] Berry GC. Molecular weight distribution. In: Encyclopedia of materials science and engineering; M. B. Bever, ed. Oxford: Pergamon Press, 1986. 3759-68.

[68] Volkenstein MV. Configurational statistics of polymeric chains. New York: Interscience Publishers, 1963.

[69] Freed KF. Renormalization group theory of macromolecules. New York: John Wiley & Sons, 1987.

[70] Berry GC, Casassa EF. Thermodynamic and hydrodynamic behavior of dilute polymer solutions. J. Polym. Sci., Part D 1970;4:1-66.

[71] Oono Y. Statistical physics of polymer solutions: conformation-space renormalization-group approach. Adv. in Chem. Phys. 1985;61:301-437.

[72] Berry GC. Thermodynamic and conformational properties of polystyrene. I. Light-scattering studies on dilute solutions of linear polystyrenes. J. Chem. Phys. 1966;44:4550-64.

[73] Yamakawa H, Fujii M. Binary cluster integrals in the theory of dilute polymer solutions. J. Chem. Phys. 1973;58:1523-8.

[74] Yamakawa H, Stockmayer WH. Statistical mechanics of wormlike chains. II. Excluded volume effects. J. Chem. Phys. 1972;57:2843-54.

[75] Yamakawa H. Statistical mechanics of wormlike chains. Pure Appl. Chem. 1976;46:135-41.

[76] Sullivan VJ, Berry GC. Light scattering studies on dilute solutions of semiflexible polyelectrolytes. Intl. J. Polym. Anal. Charact. 1995;2:55-69.

[77] Kurata M, Fukatsu M. Unperturbed dimension and translational friction constant of branched polymers. J. Chem. Phys. 1964;41:2934-44.

[78] Berry GC, Orofino TA. Branched polymers. III. Dimensions of chains with small excluded volume. J. Chem. Phys. 1964;40:1614-21.

[79] Casassa EF, Berry GC. Angular distribution of intensity of Rayleigh scattering from comblike branched molecules. J. Polym. Sci.: Part A-2. 1966;4:881-97.

[80] Solensky PJ, Casassa EF. Perturbation theory of dimensions of comb-like polymer chains with branches randomly spaced along the backbone. Macromolecules 1980;13:500-6.

[81] Casassa EF, Tagami Y. Statistical thermodynamics of polymer solutions. VI. Comblike branched molecules with branches placed randomly along the backbone. J. Polym. Sci., Polym. Phys. Ed. 1968;6:63-89.

[82] Bhandari R. Scattering coefficients for a multilayered sphere: Analytic expressions and algorithms. Appl. Opt. 1985;24:1960-7.

[83] van Zanten JH. The Zimm plot and its analogs as indicators of vesicle and micelle size polydispersity. J. Chem. Phys. 1995;102:9121-8.

[84] van Zanten JH. Unilamellar vesicle diameter and wall thickness determined by Zimm's light scattering technique. Langmuir 1994;10:4391-3.

[85] Brown W, Mortensen K. Scattering in Polymeric and Colloidal Systems. In: 2000. 586 pp.

[86] Mays H, Mortensen K, Brown W. Microemulsions studied by scattering techniques. In: Scattering in Polymeric and Colloidal Systems; W. Brown, K. Mortensen, eds. Amsterdam, Neth.: Gordon & Breach 2000. 249-325.

[87] Hahn DK, Aragon SR. Mie scattering from anisotropic thick spherical shells. J. Chem. Phys. 1994;101:8409-17.

[88] Strawbridge KB, Hallett FR. Polydisperse Mie theory applied to hollow latex spheres: an integrated light-scattering study. Can. J. Phys. 1992;70:401-6.

[89] Asano S, Sato M. Light scattering by randomly oriented spheroidal particles. Appl. Opt. 1980;19:962-74.

[90] Wyatt PJ. Scattering of electromagnetic plane waves from inhomogeneous spherically symmetric objects. Phys. Rev. 1962;127:1837-43.

[91] Yoshizaki T, Yamakawa H. Scattering functions of wormlike and helical wormlike chains. Macromolecules 1980;13:1518-25.

[92] Casassa EF. Light scattering from very long rod-like particles and an application to polymerized fibrinogen. J. Chem. Phys. 1955;23:596-7.

[93] Casassa EF. The conversion of fibrinogen to fibrin. XIX. The structure of the intermediate polymer of fibrinogen formed in alkaline solutions. J. Am. Chem. Soc. 1956;78:3980-5.

[94] Nagai K. Theory of light scattering by an isotropic system composed of anisotropic units with application to the Porod-Kratky chains. Polym. J. 1972;3:67-83.

[95] Nakamura Y, Norisuye T. Scattering function for wormlike chains with finite thickness. J. Polym. Sci.: Part B: Polym. Phys. 2004;42:1398-1407.

[96] Koyama R. Light scattering of stiff chain polymers. J. Phys. So.c Jn. 1973;34:1029-38.

[97] des Clozeaux J. Form factor of an infinite Kratky-Porod chain. Macromolecules 1973;6:403-7.

[98] Peterlin A. Light scattering by non-Gaussian macromolecular coils. In: Electromagnetic scattering; M. Kerker, ed. Elmworth, NY: Pergamon Press, 1963. 357-75.

[99] Porod G. X-ray and light scattering by chain molecules in solution. J. Polym. Sci. 1953;10:157-66.

[100] Potschke D, Hickl P, Ballauff M, Astrand P-O, Pedersen JS. Analysis of the conformation of worm-like chains by small-angle scattering: Monte Carlo simulations in comparison to analytical theory. Macromol. Theory Simulations 2000;9:345-353.

[101] Kholodenko AL. Analytical calculation of the scattering function for polymers of arbitrary flexibility using the Dirac propagator. Macromolecules 1993;26:4179-83.

[102] Pedersen JS, Schurtenberger P. Scattering Functions of Semiflexible Polymers with and without Excluded Volume Effects. Macromolecules 1996;29:7602-7612.

[103] Ter Meer HU, Burchard W. Determination of chain flexibility by light scattering. Polym. Commun. 1985;26:273-5.

[104] Porod G. The dependence of small-angle x-ray scattering on the shape and size of colloidal particles in dilute systems. IV. Acta Physica Austriaca 1948;2:255-92.

[105] Magid LJ, Han Z, Li Z, Butler PD. Tuning microstructure of cationic micelles on multiple length scales: The role of electrostatics and specific ion binding. Langmuir 2000;16:149-56.

[106] Gerber MJ, Kline SR, Walker LM. Characterization of Rodlike Aggregates Generated from a Cationic Surfactant and a Polymerizable Counterion. Langmuir 2004;20:8510-8516.

[107] Doi M, Edwards S. The theory of polymer dynamics. 1986;Clarendon Press, Oxford:

[108] Goldstein M. Scattering factors for certain polydisperse systems. J. Chem. Phys. 1953;21:1255-8.

[109] Berry GC. Thermodynamic and conformational properties of polystyrene. III. Dilute solution studies on branched polymers. J. Polym. Sci., Part A-2 1971;9:687-715.

[110] Wiscombe WJ. Improved Mie scattering algorithms. Appl. Opt. 1980;19:1505-9.

[111] Bohren CFA. Recurrence relations for the Mie scattering coefficients. J. Opt. Soc. Am. A 1986;4:612-13.

[112] Gulari E, Annapragada A, Gulari E, Jawad B. Determination of particle size distributions using light-scattering techniques. ACS Symp. Ser. 1987;332:133-45.

[113] Hodkinson JR. Particle sizing by means of the forward scattering lobe. Appl. Opt. 1966;5:839-44.

[114] Meeten GH, Navard P. Small-angle scattering of polarized light. I. Comparison of theoretical predictions for isotropic and anisotropic spheres. J. Polym. Sci.: Part B: Polym. Phys. 1989;27:2023-35.

[115] Stein RS, Srinivasarao M. Fifty years of light scattering: a perspective. J. Polym. Sci.: Part B: Polym. Phys. 1993;31:2003-10.

[116] Meeten GH. Small-angle light scattering by spherulites in the anomalous diffraction approximation. Opt. Acta 1982;29:759-70.

[117] Rhodes MB, Stein RS. Scattering of light from assemblies of oriented rods. J. Polym. Sci.: Part A-2. 1969;7:1539-58.

[118] Graessley WW. Polymer liquids & networks: Structure and properties. New York: Garland Science, 2004.

[119] Hirschfelder JO, Curtiss CF, Bird RB. Molecular theory of gases and liquids. New York: John Wiley & Sons, 1954.

[120] Cotts PM, Berry GC. Studies on dilute solutions of rodlike macroions. II. Electrostatic effects. J. Polym. Sci., Polym. Phys. Ed. 1983;21:1255-74.

[121] Benmouna M, Duval M, Strazielle C, Hakem FI. Static and dynamic light scattering from multicomponent polymer mixtures PS/PDMS/PMMA/toluene. Acta Polymerica 1996;47:29-34.

[122] Benmouna M, Duval M, Strazielle C, Hakem F-I, Fischer EW. Theory of static scattering from polymer mixtures. The case of polystyrene/polydimethylsiloxane/poly(methyl methacrylate)/toluene. Macromol. Theory Simulations 1995;4:53-65.

[123] Aven MR, Cohen C. Light scattering from dilute polystyrene in mixtures of semidilute poly(dimethylsiloxane) and tetrahydrofuran. Macromolecules 1990;23:476-86.

[124] Benoit H, Benmouna M, Wu WL. Static scattering from multicomponent polymer and copolymer systems. Macromolecules 1990;23:1511-7.

[125] Benoit H, Benmouna M, Strazielle C, Cesteros C. Light scattering from mixtures of homopolymers and copolymers. Theoretical results and experimental examples. Phys. Chem. Colloids Macromol., Proc. Int. Symp. 1987;119-25.

[126] Sato T, Norisuye T, Fujita H. Second and third virial coefficients for binary polystyrene mixtures in benzene. J. Polym. Sci.: Part B: Polym. Phys. 1987;25:1-17.

[127] Kok CM, Rudin A. Second virial coefficients of polystyrene mixtures in 2-butanone. Europ. Polym. J. 1986;22:107-9.

[128] Stepanov S, Straube E. Renormalization group evaluation of the second virial coefficient of polydisperse polymer solutions. J. Phys., Lett. 1985;46:1115-22.

[129] Tong Z, Einaga Y. Second virial coefficient of binary polystyrene mixtures in cyclohexane below the theta temperature. Polymer J. 1984;16:641-6.

[130] Noda I, Kitano T, Nagasawa M. The effect of molecular weight heterogeneity on the second virial coefficient of linear polymers in good solvents. J. Polym. Sci., Polym. Phys.Ed. 1977;15:1129-42.

[131] Welzen TL. Second virial coefficients for solutions of polystyrene mixtures obtained with low-angle laser light scattering. Brit. Polym. J. 1980;12:95-8.

[132] Wallace TP, Casassa EF. Second virial coefficient in solutions of mixtures of two polymer fractions. Polymer Preprints (Am. Chem. Soc.) 1970;11:136-41.

[133] Blum JJ, Morales MF. Light scattering of multicomponent macromolecular systems. J. Chem. Phys. 1952;20:1822.

[134] Stockmayer WH, Stanley HE. Light-scattering measurement of interactions between unlike polymers. J. Chem. Phys. 1950;18:153-4.

[135] Casassa EF. Effect of heterogeneity in molecular weight on the second virial coefficient of polymers in good solvents. Polymer 1962;3:625-38.

[136] Aelanei N, Avram E, Paduraru G. On the compatibility of polystyrene with polybutadiene and styrene-butadiene block copolymers. Anal. Stiint. .Univ. Al. I. Cuza Chimie 2002;10:237-242.

[137] Clark AH. Direct analysis of experimental tie line data (two polymer-one solvent systems) using Flory-Huggins theory. Carbohydrate Polym. 2000;42:337-351.

[138] Strazielle C, Duval M, Benmouna M. Elastic and quasielastic light scattering from mixtures of three polymers and a solvent: the effects of poly(methyl methacrylate) concentration and molecular weight on the properties of polystyrene/polydimethylsiloxane/toluene solutions. J. Polym. Sci.: Part B: Polym. Phys. 1995;33:823-32.

[139] Kent MS, Tirrell M, Lodge TP. Solution properties of polymer mixtures. Macromolecules 1992;25:5383-97.

[140] Kaddour LO, Strazielle C. The scaling laws in ternary systems: polymer-polymer-good solvent. An experimental study. New Trends Phys. Phys. Chem. Polym. 1989;229-37.

[141] Edsman K, Sundeloef LO. Interaction virial coefficients in some mixed polymer solutions. Polymer 1988;29:535-40.

[142] Kaddour LO, Strazielle C. Experimental investigations of light scattering by a solution of two polymers. Polymer 1987;28:459-68.

[143] Fukuda T, Nagata M, Inagaki H. Light scattering from polymer blend solutions. 4. Data analysis for asymmetrical dilute systems. Macromolecules 1987;20:654-8.

[144] Ogawa E, Yamaguchi N, Shima M. Estimation of the interaction parameter between polystyrene and poly(p-chlorostyrene) from osmotic pressure measurements. Polymer J. 1986;18:903-10.

[145] Kratochvil P, Strakova D, Tuzar Z. Interaction between polymers in dilute solutions of two polymers in a single solvent measured by light scattering and the compatibility of polymers. Brit. Polym. J. 1977;9:217-21.

[146] Hyde AJ. Light scattering from polymer-polymer solvent systems. In: Light scattering from polymer solutions; M. B. Huglin, ed. New York: Academic Press, 1972. 459-466.

[147] Kuhn R, Cantow HJ, Burchard W. Incompatibility of polymer mixtures. I. Light-scattering measurements of the system polystyrene-poly(methyl methacrylate)-benzene. Ang.Makromol. Chem. 1968;2:146-56.

[148] Kuleznev VN, Krokhina LS, Lyakin YI, Dogadkin BA. Investigation of the structure of solutions of polymer mixtures by light scattering. Kolloidnyi Zh. 1964;26:475-80.

[149] Benmouna M, Briber R, Hammouda B. Polymer blends, copolymers, and networks. Scattering properties and phase behavior. Macromol. Theory Simulations 1997;6:197-235.

[150] Benoit H, Benmouna M, Strazielle C, Lapp A, Ould-Kaddour L. Polymer and copolymer characterization by light and neutron scattering: theoretical considerations and experimental examples. J. Appl. Polym. Sci.: Appl. Polym. Symp. 1991;48:315-34.

[151] Benmouna M, Benoit H. Scattering from copolymer solutions at finite concentration. J. Polym. Sci., Polym. Phys.Ed. 1983;21:1227-42.

[152] Benoit H, Stockmayer WH. Influence of the interaction of assembled particles on the scattering of light. J. Phys. Radium 1956;17:21-6.

[153] Benoit H. Determination of the dimensions of anisotropic macromolecules by means of light scattering. Makromol. Chemie 1956;18/19:397-405.

[154] Benoit H, Stockmayer WH. A study of the influence of interactions on light scattered by a collection of particles. J. Phys. Radium 1956;17:21-6.

[155] Akasaka K, Nakamura Y, Norisuye T, Teramoto A. Second and third virial coefficients for polyisobutylene in heptane, an intermediate solvent. Polymer J. 1994;26:1387-95.

[156] Nakamura Y, Akasaka K, Katayama K, Norisuye T, Teramoto A. Second and third virial coefficients for polyisobutylene in cyclohexane. Macromolecules 1992;25:1134-8.

[157] Bruns W. The third osmotic virial coefficient of polymer solutions. Macromolecules 1997;30:4429-4431.

[158] Stockmayer WH, Casassa EF. The third virial coefficient in polymer solutions. J. Chem. Phys. 1952;20:1560-6.

[159] Okumoto M, Nakamura Y, Norisuye T, Teramoto A. Excluded-volume effects in star polymer solutions: four-arm star polystyrene in benzene. Macromolecules 1998;31:1615-1620.

[160] Roovers J, Toporowski PM, Douglas J. Thermodynamic Properties of Dilute and Semidilute Solutions of Regular Star Polymers. Macromolecules 1995;28:7064-70.

[161] Akasaka K, Nakamura Y, Norisuye T, Teramoto A. Second and third virial coefficients for polyisobutylene in the vicinity of the theta point. Polymer J. 1994;26:363-71.

[162] Okumoto M, Terao K, Nakamura Y, Norisuye T, Teramoto A. Excluded volume effects in star polymer solutions: four-arm star polystyrene in cyclohexane near the Q temperature. Macromolecules 1997;30:7493-7499.

[163] Cherayil BJ, Kholodenko AL, Freed KF. Semidilute polymer solutions in the theta domain: a renormalization group study. J. Chem. Phys. 1987;86:7204-17.

[164] Cherayil BJ, Douglas JF, Freed KF. Effect of residual interactions on polymer properties near the theta point. J. Chem. Phys. 1985;83:5293-310.

[165] Carnahan NF, Starling KE. Equation of state for nonattracting rigid spheres. J. Chem. Phys. 1969;51:635-6.

[166] Flory PJ, Daoust H. Osmotic pressures of moderately concentrated polymer solutions. Journal of Polymer Science 1957;25:429-40.

[167] Eichinger BE, Flory PJ. Thermodynamics of polymer solutions. III. Polyisobutylene and cyclohexane. Transactions of the Faraday Society 1968;64:2061-5.

[168] Noda I, Higo Y, Ueno N, Fujimoto T. Semidilute region for linear polymers in good solvents. Macromolecules 1984;17:1055-9.

[169] Hager BL, Berry GC, Tsai HH. Moderately concentrated solutions of polystyrene. II. Integrated-intensity light scattering as a function of concentration, temperature, and molecular weight. J. Polym. Sci., Part B: Polym. Phys. 1987;25:387-413.

[170] Flory PJ, Bueche AM. Theory of light scattering by polymer solutions. J. Polym. Sci. 1958;27:219-29.

[171] Benmouna M, Fischer EW, Bensafi A, Khaldi S. On the static scattering of linear and cyclic copolymers in solution. J. Polym. Sci., Part B: Polym. Phys. 1996;34:1629-1636.

[172] Benoit H, Benmouna M. New approach to the problem of elastic scattering from a mixture of homopolymers in a concentrated solution. Macromolecules 1984;17:535-40.

[173] Benoit H, Benmouna M. Scattering from a polymer solution at an arbitrary concentration. Polymer 1984;25:1059-67.

[174] Akcasu AZ, Benmouna M, Benoit H. Application of random phase approximation to the dynamics of polymer blends and copolymers. Polymer 1986;27:1935-42.

[175] Chen SJ, Berry GC. Moderately concentrated solutions of polystyrene. 4. Elastic and quasielastic light scattering at the Flory theta temperature. Polymer 1990;31:793-804.

[176] DeLong LM, Russo PS. Thermodynamic and dynamic behavior of semiflexible polymers in the isotropic phase. Macromolecules 1991;24:6139-55.

[177] Kinning DJ, Thomas EL. Hard-sphere interactions between spherical domains in diblock copolymers. Macromolecules 1984;17:1712-18.

[178] Kim SH, Ramsay DJ, Patterson GD, Selser JC. Static and dynamic light scattering of poly(α- methylstyrene) in toluene in the dilute region. J. Polym. Sci.: Part B: Polym. Phys. 1990;28:2023-56.

[179] Sedlak M. Polyelectrolytes in Solution. In Light Scattering: Principles and Development; W Brown, ed; Clarendon Press: Oxford 1996;120-65.

[180] Grüner F, Lehmann W. On the long time diffusion of interacting Brownian particles. In: Light Scattering in Liquids and Macromolecular Solutions; V. Degiorgio, M. Corti, M. Giglio, eds. New York: Plenum Press, 1980. 51-69.

[181] Doty P, Steiner RF. Macro-ions. I. Light scattering theory and experiments with bovine serum albumin. J. Chem. Phys. 1952;20:85-94.

[182] Burchard W. Macromolecular association phenomena. A neglected field of research? Trends Polym. Sci. 1993;1:192-8.

[183] Yue S, Berry GC, Green MS. Intermolecular association and supramolecular organization in dilute solution 2 Light scattering and optical activity of poly(pbiphenylmethyl- L-glutamate. Macromolecules 1996;29:6175-82.

[184] Tanner DW, Berry GC. Properties of cellulose acetate in solution. I. Light scattering, osmometry and viscometry on dilute solutions. J. Polym. Sci.: Polym. Phys. Ed. 1974;12:941-75.

[185] Einaga Y, Berry GC. Studies on dilute solutions of rodlike macroions: III Integrated intensity and photon correlation light scattering investigation of association. In Microdomains in Polymer Solutions; P Dubin, ed; Plenum Press; New York 1985;191-210.

[186] Yue S, Berry GC, McCullough RD. Intermolecular association and supramolecular organization in dilute solution. 1. Regioregular poly(3-dodecylthiophene). Macromolecules 1996;29:933-9.

[187] Furukawa R, Berry GC. Studies on dilute solutions of rodlike macroions. 4. Aggregation with enhanced orientational correlation. Pure Appl. Chem. 1985;57:913-20.

[188] Nicolai T, Durand D, Gimel J-C. Scattering Properties and Modelling of Aggregating and Gelling Systems. In: Light Scattering: Principles and Development; W. Brown, ed. Oxford: Clarendon Press, 1996. 201-31.

[189] Elias HG. The study of association and aggregation via light scattering. In: Light scattering from polymer solutions; M. B. Huglin, ed. New York: Academic Press, 1972. 397-457.

[190] Yoshimura S, Shirai S, Einaga Y. Light-scattering characterization of wormlike micelles of hexaoxyethylene dodecyl $C_{12}E_6$ and hexaoxyethylene tetradecyl $C_{14}E_6$ ethers in dilute aqueous solution. J. Phys. Chem. B 2004;108:15477-87.

[191] Sato T. Scattering theory for threadlike micellar solutions. Langmuir 2004;20:1095-9.

[192] Provder T, Barth HG, Urban MW. Chromatographic characterization of polymers: hyphenated and multidimensional techniques. 1995.

[193] Alb AM, Mignard E, Drenski MF, Reed WF. In Situ Time-Dependent Signatures of Light Scattered from Solutions Undergoing Polymerization Reactions. Macromolecules 2004;37:2578-2587.

[194] Reed WF. Monitoring kinetic processes in polymer solutions with time dependent static light scattering (TDSLS). Macromolecular Symposia 2002;190:131-150.

[195] Hoecker H, Shih H, Flory PJ. Thermodynamics of polystyrene solutions. 3. Polystyrene and cyclohexane. Transactions of the Faraday Society 1971;67:2275-81.

[196] Eichinger BE, Flory PJ. Thermodynamics of polymer solutions. II. Polyisobutylene and benzene. Transactions of the Faraday Society 1968;64:2053-60.

[197] Shiomi T, Izumi Z, Hamada F, Nakajima A. Thermodynamics of solutions of poly(dimethylsiloxane). 1. Solutions of poly(dimethylsiloxane) in methyl ethyl ketone, methyl isobutyl ketone, ethyl butyl ketone, and diisobutyl ketone. Macromolecules 1980;13:1149-54.

[198] Candau F, Strazielle C, Benoit H. Osmotic pressure study of linear and branched polystyrenes in solution. Determination of their thermodynamic parameters. European Polymer Journal 1976;12:95-103.

[199] Stepanek P, Perzynski R, Delsanti M, Adam M. Osmotic compressibility measurements on semidilute polystyrene-cyclohexane solutions. Macromolecules 1984;17:2340-3.

Figure Captions

1. Bilogarithmic plots of $12R^2_{G,LS}/L_zL_{z+1}$ and δ^2/δ_o^2 vs the ratio $L_w/â$ of the weight average contour length L_w to the persistence length â for the wormlike chain model. From reference 1.

2. The ratio M_{LS}/M ($= [m_{sph}(ñ,\tilde{\alpha})]^2$) of the light scattering averaged molecular weight M_{LS} for monodisperse spheres of radius R to the molecular weight M as a function of the relative refractive index ñ for the indicated values of the size parameter $\tilde{\alpha} = 2\pi R/\lambda$. The dashed lines give the limiting behavior for small ñ – 1. From reference 1.

3. The functions f_i, appearing in the reciprocal scattering factors for anisotropic chains as a function of the contour length L divided by the persistence length â: ——, f_1;— - —, f_2; - - -, f_3; and – – –, f_4 . From reference 20.

4. The ratio $R^2_{G,LS}/(3R^2/5)$ ($= y_{sph}(ñ,\tilde{\alpha})$) of the light scattering averaged mean square radius of gyration $R^2_{G,LS}$ for monodisperse spheres of radius R to the geometric square radius of gyration as a function of (a) the size parameter $\tilde{\alpha} = 2\pi R/\lambda$ for the indicated values of the relative refractive index ñ and (b) the relative refractive index ñ for the indicated values of $\tilde{\alpha}$. From reference 1.

5. Examples of $P(q,0)^{-1}$ versus $R^2_Gq^2$ for random-flight linear chains (C), rodlike chains (R), disks (D) and spheres (S); expressions for P(q,0) for these cases are given in Table 3. The insert shows the ratio of the logarithm of P(q,0) divided by P(q,0) for the coil with the same R^2_G versus $R^2_Gq^2$ for these cases. From reference 4.

6. Examples of $[P(q,0)]_{BR}$ vs. $R^2_Gq^2$ for comb-shaped branched chain polymers divided by $[P(q,0)]_{LIN}$ for linear chains with the same R^2_G (not the same molecular weight). The number of branches is indicated, along with the fraction φ of mass in the backbone of the branched chain. From reference 79.

7. The functions $(\hat{a}Lq^2/3)P(q,0)$ (upper) and $(Lq/\pi)P(q,0)$ (lower) vs $\hat{a}q$ for the Kratky–Porod wormlike chain model [5, 91], for chains of contour length L and persistence length â. For convenience of comparison, the values of $L/\hat{a}$ used are the same are among those in an alternative bilogarithmic representation $(L/2\hat{a})P(q,0)$ vs $2\hat{a}q$ presented in the literature [102]: 640, 160, 80, 40, 20, 10, 5 for the curves from top to bottom in the lower panel, and all of these except 160 in the upper panel for the curves from left to right.

8. Examples of experimental data on $qP(q,0)$/(arbitrary units) vs q/nm^{-1} for wormlike micelles.
   (a) Small-angle neutron scattering SANS on micelles formed by cetyltrimethylammonium (CTA) with 2,6 dichlorbenzoate counterions in aqueous salt solution, showing the maximum mentioned in the text, and the region, indicated by the dashed line, for which $(Lq/\pi)P(q,0)$ tends to unity, followed by the regime with decreasing $P_{III}(q,0)$, providing measure of the micellar radius R_c, as discussed in the text. From reference 105.
   (b) Light scattering (filled circles) and SANS on wormlike micelles (unfilled symbols) of CTA with a polymerized counterion (to prevent dissociation on dilution). The maximum prominent in (a) is missing owing to the smaller $L/\hat{a}$ (≈ 3) for this sample, but the regime with decreasing $P_{III}(q,0)$ is evident. Data from reference 106.

9. Examples of $P_{LS}(q,0)$ vs. $R_{G,LS}^2q^2$ for spheres with size parameter $\tilde{\alpha} = 2\pi R/\lambda = 4$ for the indicated values of the relative refractive index ñ. The angular range is 0 to 180 degrees in all cases except for ñ = 2. The RGD limiting case for very small ñ – 1 is given by the dashed curve. The dashed line gives the initial tangent. Values of $R_{G,LS}^2/(3R^2/5)$ may be seen in Figure 2. From reference 1.

10. Light scattering data on solutions of a polyelectrolyte rodlike chain (*cis*-PBO) and a multiply broken variant of the same (*ab*-PBO) in solvents with ionic strengths providing Debye screening lengths κ^{-1}/nm of 7.9 (filled circles), 2.1 (squares) and 0.8 (unfilled circles).
    (a) Upper: $[Kc/R_{VV}(0,c)]^{1/2}$ for solutions of *cis*-PBO.
        Middle: $Kc/R_{HV}(0,c)$ for solutions of *cis*-PBO.
        Lower: $[Kc/R_{VV}(0,c)]^{1/2}$ *ab*-PBO.
    (b) Upper: $[Kc/R_{VV}(\vartheta,c)]^0$ for solutions of *cis*-PBO.
        Middle: $[Kc/R_{HV}(\vartheta,c)]^0$ for solutions of *cis*-PBO.
        Lower: $[Kc/R_{VV}(\vartheta,c)]^0$ for solutions of *ab*-PBO.

From reference 76.

11. The functions $\Omega_{LS} \propto A_{2,LS}/M_W^{-\gamma}$ (curves 2 and 3) and $\Omega_{\Pi} \propto A_{2,\Pi}/M_n^{-\gamma}$ (curves 1 and 4) as a function of the polydispersity parameter $1/h = (M_w/M_n) - 1$ for flexible chain polymers with a distribution of M given by the Schulz-Zimm distribution function and $\gamma = 1/5$. The data are calculated using the arithmetic mean given by Equation 143 for curves 1 and 2, and the geometric mean discussed in the text for curves 3 and 4.

12. Bilogarithmic plots of $(\Pi M/RTc) - 1$ as a function of φ for solutions of polyisobutylene in cyclohexane, from measurements of the osmotic pressure, or converted from measurements of the vapor pressure [166, 167]. The dashed curve is computed with a fit to Equation 162 with $\chi(\varphi) = 0.42 + 0.08\varphi$, and this same expression was used with Equation 163 to compute the solid curve shown for $[K_{op}cM/\mathbf{R}(0,c)] - 1$ vs. $\varphi/2$. The straight line portion is consistent with the scaling expected for moderately concentrated solutions.

13. Bilogarithmic plots of $\chi - 1/2$ versus volume fraction φ (upper) or $\varphi/\sqrt{(1-\varphi)}$ (lower) for concentrated solutions at the Flory Theta temperature. The same data are presented and discussed as linear plots of χ vs φ in reference 118; the symbols identifying the source of the data are those used in the latter reference: circles [195]; triangles [196]; and squares [197].

14. Bilogarithmic plots of $K_{op}cM/\mathbf{R}_{Vv}(0,c)$ versus A_2Mc for moderately concentrated solutions of poly(benzyl glutatmate) in a good solvent. The curve represents the use of Equation 132 with A_3 and higher virial coefficients equal to zero. The data were collected in the temperature range 15 to 75°C for samples with $10^{-3}M_w$ equal to 277, 179, 149, and 60 [176]. From reference 9.

15. Bilogarithmic plot of $c\Gamma(c)$ versus $[\eta]c$ for solutions of polystyrene in cyclohexane at the Flory Theta temperature (34.8°C): circles [175]; squares [198]]; triangles [199]. The line represents $3A_3M/[\eta]^2 = 0.195$, i.e., $c\Gamma(c) = 0.195([\eta]c)^2$. From reference 9.

16. Bilogarithmic plots of $K_{op}cM/\mathbf{R}(0,c)$ versus A_2Mc (or $\Pi M/RTc$ versus $A_2Mc/2$) for several flexible chain polymers in good solvents. The solid curves represent the use of Eqn. 26. The data sources are identified in references 20 and 45.

Upper: $K_{op}cM/\mathbf{R}(0,c)$ for polystyrene ($0.36 \leq 10\_6Mw \leq 7.6$) in benzene (15°C);

Middle: $K_{op}cM/\mathbf{R}(0,c)$ (unfilled) and $\Pi M/RTc$ (filled) for poly(α-methyl styrene) in toluene;

Lower: $K_{op}cM/\mathbf{R}(0,c)$ for polystyrene (10_6Mw equal to 0.862 for filled and 1.50 for unfilled) in cyclopentane at T equal to the Flory Theta temperature plus 20°C (no pips) and 35°C (pips).

From reference 9.

17. Bilogarithmic plots of $b(0,c)/b(0,0)$ (or $b(q > q_{max},c)/b(0,0)$) versus $[\eta]c$ for moderately concentrated solutions of flexible chain polymers under two thermodynamic conditions; $b(0,0)^2 = R^2_{G,LS}/3$.

Upper: $b(q > q_{max},c)/b(0,0)$ determined under Flory Theta solvent conditions; the symbols are defined in Fig. 5 of reference 175. The solid curve represents $\xi_p(0,c)/(R^2_{G,LS}/3)^{1/2}$, see Equations 179-180.

Lower: $b(0,c)/b(0,0)$ determined under good solvent conditions; the symbols are for data given in reference [ref 39] for $b(0,c)$ determined by light scattering, unfilled, or neutron scattering, filled: polydimethyl siloxane, diamonds; polystyrene, squares; and poly(methyl methacrylate), triangles. The solid curve represents $\xi_p(0,c)/(R^2_{G,LS}/3)^{1/2}$, see Equations 179-180.

From reference 9.

18. Bilogarithmic plot of $b(0,c)/b(0,0)$ versus A_2M_wc for moderately concentrated solutions of poly(benzyl glutatmate) in a good solvent for the polymers described in the caption to Fig. 13 of reference 176; $b(0,0)^2 = R^2_{G,LS}/3$. The curve represents $\xi_P(0,c)/b(0,0)$ using the experimental data for $\Gamma(c)$ (see Equations 179-180). From reference 9.

19. (a) The function $P(q,c)H(q,c)$ vs $2qR$ calculated for monodisperse spheres of radius R interacting through a hard core potential. The bold curve is calculated with Equation

182, and the remaining curves were calculated with Equation 183, with the volume fraction φ equal to 0.05, 0.1, 0.2, 0.3 and 0.4 from top to bottom.

(b) The function cΓ(c) vs volume fraction for monodisperse spheres calculated with Equations 160 and 184 for curve (1) and (2), respectively.

20. H(q,c) versus $R_G^2q^2/6$ for moderately concentrated solutions of polystyrene in cyclohexane at the Flory Theta temperature (34.8°C), $M_w = 8.62 \times 10^5$, [η] = 76 ml/g, R_G = 27 nm: [η]c equal to 0.60, 1.15, 1.73, 2.68, 4.64, 4.69, 6.54 from bottom to top. The curves are drawn merely to aid the eye. From reference 9.

21. $K_{op}cM/\mathbf{R}(q,c)$ versus $u = R_G^2q^2$ for dilute to moderately concentrated solutions of poly(α-methyl styrene) in toluene (a good solvent) [178]: $M_w = 2.96 \times 10^6$ and R_G = 74 nm. [η]c equal to 0.94, 1.94, and 5.30 from bottom to top. The value of R_G^2 used was chosen to fit the data for the larger range of u, and the curves for the lower two data sets represents P(q,0) for the random-flight model. The solid curve for the most concentrated solution is calculated using the approximation $H(q,c) \approx [P(2q,c)]^2/P(q,c)$ as discussed in the text. From reference 9.

22. The function Q(q,c) corresponding to the approximation $H(q,c) \approx [P(2q,c)]^{1/2}/P(q,c)$, using Equation for P(q,c), as discussed in the text. The dashed curve gives H(q,c), and the solid curves give Q(q,c) for c_(c) equal to 5, 10 and 25 from bottom to top, respectively. From reference 9.

23. The dependence of the structure factor on qR for polystyrene spheres (R = 45 nm) immersed in deionized water, with the number concentration n/particles·mm^{-3} = 2.53, 5.06, 7.59 and 10.12 for the circles with increasing depth of the shading, respectively; adapted from figures in reference 179. From reference 1.

24. Illustrations of $KcM/\mathbf{R}(q,c)$ for two extreme forms of association observed with solutions. In type I association (— —), the aggregates form a loose supramolecular structure, of a type that may lead to gelation. In type II association (——), the aggregates are more

compact, giving much enhanced scattering preferentially at small scattering angle. The scattering from the fully dissociated polymer is also shown (- - - -).

25. Scattering functions for an illustrative example of a flexible chain polymer undergoing end-to-end dimerization. (a) dependence on angle, calculated as discussed in the text for a reduced equilibrium constant $K_{eq} = 0.1$ and the indicated values of $A_{2,M}Mc$, with the constant equal to zero or 0.2 for the solid and dashed curves, respectively; (b) scattering extrapolated to zero angle as a function of $A_{2,M}Mc$, for the indicated values of K_{eq}. From reference 1.

26. Light scattering data for aqueous solutions of wormlike micelles of hexaoxyethylene dodecyl ether [190].

(a) Bilogarithmic plot of $Kc/\mathbf{R}(0,c)$ vs c at the indicated temperatures. The dashed and solid lines are placed with slopes –1/2 and 2 as discussed in the text.

(b) Bilogarithmic plot of $Kc/\mathbf{R}(0,c) - M_w^{-1}$ vs c at the temperatures indicated by the symbols defined in (a). The line has slope 2.

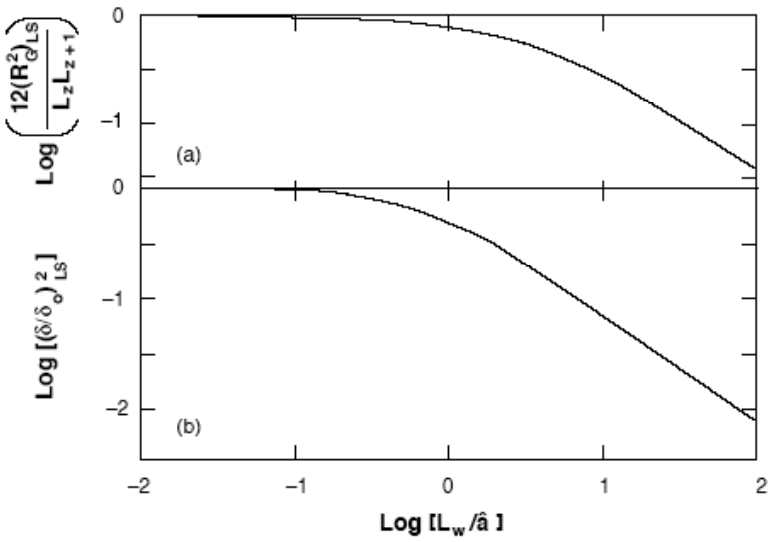

1. Bilogarithmic plots of $12R^2_{G,LS}/L_zL_{z+1}$ and δ^2/δ_o^2 vs the ratio $L_w/\hat{a}$ of the weight average contour length L_w to the persistence length â for the wormlike chain model. From reference 1.

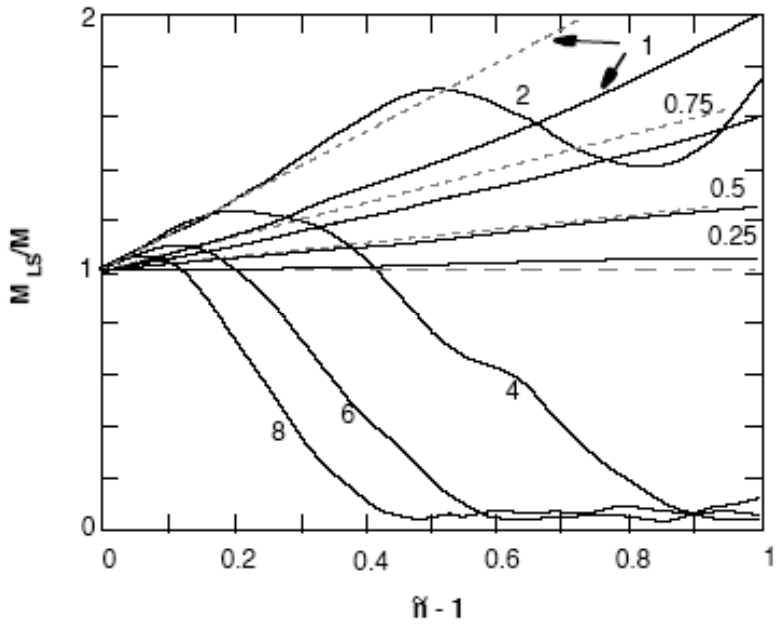

2. The ratio M_{LS}/M ($= [m_{sph}(\tilde{n},\tilde{\alpha})]^2$) of the light scattering averaged molecular weight M_{LS} for monodisperse spheres of radius R to the molecular weight M as a function of the relative refractive index ñ for the indicated values of the size parameter $\tilde{\alpha} = 2\pi R/\lambda$. The dashed lines give the limiting behavior for small ñ – 1. From reference 1.

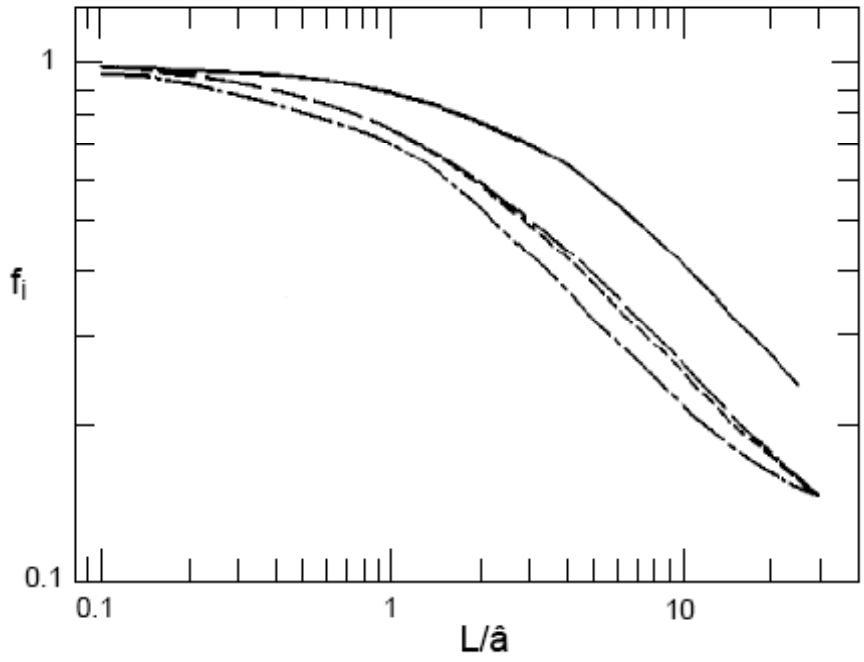

3. The functions f_i, appearing in the reciprocal scattering factors for anisotropic chains as a function of the contour length L divided by the persistence length â: ——, f_1;— - —, f_2; - - -, f_3; and – – –, f_4 . From reference 20.

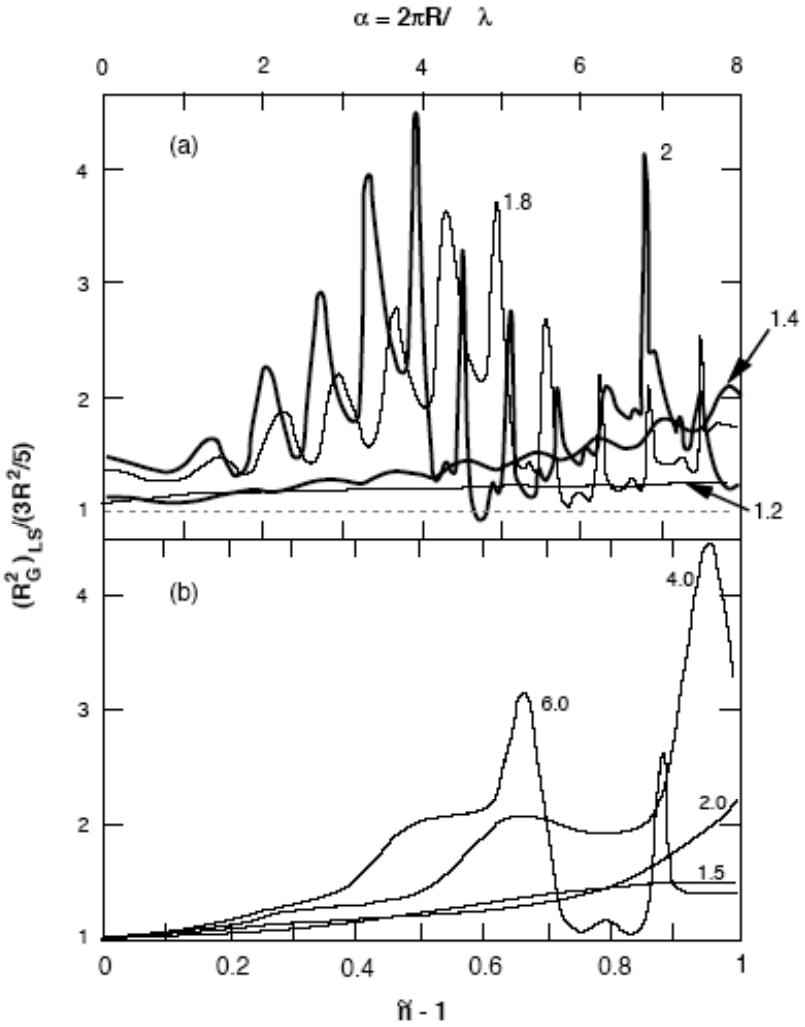

4. The ratio $R^2_{G,LS}/(3R^2/5)$ (= $y_{sph}(\tilde{n},\tilde{\alpha})$) of the light scattering averaged mean square radius of gyration $R^2_{G,LS}$ for monodisperse spheres of radius R to the geometric square radius of gyration as a function of (a) the size parameter $\tilde{\alpha} = 2\pi R/\lambda$ for the indicated values of the relative refractive index ñ and (b) the relative refractive index ñ for the indicated values of $\tilde{\alpha}$. From reference 1.

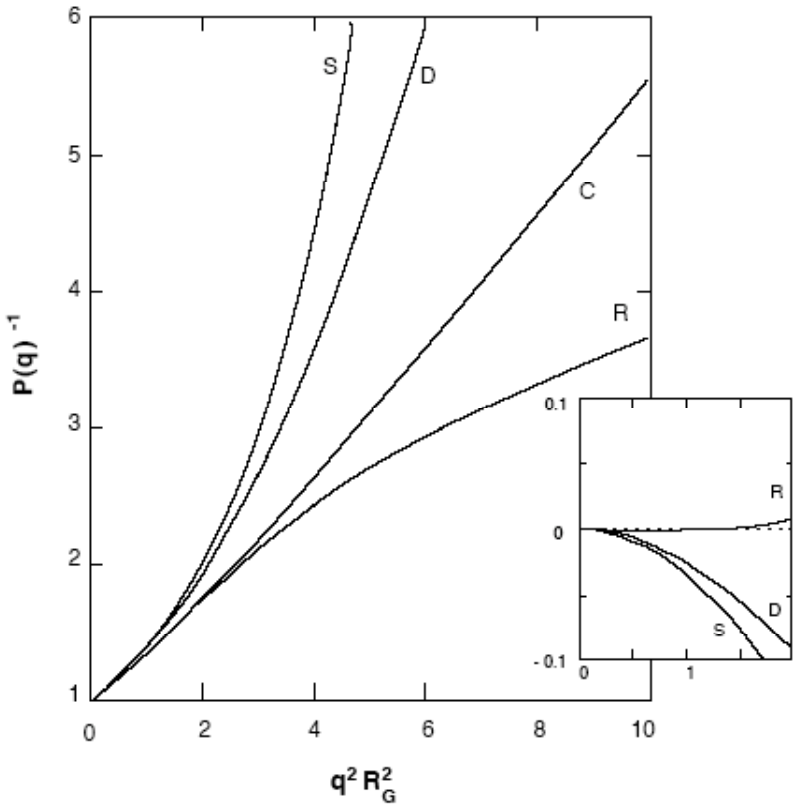

5. Examples of $P(q,0)^{-1}$ versus $R_G^2q^2$ for random-flight linear chains (C), rodlike chains (R), disks (D) and spheres (S); expressions for P(q,0) for these cases are given in Table 3. The insert shows the ratio of the logarithm of P(q,0) divided by P(q,0) for the coil with the same R_G^2 versus $R_G^2q^2$ for these cases. From reference 4.

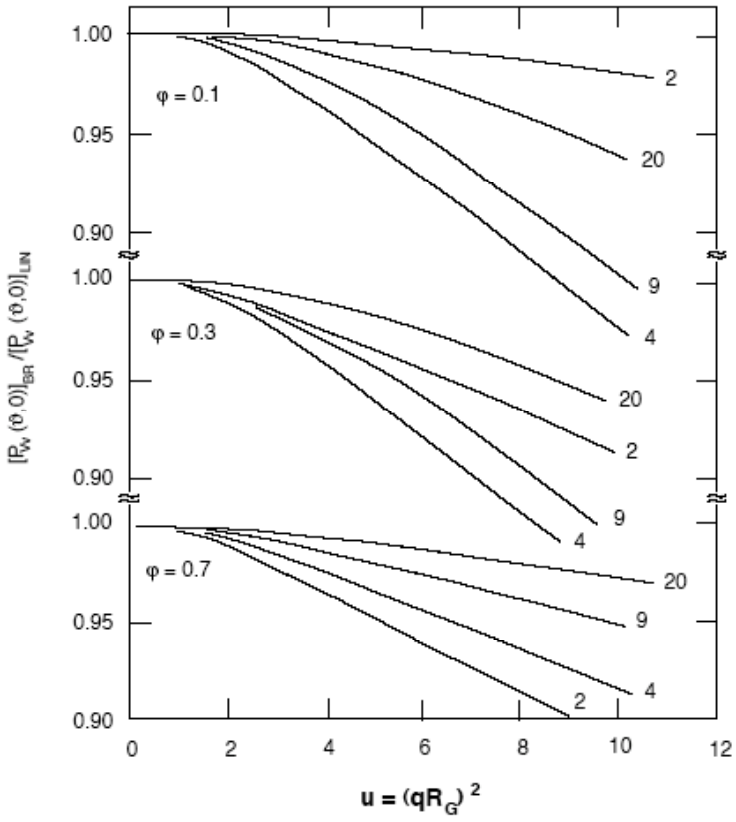

6. Examples of $[P(q,0)]_{BR}$ vs. $R_G^2q^2$ for comb-shaped branched chain polymers divided by $[P(q,0)]_{LIN}$ for linear chains with the same R_G^2 (not the same molecular weight). The number of branches is indicated, along with the fraction φ of mass in the backbone of the branched chain. From reference 79.

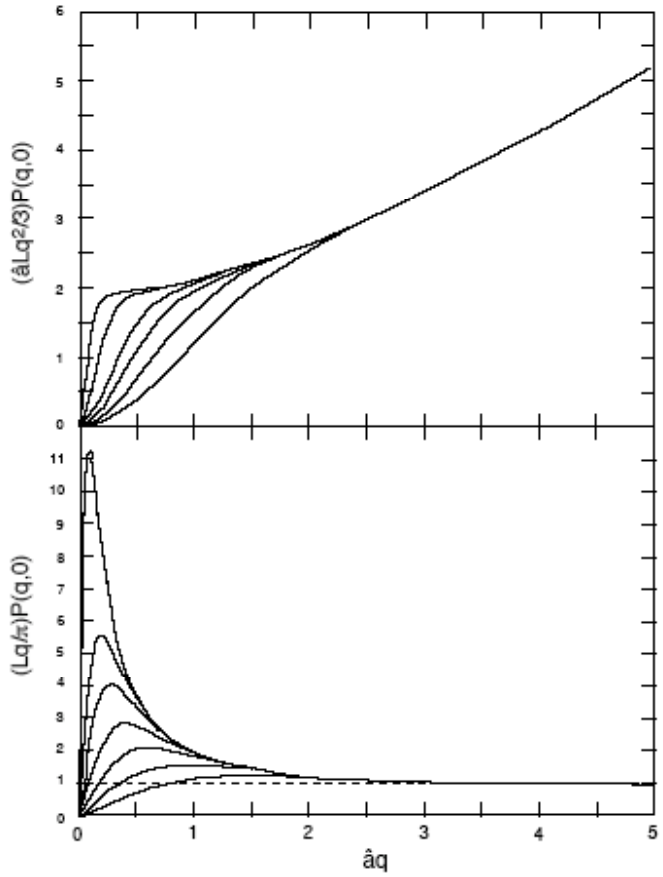

7. The functions ($\hat{a}Lq^2/3$)P(q,0) (upper) and (Lq/π)P(q,0) (lower) vs âq for the Kratky–Porod wormlike chain model [5, 91], for chains of contour length L and persistence length â. For convenience of comparison, the values of L/â used are the same are among those in an alternative bilogarithmic representation (L/2â)P(q,0) vs 2âq presented in the literature [102]: 640, 160, 80, 40, 20, 10, 5 for the curves from top to bottom in the lower panel, and all of these except 160 in the upper panel for the curves from left to right.

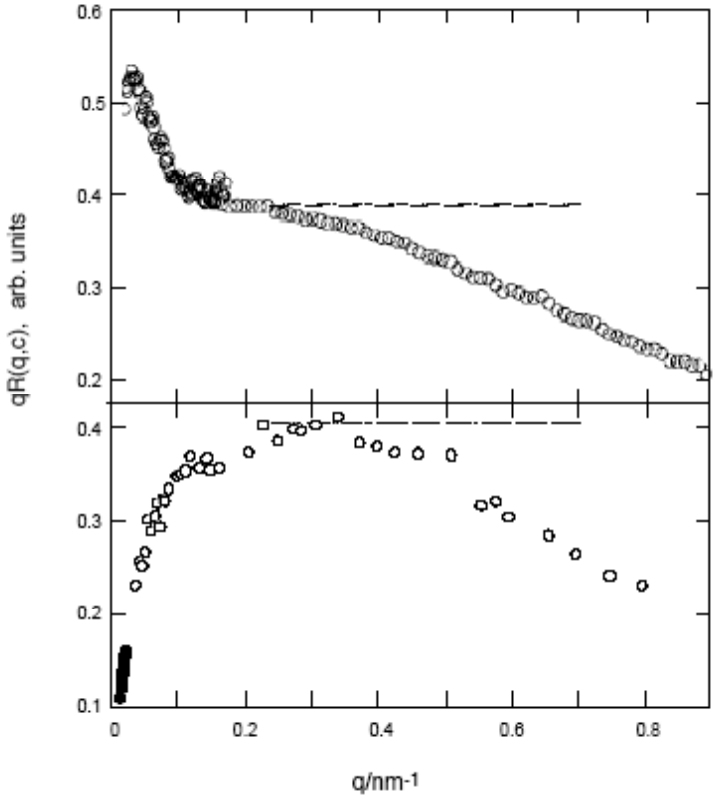

8. Examples of experimental data on qP(q,0)/(arbitrary units) vs q/nm^{-1} for wormlike micelles.
   (a) Small-angle neutron scattering SANS on micelles formed by cetyltrimethylammonium (CTA) with 2,6 dichlorbenzoate counterions in aqueous salt solution, showing the maximum mentioned in the text, and the region, indicated by the dashed line, for which $(Lq/\pi)P(q,0)$ tends to unity, followed by the regime with decreasing $P_{III}(q,0)$, providing measure of the micellar radius R_c, as discussed in the text. From reference 105.
   (b) Light scattering (filled circles) and SANS on wormlike micelles (unfilled symbols) of CTA with a polymerized counterion (to prevent dissociation on dilution). The maximum prominent in (a) is missing owing to the smaller L/â (≈ 3) for this sample, but the regime with decreasing $P_{III}(q,0)$ is evident. Data from reference 106.

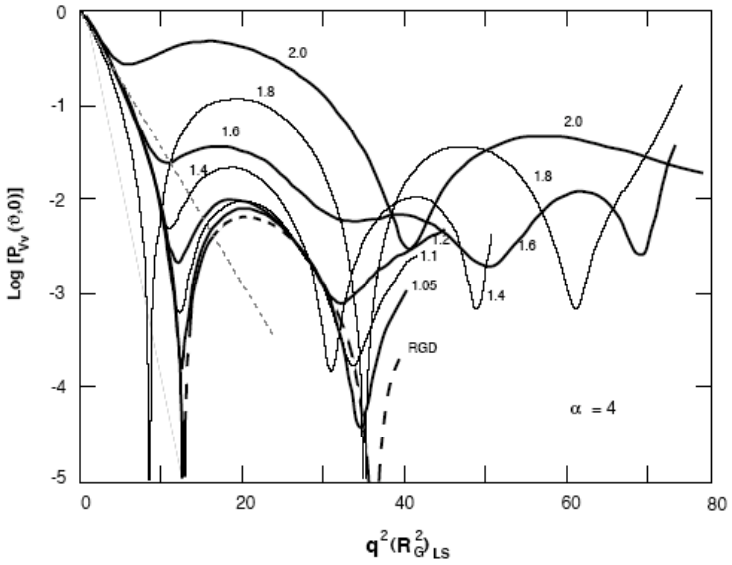

9. Examples of $P_{LS}(q,0)$ vs. $R^2_{G,LS}q^2$ for spheres with size parameter $\tilde{\alpha} = 2\pi R/\lambda = 4$ for the indicated values of the relative refractive index $\tilde{n}$. The angular range is 0 to 180 degrees in all cases except for $\tilde{n} = 2$. The RGD limiting case for very small $\tilde{n} - 1$ is given by the dashed curve. The dashed line gives the initial tangent. Values of $R^2_{G,LS}/(3R^2/5)$ may be seen in Figure 2. From reference 1.

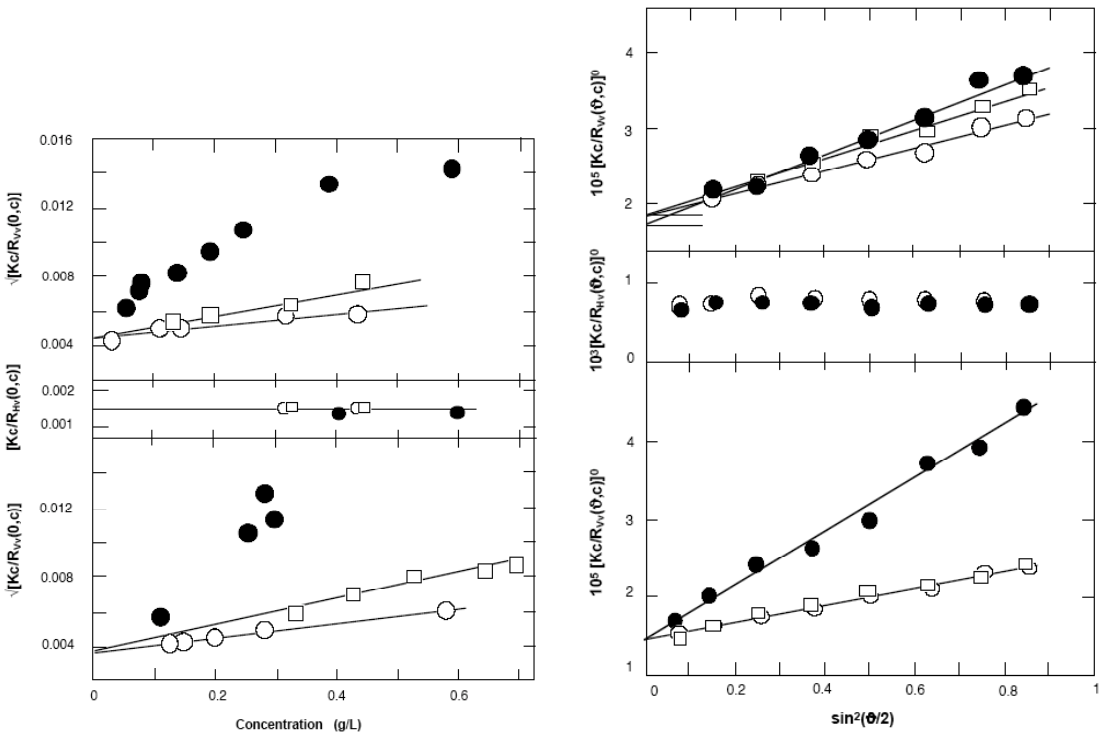

10. Light scattering data on solutions of a polyelectrolyte rodlike chain (*cis*-PBO) and a multiply broken variant of the same (*ab*-PBO) in solvents with ionic strengths providing Debye screening lengths κ^{-1}/nm of 7.9 (filled circles), 2.1 (squares) and 0.8 (unfilled circles).

    (a) Upper: $[Kc/R_{Vv}(0,c)]^{1/2}$ for solutions of *cis*-PBO.
    Middle: $Kc/R_{Hv}(0,c)$ for solutions of *cis*-PBO.
    Lower: $[Kc/R_{Vv}(0,c)]^{1/2}$ *ab*-PBO.

    (b) Upper: $[Kc/R_{Vv}(\vartheta,c)]^0$ for solutions of *cis*-PBO.
    Middle: $[Kc/R_{Hv}(\vartheta,c)]^0$ for solutions of *cis*-PBO.
    Lower: $[Kc/R_{Vv}(\vartheta,c)]^0$ for solutions of *ab*-PBO.

    From reference 76.

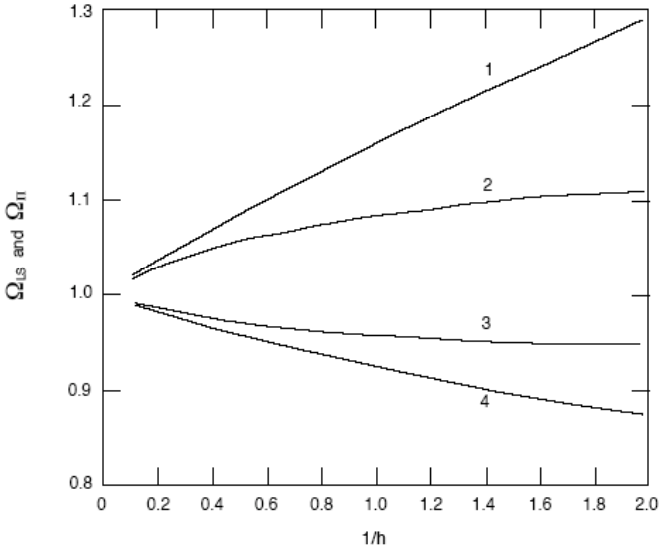

11. The functions $\Omega_{LS} \propto A_{2,LS}/M_W^{-\gamma}$ (curves 2 and 3) and $\Omega_{\Pi} \propto A_{2,\Pi}/M_n^{-\gamma}$ (curves 1 and 4) as a function of the polydispersity parameter $1/h = (M_w/M_n) - 1$ for flexible chain polymers with a distribution of M given by the Schulz-Zimm distribution function and $\gamma = 1/5$. The data are calculated using the arithmetic mean given by Equation 143 for curves 1 and 2, and the geometric mean discussed in the text for curves 3 and 4.

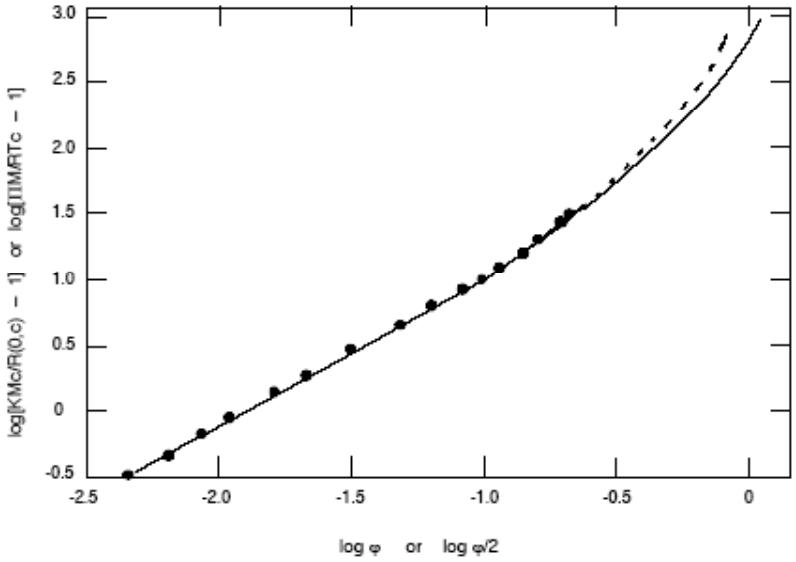

12. Bilogarithmic plots of (ΠM/RTc) – 1 as a function of φ for solutions of polyisobutylene in cyclohexane, from measurements of the osmotic pressure, or converted from measurements of the vapor pressure [166, 167]. The dashed curve is computed with a fit to Equation 162 with $\chi(\varphi) = 0.42 + 0.08\varphi$, and this same expression was used with Equation 163 to compute the solid curve shown for $[K_{op}cM/\mathbf{R}(0,c)] - 1$ vs. φ/2. The straight line portion is consistent with the scaling expected for moderately concentrated solutions.

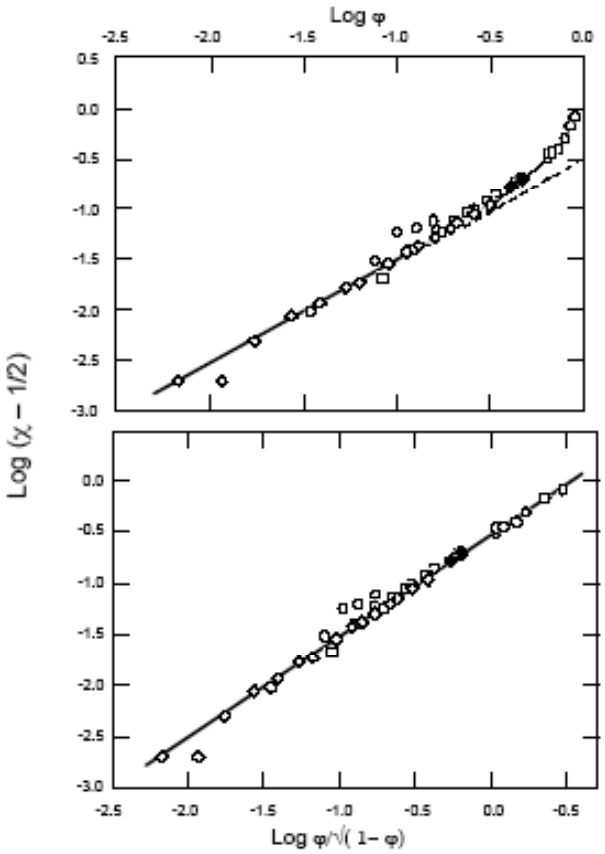

13. Bilogarithmic plots of $\chi - 1/2$ versus volume fraction φ (upper) or $\varphi/\sqrt{(1-\varphi)}$ (lower) for concentrated solutions at the Flory Theta temperature. The same data are presented and discussed as linear plots of χ vs φ in reference 118; the symbols identifying the source of the data are those used in the latter reference: circles [195]; triangles [196]; and squares [197].

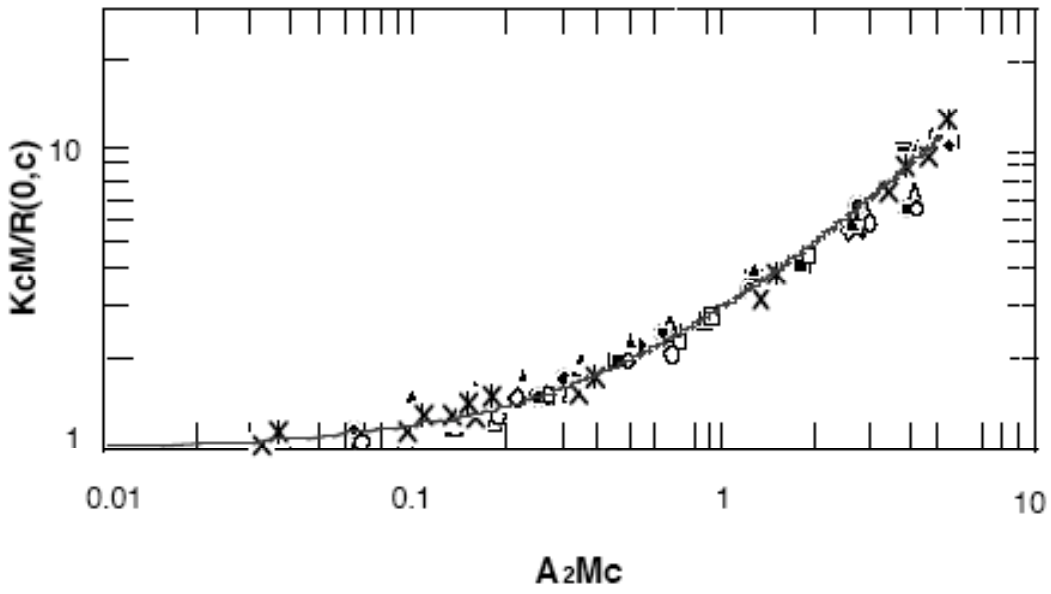

14. Bilogarithmic plots of $K_{op}cM/\mathbf{R}_{Vv}(0,c)$ versus A_2Mc for moderately concentrated solutions of poly(benzyl glutatmate) in a good solvent. The curve represents the use of Equation 132 with A_3 and higher virial coefficients equal to zero. The data were collected in the temperature range 15 to 75°C for samples with $10^{-3}M_w$ equal to 277, 179, 149, and 60 [176]. From reference 9.

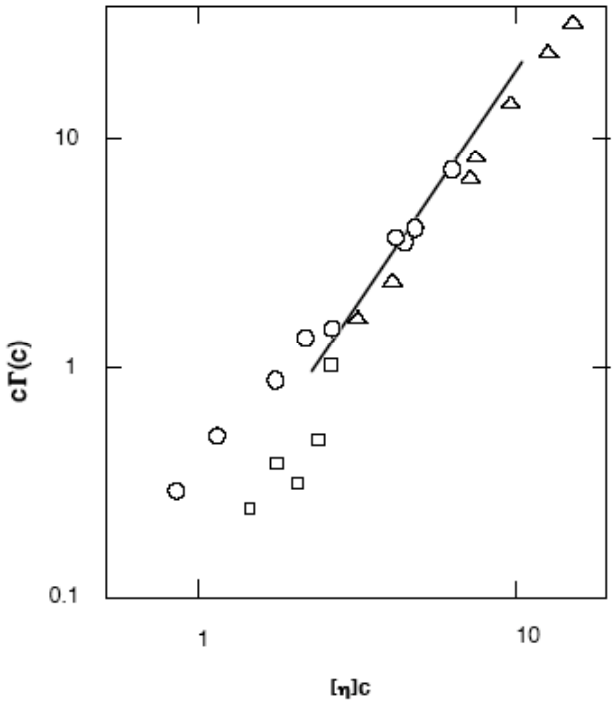

15. Bilogarithmic plot of cΓ(c) versus [η]c for solutions of polystyrene in cyclohexane at the Flory Theta temperature (34.8°C): circles [175]; squares [198]]; triangles [199]. The line represents $3A_3M/[\eta]^2 = 0.195$, i.e., $c\Gamma(c) = 0.195([\eta]c)^2$. From reference 9.

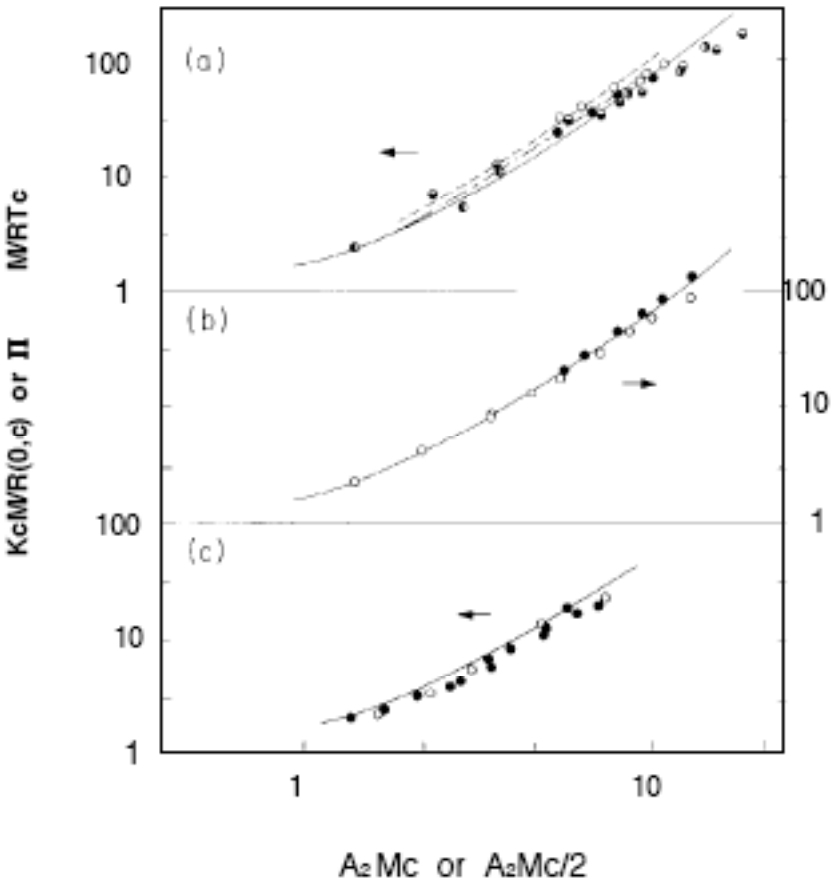

16. Bilogarithmic plots of $K_{op}cM/\mathbf{R}(0,c)$ versus A_2Mc (or $\Pi M/RTc$ versus $A_2Mc/2$) for several flexible chain polymers in good solvents. The solid curves represent the use of Eqn. 26. The data sources are identified in references 20 and 45.

    Upper: $K_{op}cM/\mathbf{R}(0,c)$ for polystyrene ($0.36 \leq 10\_6Mw \leq 7.6$) in benzene (15°C);

    Middle: $K_{op}cM/\mathbf{R}(0,c)$ (unfilled) and $\Pi M/RTc$ (filled) for poly(α-methyl styrene) in toluene;

    Lower: $K_{op}cM/\mathbf{R}(0,c)$ for polystyrene (10_6Mw equal to 0.862 for filled and 1.50 for unfilled) in cyclopentane at T equal to the Flory Theta temperature plus 20°C (no pips) and 35°C (pips).

    From reference 9.

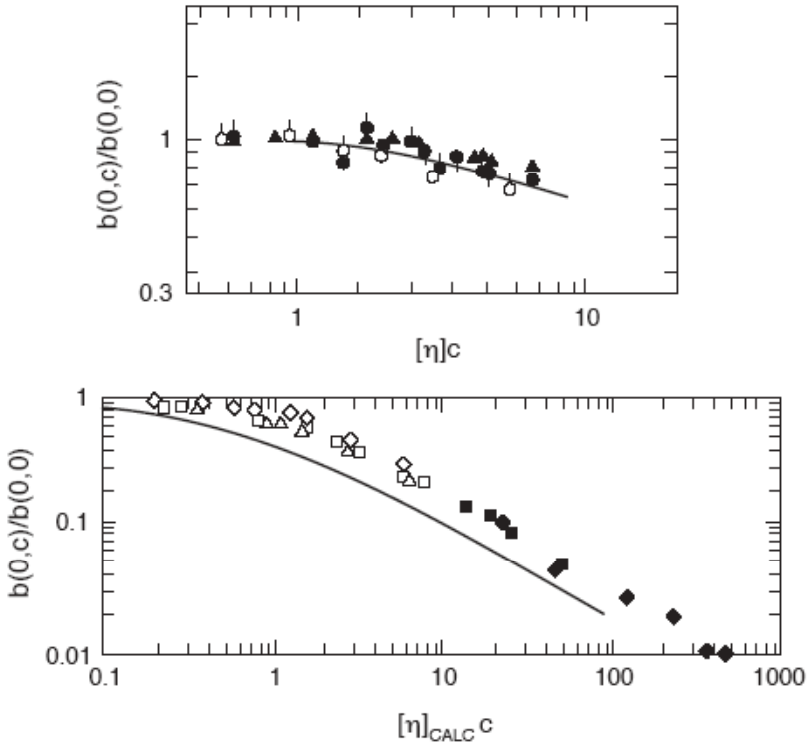

17. Bilogarithmic plots of b(0,c)/b(0,0) (or b(q > q_{max},c)/b(0,0)) versus [η]c for moderately concentrated solutions of flexible chain polymers under two thermodynamic conditions; $b(0,0)^2 = R^2_{G,LS}/3$.

Upper: b(q > q_{max},c)/b(0,0) determined under Flory Theta solvent conditions; the symbols are defined in Fig. 5 of reference 175. The solid curve represents $\xi_p(0,c)/(R^2_{G,LS}/3)^{1/2}$, see Equations 179-180.

Lower: b(0,c)/b(0,0) determined under good solvent conditions; the symbols are for data given in reference [ref 39] for b(0,c) determined by light scattering, unfilled, or neutron scattering, filled: polydimethyl siloxane, diamonds; polystyrene, squares; and poly(methyl methacrylate), triangles. The solid curve represents $\xi_p(0,c)/(R^2_{G,LS}/3)^{1/2}$, see Equations 179-180.

From reference 9.

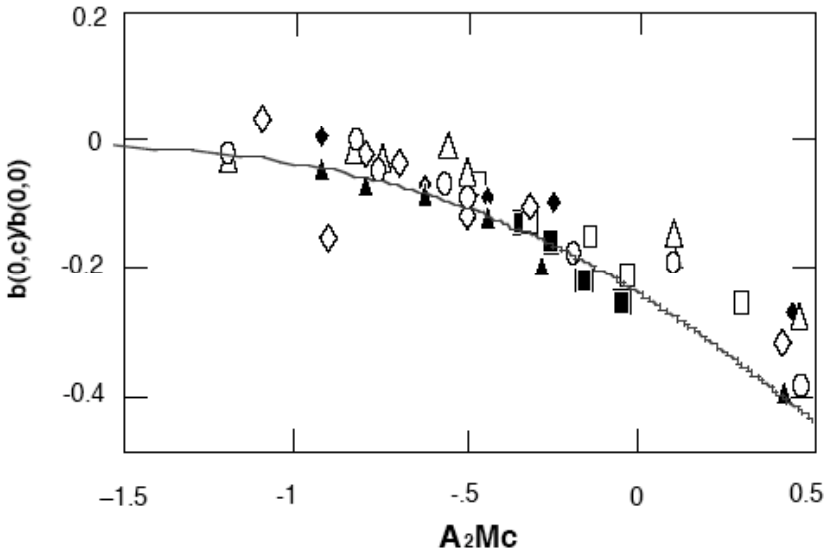

18. Bilogarithmic plot of b(0,c)/b(0,0) versus A_2M_wc for moderately concentrated solutions of poly(benzyl glutatmate) in a good solvent for the polymers described in the caption to Fig. 13 of reference 176; $b(0,0)^2 = R^2_{G,LS}/3$. The curve represents $\xi_P(0,c)/b(0,0)$ using the experimental data for $\Gamma(c)$ (see Equations 179-180). From reference 9.

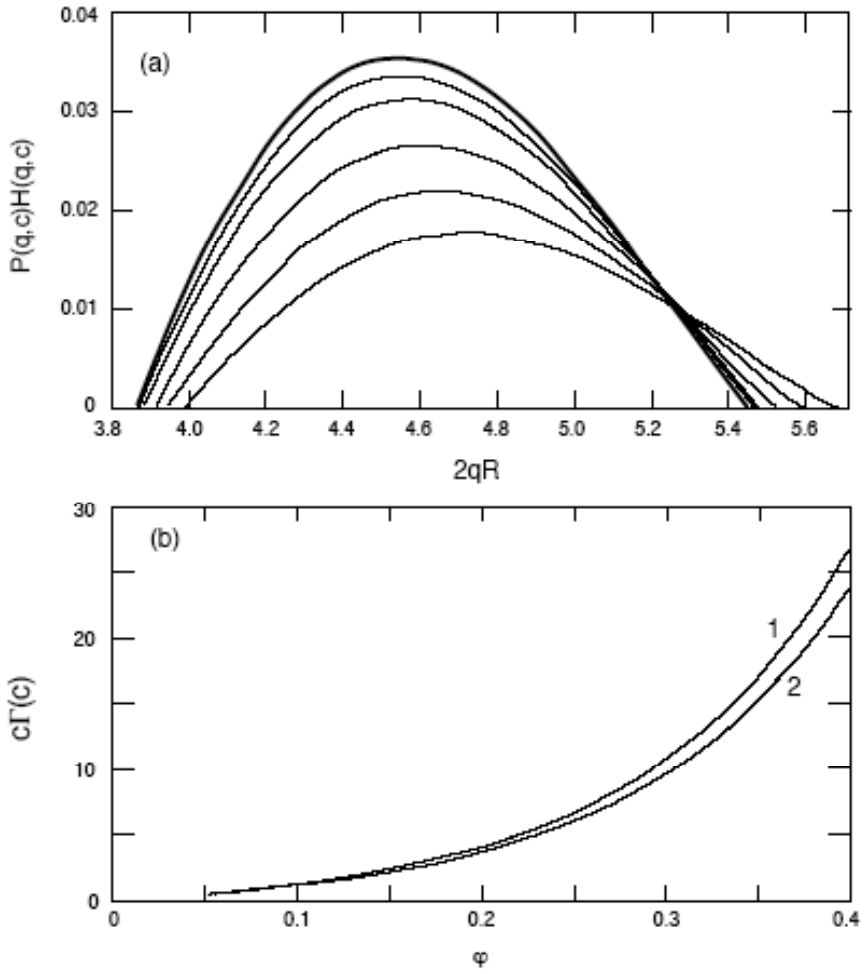

19. (a) The function P(q,c)H(q,c) vs 2qR calculated for monodisperse spheres of radius R interacting through a hard core potential. The bold curve is calculated with Equation 182, and the remaining curves were calculated with Equation 183, with the volume fraction φ equal to 0.05, 0.1, 0.2, 0.3 and 0.4 from top to bottom.

(b) The function cΓ(c) vs volume fraction for monodisperse spheres calculated with Equations 160 and 184 for curve (1) and (2), respectively.

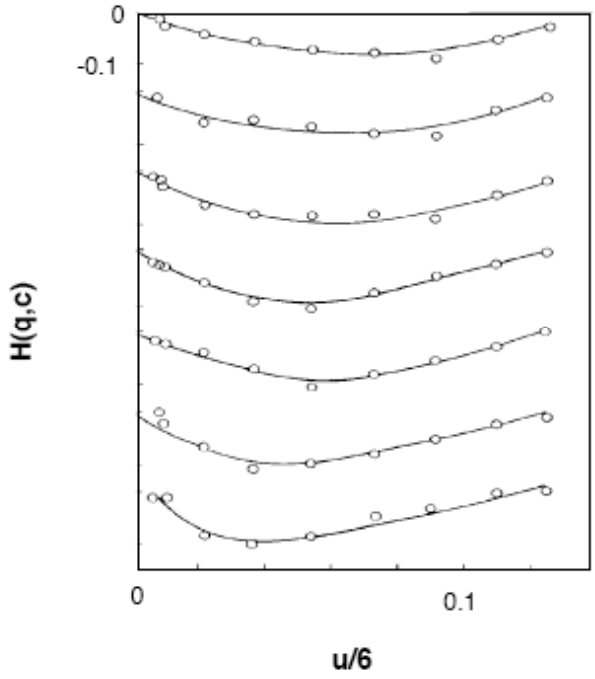

20. H(q,c) versus $R_G^2q^2/6$ for moderately concentrated solutions of polystyrene in cyclohexane at the Flory Theta temperature (34.8°C), $M_w = 8.62 \times 10^5$, $[\eta] = 76$ ml/g, $R_G = 27$ nm: $[\eta]c$ equal to 0.60, 1.15, 1.73, 2.68, 4.64, 4.69, 6.54 from bottom to top. The curves are drawn merely to aid the eye. From reference 9.

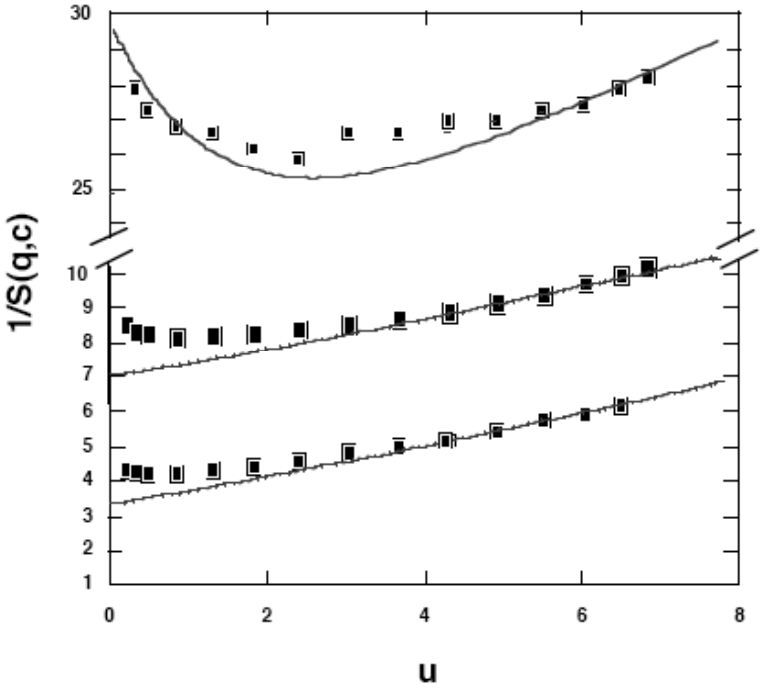

21. $K_{op}cM/\mathbf{R}(q,c)$ versus $u = R_G^2q^2$ for dilute to moderately concentrated solutions of poly(α-methyl styrene) in toluene (a good solvent) [178]: $M_w = 2.96 \times 10^6$ and $R_G = 74$ nm. $[\eta]c$ equal to 0.94, 1.94, and 5.30 from bottom to top. The value of R_G^2 used was chosen to fit the data for the larger range of u, and the curves for the lower two data sets represents P(q,0) for the random-flight model. The solid curve for the most concentrated solution is calculated using the approximation $H(q,c) \approx [P(2q,c)]^2/P(q,c)$ as discussed in the text. From reference 9.

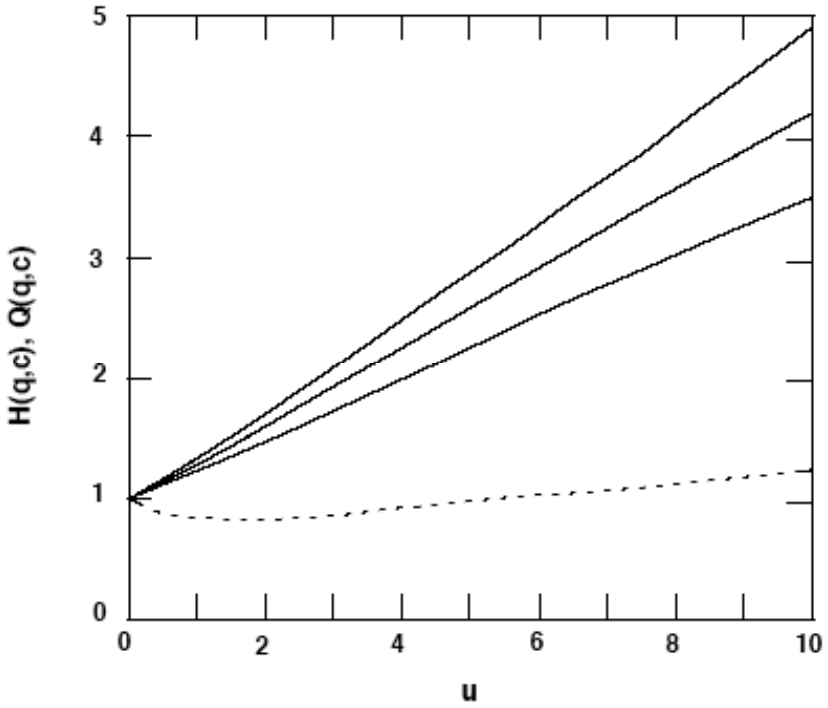

22. The function Q(q,c) corresponding to the approximation $H(q,c) \approx [P(2q,c)]^{1/2}/P(q,c)$, using Equation for P(q,c), as discussed in the text. The dashed curve gives H(q,c), and the solid curves give Q(q,c) for c_(c) equal to 5, 10 and 25 from bottom to top, respectively. From reference 9.

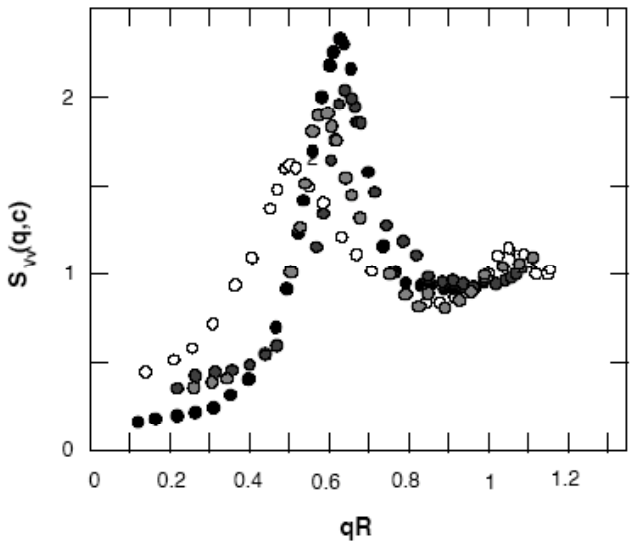

23. The dependence of the structure factor on qR for polystyrene spheres (R = 45 nm) immersed in deionized water, with the number concentration n/particles·mm^{-3} = 2.53, 5.06, 7.59 and 10.12 for the circles with increasing depth of the shading, respectively; adapted from figures in reference 179. From reference 1.

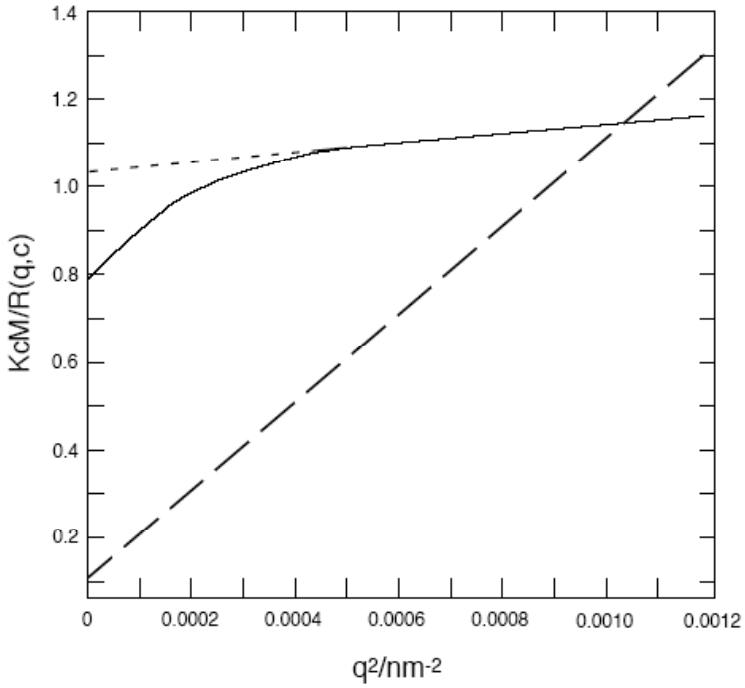

24. Illustrations of KcM/**R**(q,c) for two extreme forms of association observed with solutions. In type I association (— —), the aggregates form a loose supramolecular structure, of a type that may lead to gelation. In type II association (——), the aggregates are more compact, giving much enhanced scattering preferentially at small scattering angle. The scattering from the fully dissociated polymer is also shown (- - - -).

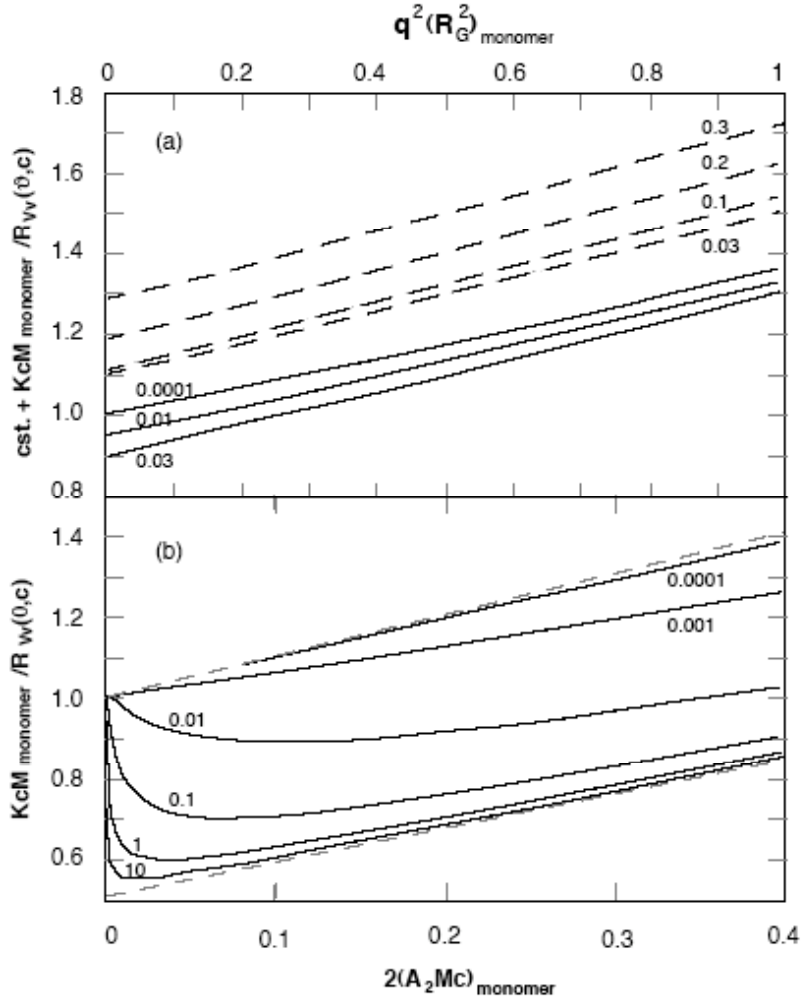

25. Scattering functions for an illustrative example of a flexible chain polymer undergoing end-to-end dimerization. (a) dependence on angle, calculated as discussed in the text for a reduced equilibrium constant $K_{eq} = 0.1$ and the indicated values of $A_{2,M}Mc$, with the constant equal to zero or 0.2 for the solid and dashed curves, respectively; (b) scattering extrapolated to zero angle as a function of $A_{2,M}Mc$, for the indicated values of K_{eq}. From reference 1.

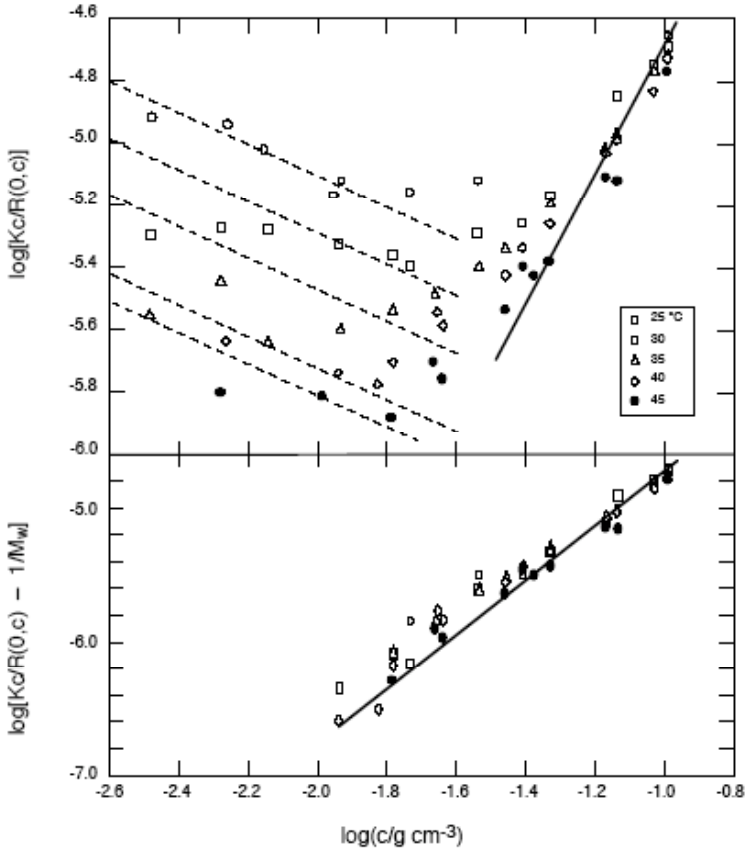

26. Light scattering data for aqueous solutions of wormlike micelles of hexaoxyethylene dodecyl ether [190].

(a) Bilogarithmic plot of Kc/**R**(0,c) vs c at the indicated temperatures. The dashed and solid lines are placed with slopes –1/2 and 2 as discussed in the text.

(b) Bilogarithmic plot of Kc/**R**(0,c) – M_w^{-1} vs c at the temperatures indicated by the symbols defined in (a). The line has slope 2.